(2)

Baylor Research Foundation

Biomedical Free Electron Laser Studies
Annual Report 1987-88

Principal Investigator: J.L. Matthews, Ph.D.
Contract Number: N00014-86-K-0186

BAYLOR RESEARCH FOUNDATION
FEL EXECUTIVE SUMMARY
Annual Report 1987

This submission by the Baylor Research Foundation, Dallas, Texas is the annual report of ONR contract N00014-86-K-0186, Biomedical and Material Science Applications of the Free Electron Laser. This submission is for projects submitted for work during 1986-88 project years.

The Baylor Research Foundation (BRF) is part of Baylor University Medical Center in Dallas, Texas. BRF is uniquely qualified to provide continued successful research where basic science can be brought to clinical applications. Baylor University Medical Center is the second largest not-for-profit hospital in the United States. The use of lasers in medicine is strongly apparent as seventy physicians currently use lasers in their clinical practice at Baylor.

A financial summary is provided in the annual report. Annual budget for this contract was $600,000 per year for two years. The following projects represent a continuation of preliminary work performed under this program. Some of the work described was reported at the annual meeting in Salt Lake City, Utah in May 1988.

PHOTOSENISTIZING DYES FOR THE REMOVAL OF INFECTIOUS AGENTS FROM BLOOD

Until 1985, little effort had been expended upon the study of transmission of infectious agents by banked-blood products, although a report of transmission of viral hepatitis (HVB) in banked blood has been known since 1938 (Junet and Junet, 1938). Since that time, other studies of HVB by Attere et. al. (1972) suggest that the risk of post-transfusion hepattis may be as high as 7-10% of all blood recipients. In addition to HVB, other agents such at Cytomegalovirus (CMV) and Epstein-Barr virus (EBV) are known to be transmitted in banked blood and to cause disease (Battle and Hewlett, 1958; Land and Hanshaw, 1969). Land and Hanshow (op. cit.) believe that up to 35% of transfused patients showed laboratory evidence of CMV infection. More recently, AIDS caused by HIV virus is of growing concern due to the difficulty of evaluating the possibility of infection with the virus prior to the appearance of antibodies.

We have now published data on killing HIV, CMV, Herpes, etc. virus using DHE and laser light in which viral kill was 99.999% (limit of detection). Blood quality was unchanged. In a quest for more effective dyes requiring less energy and being activated at wavelengths more separated from hemoglobin, we have focused our study on the dye 3, 3^1-diethyloxatricarbocyanine ($DIOC_2(7)$). Previous studies on carbocyanine by others had shown take-up by lymphocytes (Montcucco et. al, 1979) and take-up by lipoproteins (Barbara and Webb, 1981). To date, we have examined binding of $DIOC_2(7)$ to plasma proteins, lymphocytes, and to erythrocytes. Experiments described within suggest strong partitioning of $DIOC_2(7)$ by lymphocytes with little reversibility and essentially reversible partitioning by erythrocytes.

Photokilling of a mixed population of human lymphocytes (-90%) and monocytes

(-10%) obtained by centrifugation of the buffy coat of sedimented blood in a ficoll-hypaque density gradient using $DiOC_2(7)$ was examined. Effects of both dye concentration and light fluence at 630 and 708 nm wavelengths were examined. Studies continue to examine the wavelengths over the range of 650-720 nm in order to obtain the action spectrum.

INTRACELLUAR PARASITE-FLUORSCENT PROBE INTERACTION

Chagas disease, a debilitating and often fatal condition, affects over 30 million human beings. Although *Trypanosoma cruzi* , the etiologic agent of Chagas disease, has been cultured in various mammalian cells since 1935, drug toxicity studies have been difficult to assess due to the differences in intra- and extracellular parasite physiology. The use of differential centrifugation and gradient sedimentation techniques described by Carvalho and de Souza for the separation of amastigotes and trypomastigotes and culture lines described by other investigators are significant advances for the development of drugs in the prophylaxis and treatment of Chagas disease.

Photoactivatable dyes Photofrin II (Dihematoporphyrin Ether) and HEVD (hydroxy ethlvinyl deuteroporphyrin) were investigated for their affinity for intracellular forms of Trypanosoma cruzi and Toxoplasma gondii. Both dyes were found to localize intracellularly in infected and non-infected cells and be specifically bound to dividing parasites.

Since both infected and uninfected cells sequestered dyes, irradiation resulted in the destruction of all cells. Thus it was necessary to develop strategies for the sole destruction of intracellular parasites. Interaction between porphyrins and chloroquine diphosphate resulted in the red shifts of emission spectra when combined with amastigotes and trypanosome stages of Trypanosoma cruzi. Chloroquine diphosphate was selected for *in vitro* tissue culture porphyrin activation studies. Results of these studies were unpredictable. Studies to determine why some failures resulted suggested that the porphyrins would aggregate when bound to the intracellular, amastigote forms. This aggregation may be due to localized charge differences, i.e. pH between the parasite and the cytosol. Studies on dye-light and aggregate reactions are ongoing.

FLUORESCENCE AND PHOSPHORESCENCE SPECTROSCOPIC STUDIES OF THIN FILAMENT PROTEINS

This study focused on the thin filament proteins actin and tropomyosin. Other work to be reported under a different study is directed to myosin in muscle protein. The idea behind this study is to expand our protein flexibility studies to include the thin filament protein assembly. The two systems really complement each other. The benefits of this approach includes sharing the protein samples, fluorescence probes, common biological assays, and similar instrument set-up.

We isolated and purified actin and tropomyosin from rabbit skeletal muscle and covalently labeled them with three dual fluorescence/phosphorescence probes--eosin maleide, eosin iodoacetic acid, and erythrosin B iodoacetic acid. These probes react specifically only to the free sulfhydryls in proteins at pH 8.4.

The fluorescence and phosphorescence spectral properties were characterized under a variety of conditions. The spectral properties investigated include steady state excitation and emission spectra, and fluorescence polarization spectra. The phosphorescence decay kenetics was investigated using a pulsed nitrogen laser and a transient digitized oscilloscope The real time phosphorescence decay curves were analyzed by curve-fitting technique The phosphorescence decay curves were best characterized by a two-exponential fit. These data are being used to better characterize the protein functional structure.

SPECTROSCOPIC CHARACTERIZATION OF SIX NEW NOVEL FLUORESCENT PROBES

Although quite a few organic dyes already exist which have been proved to be effective in photodynamic therapy for cancer cell kill, e.g., hematoporphyrin and its many derivatives, the existing compounds are mostly unpurified and the effective ingredient is not known. Some of these compounds have also proved to posses undesirable side effects. The search for better dyes with no or the least toxicity and more desirable spectral characteristics is an essential task that we are continuing to pursue.

The main purpose of the present study are (1) to characterize the absorption and fluorescence spectral properties of these novel probes; (2) to try correlating spectral characteristics with (a) the position of the substituents and (b) the type of functional groups; and (3) to investigate the potential application in photodynamic therapy as well as in hydrodynamic studies of protein macromolecular assembly.

We have successfully synthesized more than a dozen interesting fluorescent dyes and found two pyrene and two coumarin derivatives particularly attractive. All four compounds emit in the green and exhibit extremely high fluorescence yield. One of our original objective set out in the beginning is to achieve wavelength shift as long as possible into the red region. Although so far we have only obtained dyes which absorb mainly in the blue-green region, we believe that by deductive reasoning and comparing spectra feature with the position and the chemical characteristics of the substituent in the coumarin and pyrene side chains we have grasped the key in synthesizing dyes that will have further wavelength shift into the red region.

LASER SPECTROSCOPIC STUDIES OF PROTEIN STRUCTURE AND FLEXIBILITY

The most recent evidence on myosin reinforces the fundamental importance of the 'head' region of this protein in contractile function (Hynes et al., 1987). It appears that the flexibility and relative dynamic motional properties of the major structural 'subdomains' are functional in the contractile process. Thus, experiments have been undertaken with myosin labeled with specifically attached probes capable of monitoring (1) rather fast, 'localized' motions, as well as (2) relatively slower, 'global' rotations. Spectroscopically, these could be related to singlet-state (fluorescence) and triplet-state (phosphorescence) luminescence measurements. The photophysical properties of the probe eosin have been shown to be useful for both types.

We have initiated fluorescence anisotropy measurements of myosin labeled at specific sites with a probe of relatively short excited singlet lifetime in an effort to acquire additional information on the dynamics of such motions. Steady-state and time-resolved measurements were carried out at different excitation wavelengths in order to increase the information available on the probe's rotational modalities by photoselecting transition dipole moments exhibiting significantly different orientations (Wegener, 1985;

VanderMeulen and Wegener, 1985; VanderMeulen et al., 1986). Recent modifications on the FEL should allow us to test the pulse systems on the FEL.

NEAR-ULTRAVIOLET EFFECTS ON CELLULAR TISSUE COMPONENTS: DIRECT PHOTOINDUCED CHANGES OF PROTEINS

The potential role of light in the etiology of malignancy and a concern for the side-effects of current and proposed surgical uses of lasers make the study of photooxidative processes in tissue components a subject of biomedical interest. Moreover, studies of photoinduced changes in proteins could yield interesting insights into subtleties of structure, conformation, and dynamics important to biological function.

Using the protein lysozyme as a model, photoinduced oxidative changes were studied using near-UV irradiation, primarily with a nitrogen (337 nm) laser, with no specifically added sensitizing compounds. Near-UV irradiation of tryptophan alone (an amino acid component which is found in key positions in the structure of lysozyme) under similar conditions was also examined to extend the relevant background database, using HPLC, TLC, absorption and fluorescence spectrometry.

Enhancement of photochanges with deuterium oxide, compared to water as solvent, is consistent with a mechanism mediated by singlet oxygen. Involvement of peroxide and radicals have not been strictly ruled out. Exposures to laser light that resulted in 15% loss of tryptophan fluorescence produced no measurable loss in enzymatic activity. Fluorescence quenching experiments on irradiated lysozyme at low conversion percentages suggest that an exposed residue (Trp-62) is favored as an initial target of attack. Implications for enzyme mechanisms are discussed in the published article.

CURRENT STATE OF LEUKEMIA AND AUTOLOGOUS BONE MARROW PURGING

Photodynamic therapy can be simply defined as a chemical reaction activated by light. An ideal purging agent kills 100% of the tumor cells while 100% of the normal cells are spared. In an effort to approach these ideals, we have utilized Merocyanine 540 (MC 540) mediated, laser light induced photodynamic purging of bone marrow cells. Our early findings were very encouraging because we were able to attain a 99.999% kill of leukemic cells and survival of 55% of the normal marrow cells with 25% survival of normal hematopoietic progenitor cells, a significant improvement over the chemotherapeutic approach. More recently by using 0.25% human albumin instead of fetal bovine serum, we have been able to retain 99.9999% of leukemic cell killing efficiency while markedly extending the normal cell survival to 80% (Gulliya et al, 1987, 1988). Under these conditions, 40% of the granulocyte-macrophage colony forming cells also survived the treatment. It is important to note that the use of laser light has virtually eliminated the non-specific cytotoxicity observed by day light sources alone. Exposure to daylight source alone has been reported to kill 25% to 65% of cells (Sieber et al; 1986).

We have been successful in killing non-hodgkins lymphoma cells with the same efficiency. There was > 6 log reduction in clonogenic lymphoma stem cells while as much as 50% of the normal marrow CFU-GM cells survived the treatment. In these studies, the effect of recombinant interferon alpha (IFN) was also investigated. It was observed that

the presence of low levels of IFN interferes with the complete elimination of leukemic cells but not lymphoma cells by photodynamic therapy. These results are of clinical importance because many leukemic and lymphoma patients are treated with IFN as well. At present, we are investigating the effect of photochemotherapy on the elimination of small cell lung carcinoma, adenocarcinoma and breast cancer cells.

OPTICAL PROPERTIES OF BIOLOGICAL MATERIALS

Interaction of electromagnetic radiation with biological materials ranging from macromolecules to organized tissue and organs is most conveniently characterized by measurement of the various fractions of incident radiation intensity that are transmitted, T, absorbed, A, and remitted (reflected and back scattered) R. Since these quantities account for all direct physical effects of the interaction, (T+A+R) = 1. Typically, T, A, and R of a specific biological material depend upon both the chemical and structural properties of the material and upon the wavelength of the incident radiation. With knowledge of these electromagnetic properties, the fraction incident light energy transferred to a particular tissue and the variation of its intensity with depth of penetration into that tissue may be computed. This capability will allow a choice of laser radiation wavelengths to effect either optimum light penetration or absorption to achieve a desired clinical effect at a desired depth in tissue, and correlation of biological or therapeutic effects and radiation energy density within the volume of tissue at specified incident wavelength over the output spectrum of the FEL at pulse energies where optical effects are linear.

Results of preliminary measurements of the remittance and transmittance of layers of blood-free agar of thickness ranging between 1 and 7 nm. The observed decrease in both optical quantities agrees qualitively with prediction of Kubelka Theory (1948). Small fluctuations of measured values about curves of best fit are possibly due to minor fluctuations in sample alignment relative to the beam and possible inclusion of small air bubbles between the agar surface film and the coverslip. We are working to identify and eliminate the sources of these fluctuations before proceeding to work with blood-agar suspensions and whole blood.

PHOTOSENSITIZING DYES FOR THE REMOVAL OF INFECTIOUS AGENTS FROM BLOOD

Until 1985, (see review in 1985 Federal Register 50:5612-5723) little effort had been expended upon the study of transmission of infectious agents by banked-blood products, although a report of transmission of viral hepatitis (HVB) in banked blood has been known since 1938 (Junet and Junet, 1938). Since that time, other studies of HVB by Attere et. al. (1972) suggest that the risk of post-transfusion hepattis may be as high as 7-10% of all blood recipients. In addition to HVB, other agents such at Cytomegalovirus (CMV) and Epstein-Barr virus (EBV) are known to be transmitted in banked blood and to cause disease (Battle and Hewlett, 1958; Land and Hanshaw, 1969). Land and Hanshow (op. cit.) believe that up to 35% of transfused patients showed laboratory evidence of CMV infection. More recently, AIDS caused by HIV virus is of growing concern due to the difficulty of evaluating the possibility of infection with the virus prior to the appearance of antibodies.

Clinically realistic and successful application of special photodynamic techniques (Skiles et. al., 1985) for killing of infectious agents in blood products require relatively rapid volume of flow through-put in an irradiating beam of light. Ths means that a flow-through cell must be designed in such a way that relatively thick (> 1mm) layers of whole blood would have to be processed at high flow rates. These scale-ups from equipment designed by us, and in current use in our laboratories, would require increasing the light fluence to higher levels; equaling or even exceeding the value of 53 J/cm^2 where our previous experience with irradiation of blood containing malarial parasites suggests that onset of hemolysis of non-infected erythrocyte became important. Hemolysis of erythrocytes with 630 nm light in the presence of a photosensitizer potentially could be caused by photochemical attack and by cell heating due to light absorption by the heme group of hemoglobim. Lamola and co-workers (1973) have reported porphyrin-mediated photosensitization of erythrocytes. Recently Tan and co-workers (1987) have reported thermally induced hemolysis of whole blood in 100-1000 micron diameter glass capillary tubes at a fluences between 1 to 16 J/cm^2 with pulsed 577 nm dye laser light. This coupling of optical energy to normal erythrocyte is almost certainly due to absorption by the heme group of hemoglobin, since the value of the extinction coefficient of hemoglobin at 577 nm is approximately 1×10^4, $LM^{-1}\ cm^{-1}$.

Large increases in both the thickness of the blood layer and in the flow rate envisioned as requisite for clinical use of photosensitized killing of infectious agents in dye-treated blood would require a large increase in incident fluence and irradiance of the photosensitizing light. Possibly one effect of high fluence 630 nm irradiation would be significant hemolysis, since at this wavelength, the extinction coefficient is $3 \times 10^2\ LM^{-1}\ cm^{-1}$ (Makinen and Eaton, 1973). We are exploring the use of photosensitizing dyes other than the porphyrin-based HPD and DHE. In order to minimize the effect of light absorption in inducing photothermal hemolysis of erythrocytes, we have selected photosensitizing dyes which absorb at longer wavelengths in the far red to near IR range, 650 - 850 nm. Examination of absorption spectra for hemoglobin and oxygemoglobin (McKinen and Eaton, 1973) show that the absorbance value for the hemoglobin species in this range is approximately 30% of the value at 630 nm. The use of photosensitizers absorbing in wavelength range of 650 to 850 nm should significantly decrease the light irradiance and fluence values needed to achieve photokill of infectious agents in blood without photothermal damage to erythrocytes.

DYE STUDIES

Initially we focused our study on killing enveloped viruses including HIV I using dihematoporphyrin ether (DHE) as a photosensitizer with activation using 630 nm light (see attached paper). In examination of dyes which absorb in the far red spectrum, we have focused study initially on the dye 3, 3^1-diethyloxatricarbocyanine ($DIOC_2(7)$). Previous studies on carbocyanine by others had shown take-up by lymphocytes (Montcucco et. al, 1979) and take-up by lipoproteins (Barbara and Webb, 1981). Additional unpublished studies in our laboratory showed binding of carbocyanines to lysosomes. These studies suggested that $DIOC_2(7)$ and dyes differing only in having longer lipid tail attached at the 3, 3^1 nitrogens might be suitable candidates for killing of both intracellular and free enveloped viruses including HIV-I and the AIDS virus.

To date, we have examined binding of $DIOC_2(7)$ to plasma proteins, lymphocytes, and to erythrocytes. Experiments described below suggest strong partitioning of $DIOC_2(7)$ by lymphocytes with little reversibility and essentially reversible partitioning by erythrocytes.

Binding of DIOC2(7) to Plasma Proteins

Shifts in peak optical absorption wavelength are observed upon equilibration of $DIOC_2(7)$ (0.5 micromolar) in phosphate buffered saline (PBS) (pH = 7.3), in PBS containing 6 mg/ml of human serum albumin (HSA) and in PBS containing 10% human serum. Extensive take-up of the tricarbocyanine by the proteins is demonstrated by absence of the 678 nm peak scan in PBS in the 685 and 695 nm peaks exhibited by the dye in HSA and in serum, respectively (Figures 1,2,3).

Binding of $DIOC_2(7)$ to Erythrocytes

Binding of $DIOC_2(7)$ to human erythrocytes at normal hematocrit and in the presence of undiluted human plasma was studied. Erythrocytes were harvested from whole blood by centrifugation and resuspended in whole plasma to give a hematocrit of 46. $DIOC_2(7)$ was added to various samples to cover the concentration range 0 to 10 micromolar in plasma phase only. Dye was also added to whole plasma containing no cells to cover the same dye concentration range. After allowing the samples to equilibrate for 1 hour fluroescence emission intensity values (680 nm excitation, 700 nm emission) for the plasma fractions were recorded. Data for dye equilibrated in plasma only and plasma with erythrocytes (HCT = 46) are shown in Figure 4. No sensible difference in the fluorescence emission intensity is noted. This suggests that take-up of the dye by erythrocytes in plasma of $DIOTC_2(7)$ concentration below 10 micromolar is small and perhaps negligible. This result is probably due to the competitive binding of the dye by plasma proteins. We are further investigating this possibility. If dye binding to the erythrocytes is negligible, potential photodynamic damage to these cells may be minimized.

Binding of $DIOTC_2(7)$ to Lymphocytes and Monocytes

A mixed population of lymphocytes ($\simeq$90%) and monocytes ($\simeq$10%) were obtained by centrifugation of the buffy coat of sedimented whole blood in a ficoll-hypaque density gradient. The cells were resuspended in whole plasma to give 1 x 10^4 cells per cubic millimeter or the approximate upper limit of the entire normal whole blood cell population in whole blood. $DIOTC_2(7)$ was added to the cell suspension and to whole plasma

emission intensity was recorded after 1 hour equilibration as described above in the study on erythrocytes. Plots of fluorescence intensity versus original concentration of the dye in the plasma for plasma with and without cells are different (Figure 5). The decrease in fluorescence emission of plasma previously equilibrated with the cells reflects binding and retention of the dye by the lymphocyte-monocyte population. At an original dye concentration of 10 μm in the plasma, the cells at 1 x 10^4 per mm^3 sequester approximately 3 micromoles of the dye from a 1 ml sample. Using an average cell diameter of 15 microns leads to an estimated cellular concentration of ≃ 170 micromolar or about 17 times the initial extracellular value.

$DIOC_2(7)$ Photosensitized Killing of Lymphocytes and Monocytes

Photokilling of a mixed population of human lymphocytes (-90%) and monocytes (-10%) obtained by centrifugation of the buffy coat of sedimented blood in a ficoll-hypaque density gradient using $DiOC_2(7)$ was examined. Effects of both dye concentration and light fluence at 630 and 708 nm wavelengths were examined.

To study effect of dye concentration, cells in RPMI medium (10% fetal calf serum) were allowed to take up dye for 30 minutes. The suspension was 1 or 2 or 10 μm in dye concentration. Light exposure times at an irradiance of 11 mw/cm^2 were adjusted to give fluence of either 1, 4 or 10 J/cm^2. Cell survival was judged on basis of Trypan Blue dye exclusion after maintaining irradiated cells for 24 hours at 37.5°C in fresh RPMI medium. The preliminary resulte expressed as percent cell survival are summarized in Figure 6. Camparison of the values of light fluence required at 630 nm and 700 nm to achieve equal cell kill shows that irradiation at 700 nm (near the peak absorption) is about twice as effective as irradiation at 630 nm.

To study effect of light fluence at 630 nm on lymphocyte survival, the cell preparation in RPMI medium (10% calf serum) was exposed to 10 μm $DiOC_2(7)$ for 30 minutes. Subsequent irradiation at 630 nm with an irradiance of 11 mw/cm^2 was carried out. Results shown in Figure 7 show the knee in the cell survival curve arising from cellular repair.

Dark toxicity to lymphocytes at 1, 2, and 10 micromolar $DIOTC_2(7)$ was examined since other carbocyanines have been reported to inhibit mitochondrial respiration in lymphocytes (Montecucco, et. al., 1979). We evaluated dark toxicity upon 30 mm exposure to medium containing 10% fetal calf serum. Killing of lymphocytes in the absence of light ranged from 1-5% at 1 micromolar dye to 3% at 10 micromolar dye. Montecucco's experiments were done with the dye being taken up from solution containing no protein available for dye binding. Since absorption and fluorescence spectra indicate significant binding of the dye to plasma proteins significant differences in dye sequestration and dark lethality may be reflected in these experiments.

We are currently extending light dose response studies to wavelengths over the range of 650-720 nm in order to obtain the action spectrum.

References

Battle and Hewlett (1958) Cleveland Clin. Quart. 25:112-117.
Lamola, A., T. Yamane, and A. Trozzolo (1973) Science 179:1131.

Skiles, H., M. Judy and J. Newman (1985) Abstract A38, American Society of Microbiologists.
Montecucco, C., Pozzan, T., and Rink, T. (1979) Biochim. and Biophys. Acta 552:552-557.
Barak, L. and Webb, W. (1981) J. Cell Biology 90:595-604.
Tan, O. and S. Kennedy (1987) Abstract 21. Lasers in Surg. and Med. 7-73.

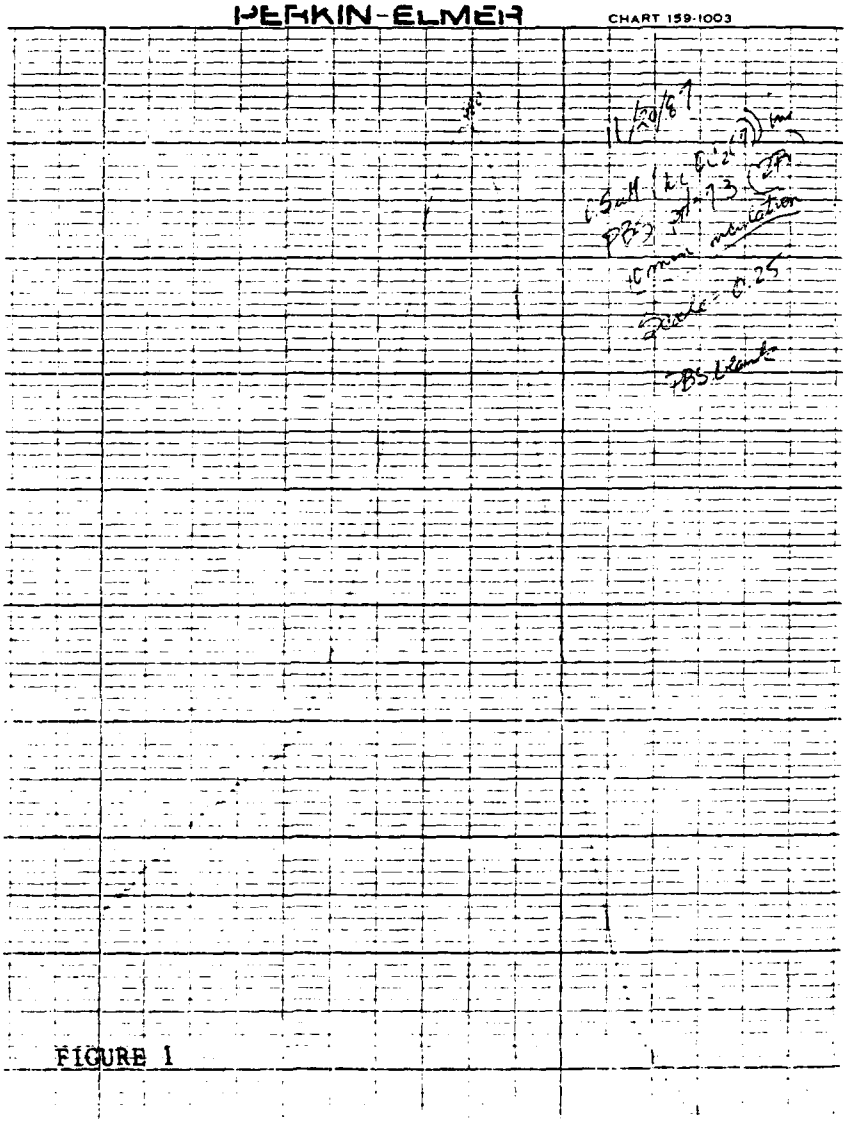

FIGURE 1

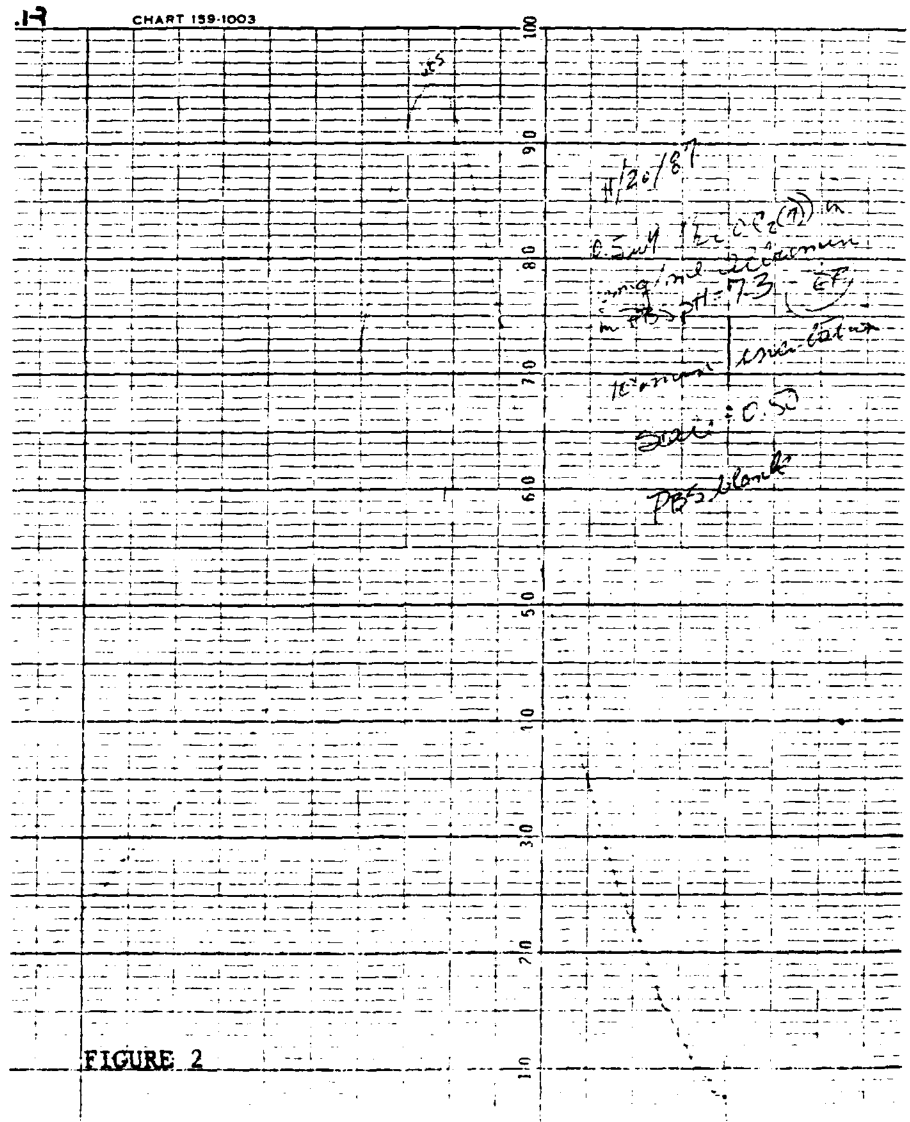

FIGURE 2

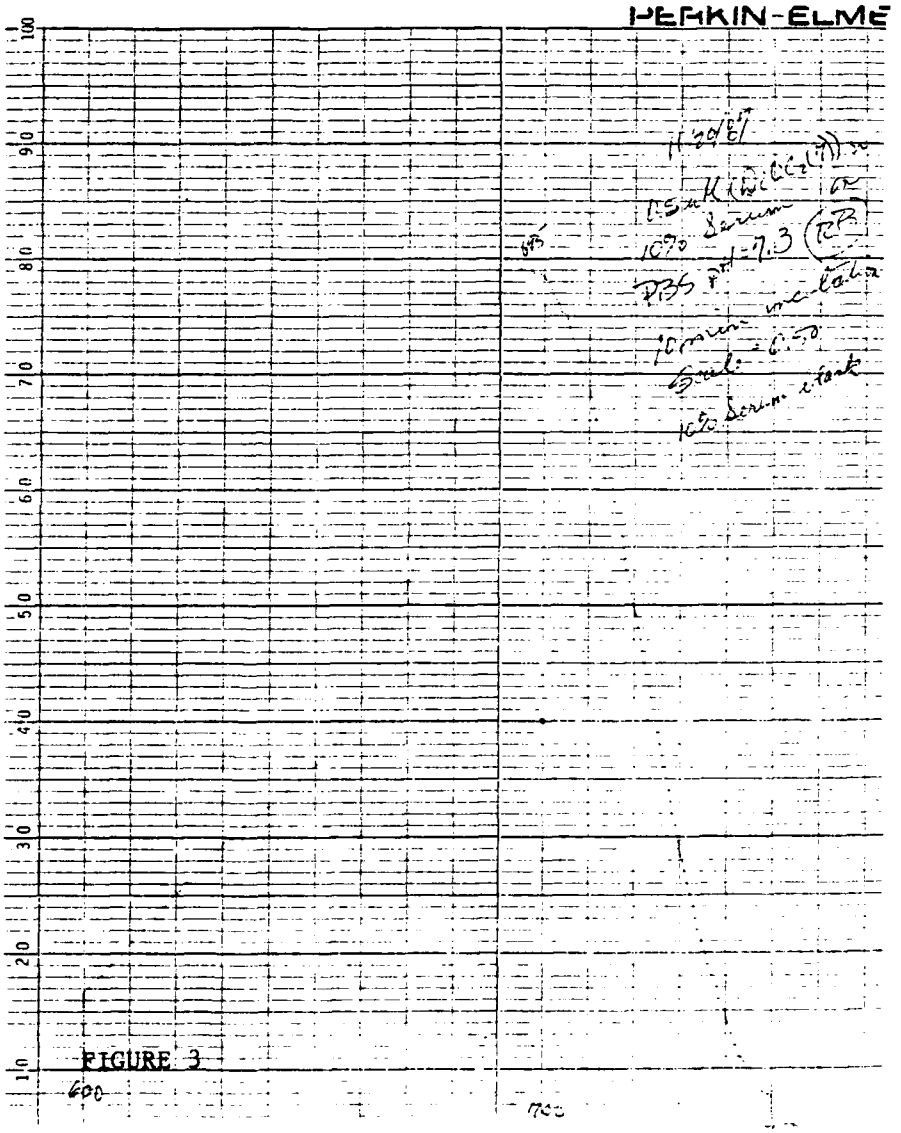

FIGURE 3

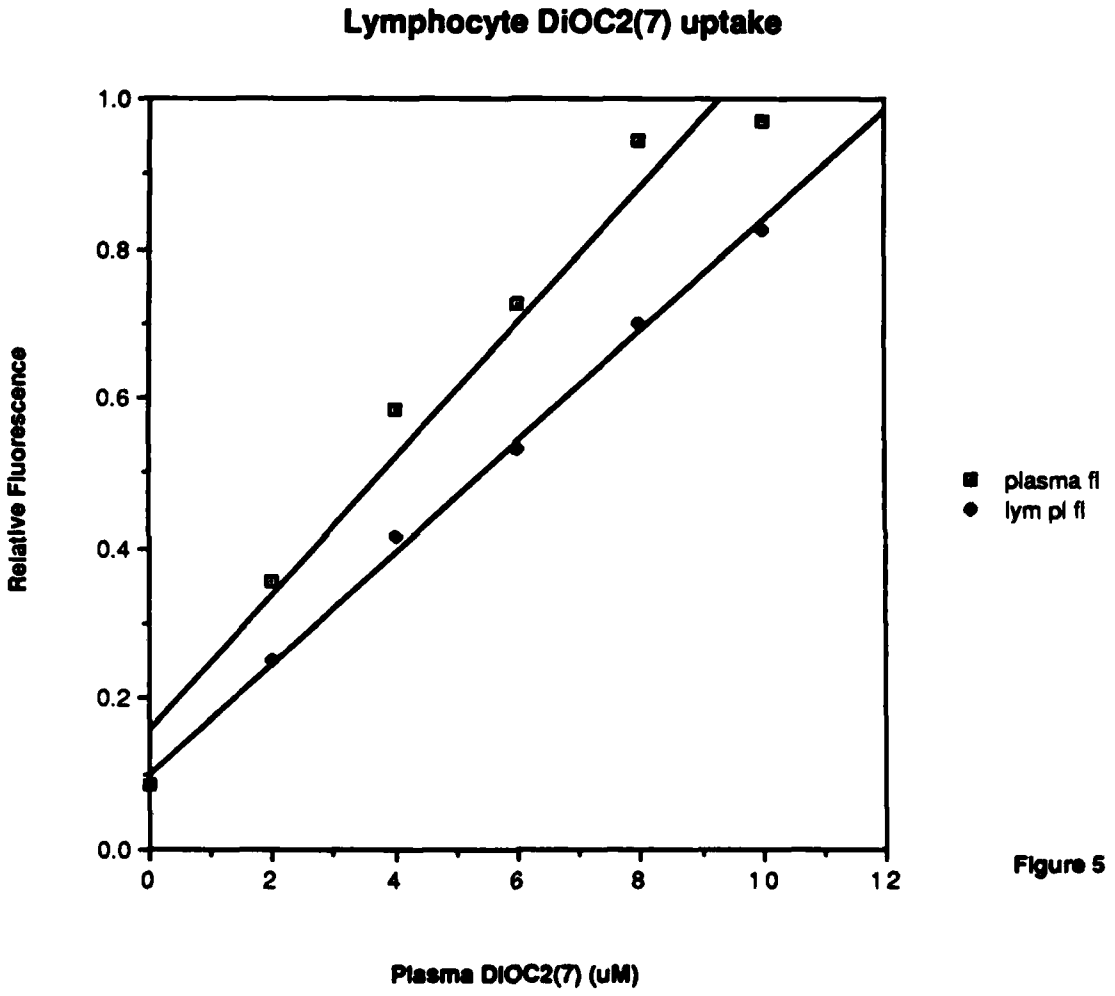
Lymphocyte DiOC2(7) uptake
Relative Fluorescence
1.0
0.8
0.6
0.4
0.2
0.0
0
2
4
6
8
10
12
Plasma DIOC2(7) (uM)
plasma fl
lym pl fl

Figure 5

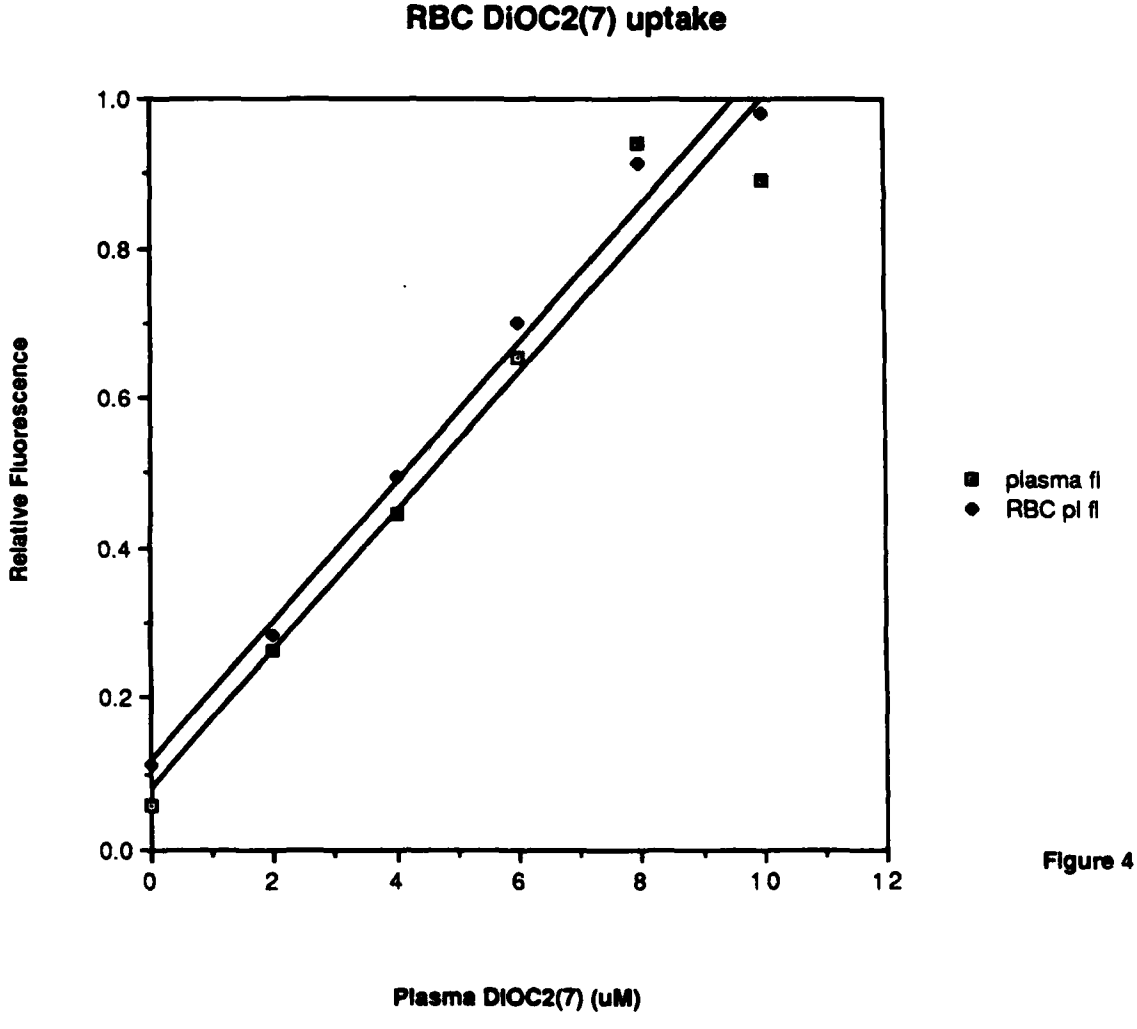
RBC DiOC2(7) uptake
Relative Fluorescence
1.0
0.8
0.6
0.4
0.2
0.0
0
2
4
6
8
10
12
Plasma DiOC2(7) (uM)
plasma fl
RBC pl fl

Figure 4

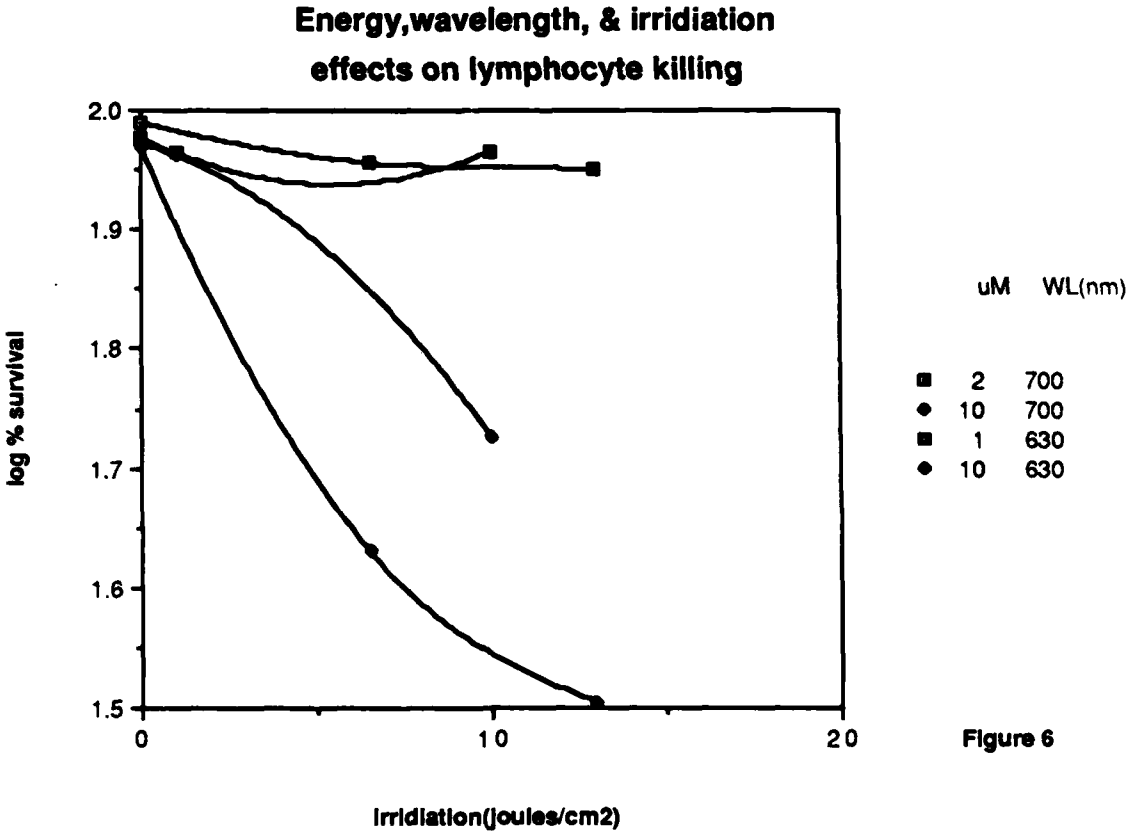
Energy,wavelength, & irridiation
effects on lymphocyte killing
2.0
1.9
1.8
1.7
1.6
1.5
log % survival
0
10
20
Irridiation(joules/cm2)
uM WL(nm)
2 700
10 700
1 630
10 630

Figure 6

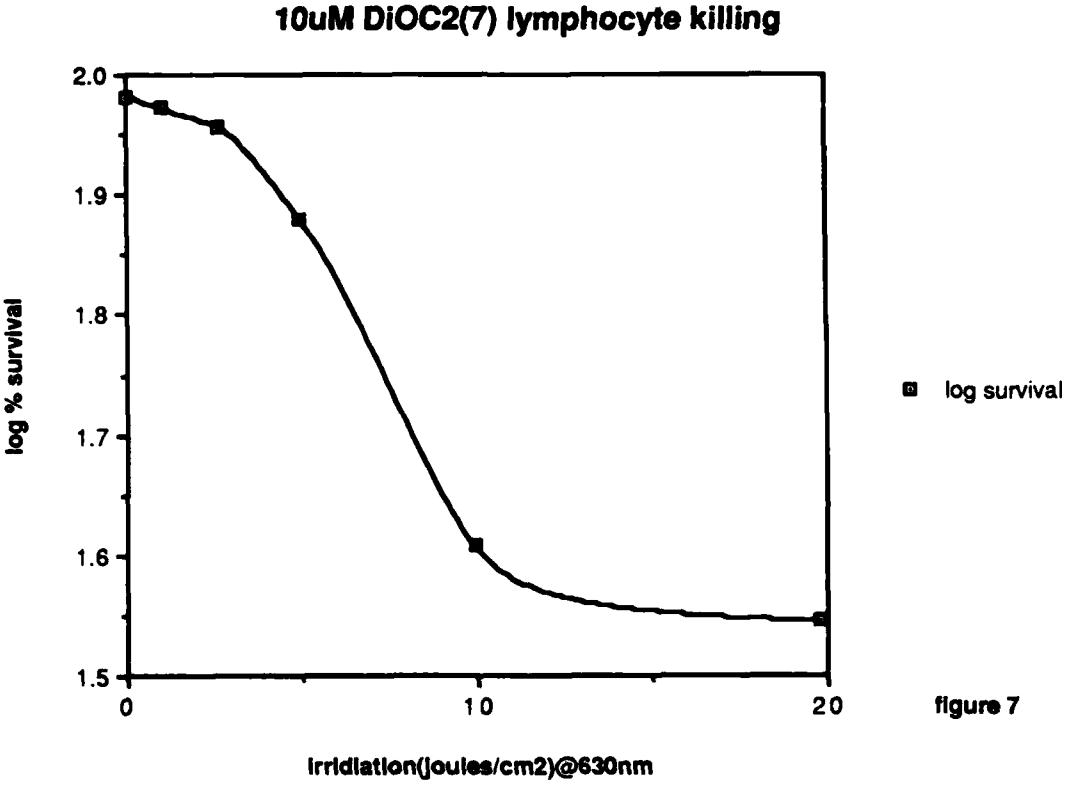
10uM DiOC2(7) lymphocyte killing
2.0
1.9
1.8
1.7
1.6
1.5
log % survival
0
10
20
Irridiation(joules/cm2)@630nm
log survival

figure 7

INTRACELLULAR PARASITE-FLUORESCENT PROBE INTERACTION

The efficacy of potentially photoactivatable and nonphotoactivatable dyes as preventive agents of infectious diseases have employed the human fibroblast cell line, CCD-27, the mouse fibroblast cell line NIH 3T3 and two human intracellular protozoan parasites Trypanosoma cruzi and Toxoplasma gondii.

The use of intracellular protozoan parasites and cell monolayers grown on flat transparent supports has two advantages in that the ability of the dye to bind to and inactivate extra and intracellular forms can be assessed. Photoactivatable dyes Photofrin II (dihematoporphyrin ether) and HEVD (hydroxyethyl vinyl deuteroporphyrin) were investigated for their affinity for intracellular forms of Trypanosoma cruzi and Toxoplasma gondii. Both dyes were take-up intracellularly by infected and non-infected cells and be specifically bound to dividing parasites.

Fluorescent microscopy showed that both infected and noninfected cells sequester dyes. When these cells were incubated with concentrations of 15 μg/ml porphyrin in tissue culture media, irradiation with 630 nm light at a power of 2 joules/cm^2 both infected and noninfected cells exhibit gross pathological changes (cytoplasmatic destruction, pyknotic nucleic). Thus it was necessary to develop strategies for the sole destruction of intracellular parasites.

After equilibration with either DHE of HEVD for 24 hours fluorescence emission and excitation measurements were made on intact T. cruzi suspended in D-PBS after washing. For both porphyrins fluorescence emission and excitation maxima were located at 634 and 412 nm respectively. Shifts of these peaks were observed in our laboratory from their values of 617 and 397 nm in aqueous medium upon binding with liposomes, erythrocytes and lymphocytes. The observed large red shift probably reflects binding of the porphyrins in a lipid environment within the trypanosome.

Chloroquine diphosphate was selected for *in vitro* tissue culture porphyrin activation studies due to reports of other investigators and equilibrium dialysis investigations that indicate chloroquine diphosphate induces monomerization of porphyrin aggregates. Monomeric porphyrins are more toxic than aggregates. Results of these studies were unpredictable. Studies to determine why some failures resulted suggested that the porphyrins would aggregate when bound to the intracellular, amastigote forms. This aggregation may be due to localized charge differences, i.e. pH between the parasite and the cytosol.

Methodology of Trypanosome Studies

Trypomastigotes were isolated from peripheral blood of Trypanosoma cruzi-Telahuen strain infected Rockland-Wistar mice. Trypomastigotes were purified from peripheral blood by gradient centrifugation at 500 X g for 30 min at room temperature utilizing LSM (Litton/Bionetics, Kensington, MD). Trypomastigotes were aseptically harvested from the blood/LSM interface, washed 3 X with Dulbecco-PBS (D-PBS), without calcium or magnesium, and added to sub-confluent 25 cm^2 culture flasks of NIH 3T3 and CCD-27 cells for amastigote and trypomastigote cultivation. Cells were maintained in Opti-MEM (Gibco/BRL, Gaithensburg, MD) containing 4 percent Fetal Bovine Serum (FBS) and antibiotics (100 U penicillin 100 μg streptomycin/ml). Cells to be used for microscopic

studies were cultured in 12 well cluster dishes containing 18 mm diameter No. 1 cover slips.

Cell cultures infected with the parasite were exposed to 15 μg/ml dihematoporphyrin ether (DHE) (Photomedica, Inc. Raritan, NJ)) and 2,4 (4,2)-hydroxyethyl vinyl deutoporphyrin (HEVD) (Porphyrin Products, Logan, UT) respectively in complete Opti-MEM. Other groups were not treated with the porphyrins and were designated negative controls. Infected cells were viewed and photographed with the aid of an Olympus Vanox-AHT microscope utilizing transmitted light and 400 nm excitation and 570 nm barrier filters for epifluorescence dye localization.

Cultures of 48 hrs. post-porphyrin labeled infected and non-infected cells were irradiated with 630 nm light at an energy density of 2 joules/cm^2 to determine direct photoactivatable damage. Chloroquine diphosphate (Sigma Chemical Co., St. Louis, MO.) was added to achieve a final concentration of 7.75 μM in culture media to ameliorate photoirradiation damage of the non-infected cells that had minimal porphyrin uptake, as well as elicit parasite inactivation. Porphyrin labeled and unlabeled infected cells were exposed to 7.75 μM chloroquine diphosphate for 24 hrs. In order to assess inactivation following chloroquine diphosphate exposure, culture medium containing extracellular forms (trypomastigotes and spheromastigotes) were collected, washed 3X with complete culture media, resuspended to its original volume and added to non-infected cells. Cover slips from treated cultures were fixed in 100 percent methanol and tinctured with Giemsa stain. Infected and non-infected cells were observed microscopically for chloroquine or porphyrin toxicity. The inactivation of the treated and non-treated extracellular trypanosomes was assayed by introducing these culture supernates into virgin cell cultures. Cover slips were treated as described previously and inactivation was assayed by determining the presence or absence of intracellular development in 200 host cells.

Chloroquine/porphyrin interaction was determined by investigating the binding of ^{14}C-chloroquine diphosphate (sp act 2.62 mCi/mMole) (Amersham, Arlington Heights, ILL) to intra- and extracellular porphyrin labeled and unlabeled T. cruzi at a concentration of 7.75 μM. Intracellular binding studies utilized triplicate confluent, 50 percent infected NIH 3T3 cells on 18 mm diameter coverslips. Cultures were prelabeled for 24 hr with 15 μg/ml DHE and HEVD respectively. Additional infected NIH 3T3 cells time-matched sham triplicates were maintained for chloroquine binding in the absence of porphyrin and background and chemiluminescence determinations. Triplicates consisted of nonporphyrin/nonchloroquine treated, nonporphyrin/chloroquine treated, and porphyrin/chloroquine treated cultures. After exposure of appropriate cultures to chloroquine for 24 hr., all triplicates were washed 3X with D-PBS, coverslips removed, air dried and placed in scintillation vials containing 10 ml of counting fluid (125 g napthalene, 7.5 g PPO, 0.377g POPOP to 1L with scintillation grade p-dioxane) and counted in a Tracor Mark III (Chicago, ILL) scintillation counter.

The binding of chloroquine to extracellular predominately trypomatsigotes was determined from porphyrin labeled and nonlabeled triplicate confluent NIH 3T3 infected cells after parasitemia reached 80 percent. When this parasitemia was attained monolayers were washed 3X with D-PBS. To one triplicate, ^{14}C-chloroquine diphosphate was added to 7.75 μM in culture medium. Identical triplicates were incubated with 15 μg/ml DHE and HEVD in culture medium. After 24 hr, extracellular *T. cruzi* were harvested from tissue culture media by pelleting at 1000 X g for 3 min. Sloughed NIH 3T3 cells and porphyrin aggregates were removed by overlaying the resuspended pellet on a 1:1 dilution of LSM in culture medium and centrifuged at 500 X g for 40 min. The interface was collected and washed 3 X with culture medium. Extracellular forms were then filtered through a 0.22 μ

nylon Acrodisc (Gelman, Sciences, Ann Arbor, MI) and the filter counted as previoulsy described. ^{14}C-chloroquine binding at 0,1,2,4,8, and 24 hrs. after the addition of 7.75 μm ^{14}C-chloroquine diphosphate to extracellular parasites was determined. The percent radionucleotide bound of the total available ^{14}C-chloroquine diphosphate was determined for each time point by filtration through a 0.22 μ nylon Acrodisc and counting both the membrane and the filtrate.

Table 1.

Inactivation of Trypanosome Infectability by Porphyrins, following 7.75 μM Chloroquine Diphosphate Addition.

Percent reduction in number of Infected NIH 3T3 cells.

Chloroquine Diphosphate	12%
HEVD-Chloroquine diphosphate	42%
DHE-Chloroquine diphosphate	50%

Table 2.

Incorporation of ^{14}C-Chloroquine Diphosphate by Trypanosoma cruzi Telahuen strain infected NIH 3T3 cells.

	Picomoles Incorporated	Percent Increase
^{14}C-Chloroquine Diphosphate	138	--
DHE-^{14}C-Chloroquine Diphosphate	167	21
HEVD-^{14}C-Chloroquine Diphosphate	497	260

Table 3.

Percent of Binding of ^{14}C-Chloroquine diphosphate to extracellular Trypanosoma cruzi-Telahuen strain forms after 24 h exposure to porphyrin.

Time	HEVD-^{14}C-Chloroquine Diphosphate	DHE-^{14}C-Chloroquine Diphosphate
0	49.8	3.5
1	54.2	47.9
2	47.9	52.2
4	42.5	39.8
8	40.7	43.5
24	24.1	17.8

Two fluorescent probes (rhodamine 123 and 3, 3'-dihexyloxacarbocyanine iodide) were employed to investigate parasite membrane potentials and organellar structure. Serendipidously, both of these fluorgenic compounds were found to be highly toxic to intracellular trypanosomes and also be taken up by them under in vitro conditions. These compounds did not appear to be toxic to either mammalian cell cultures or white mice. These dyes are currently being studied to maximize their effeciency for parasite destruction and prophylaxis of infection.

Fluroescence and Phosphorescence Spectroscopic
Studies of Thin Filament Proteins

Introduction

Movement is a ubiquitous feature of all living systems. Cell motility is essential for all types of cellular activities and vital for the survival of all organisms. Two important areas which involved intricate interaction of contractile proteins have been, for a long time, research subjects in our laboratory, e.g. see Lin and Dowben (1983a and 1983b). Specifically, we are interested in (1) the elucidation of muscle contraction mechanism and (2) the regulatory mechanism of heart contractility.

In our laboratory, fluorescence techniques (Lin, 1982; Lin and Dowben, 1982; Dowben and Lin, 1987) have been used to monitor various physical and chemical properties associated with the muscle contractile proteins. The overall objective of this project is to provide, at the molecular level, information bearing on the mechanism of contraction in cardiac and skeletal muscles.

While fluorescence probes typically provide information on events taken place in few picoseconds to several hundred nanoseconds, the phosphorescence probes, on the other hand, afford study on physical chemical events occurring in few microseconds to several hundred milliseconds and beyond. Dual fluorescence-phosphorescence probes are readily available in pure forms. We have been interested in exploring the usefulness of these probes in a variety of time-resolved techniques for extracting information regarding the hydrodynamic properties of muscle thin and thick filaments. The present communication is focusing on the thin filament proteins while the thick filament protein which has also been studied using similar probes and techniques is reported in a separate communication by VanderMeulen et.al.

Unique Features of FEL Associated with This Project

Conventional pulsed lasers have been traditionally used in all previous studies in fluorescence anisotropy decay experiments. Although ion and gas lasers are much easier to operate and many different types are readily available, they are more limited in tunability. The advantage of using FEL as the pulsed light source for our experiments is the identical pulse shape and profile the FEL provides at all wavelengths. This benefit is critical for the dual wavelength requirement of the eosin phosphorescence experiments.

Collaboration with the Photon Research Laboratory (Prof. John Madey, FEL Program Director) at Stanford University

In collaboration with the Stanford FEL scientists, we made plans to conduct studies on the flexibility of myosin and actin filaments labeled with dual fluorescence and phosphorescence probes, eosin and erythrosin using the unique set-up at Dr. Madey's laboratory.

We made our first site visit to Stanford Photon Research Laboratory and met the scientists and administrators in early October. They demonstrated successfully their prototype Mark III free electron laser which outputs 2 to 10 micron infrared laser with an impressive 5 megawatt power (ca. 500mJ per pulse) with pulse width of about 2 to 4 microsecond per macropulse. We made plans to make use of the higher harmonic laser line at ca. 500 nm wavelength for our phosphorescence anisotropy decay studies of various contractile

Our second visit to Stanford took place in Mid-November. The main purpose of this trip was to investigate the feasibility of using the Stanford FEL for the various phosphorescence anisotropy experiments we proposed previously with eosin and erythrosin B labeled actin, trypomyosin, and myosin. Prior to the trip, we had made drill runs in our site using Molectron nitrogen laser as the light source and made certain that everything was working properly.

We took these labeled proteins and our anisotropy decay apparatus and spent three days doing experiments in Stanford University FEL laboratory (November 17-20). We attempted the use of the high harmonic FEL visible output at 520 to 530 nm as a pulse light source for phosphorescence anisotropy decay experiments.

The Stanford scientists were very cordial and cooperative, and generously allotted to us three day shifts for our experiments. We successfully set up our equipments after overcoming some minor computer hardware problems due to shipment abuse.

The Stanford FEL lased beautifully in the infrared with the principal lasing wavelength around 3.62 micron. We selected the seventh harmonic, at 517 nm (3.62 μm/7), with narrow bandpass filter and tried a couple of labeled samples which we were sure worked while in Dallas. Although we could see the visible green laser, the intensity was not strong enough to give us adequate signals for performing phosphorescence experiments (although the laser intensity was adequate for fluorescence decay experiments). Dr. Steve Benson, the chief FEL operator, after learning our problem, was kind enough to take the trouble of changing the lasing fundamentals and tried different high harmonics, the fifth and sixth, giving 525 and 530 nm output. However, the intensity was still below the threshold for conducting any real phosphorescence experiments.

Overall, we didn't quite accomplish what we had hoped for in the second trip, but we gained some first hands-on experience which was essential for us to get into the next stage.

We have good reason to believe that the FEL can now be operated in a slightly different configuration that may provide a better green visible output. Dr. Steve Benson is working on making the third-harmonic (around 1.02 to 1.06 micron wavelength) lase and had some success. We plan to frequency double it to 520 to 530 nm using a KDP crystal.

Experimental Procedures

Thin filament proteins actin and tropomyosin, isolated from rabbit skeletal muscle, were prepared following procedures developed in our laboratory over the years. Actin is prepared from acetone powder using the method of Spudich and Watts (1971). Tropomyosin was isolated based on methods of Ebashi et al (1968), Hartshorne and Mueller (1969). Tropomyosin was purified, free of troponin, by using hydroxyapatite chromatography based on the method of Eisenberg and Kiely (1974).

Actin and tropomyosin were covalently labeled with three dual fluorescence/ phosphorescence probes --- eosin maleide, eosin iodoacetic acid, and erythrosin B iodoacetic acid. The probes were dissolved as high concentration stock solution (about 8 mM) in dimethylforamide-glycerol and kept frozen at -20°C. Small aliquots of dye solution were added to protein solutions and let react for one hour. The reaction was stopped with the addition of mercaptoethanol. To remove the dye unreacted to the protein, the

(Beckman Instrument Inc., Fullerton, California) to assure complete removal of unconjugated dye.

These probes react specifically only to the free sulfhydryls in proteins at pH 8.4. Previous studies (Lin, 1978) suggest that these probes linked to actin at cys-374 residue while in tropomyosin they atacted to cys-190 residue.

Results and Discussion

The fluorescence and phosphorescence spectral properties were characterized under a variety of conditions. The spectral properties investigated include steady state excitation and emission spectra, and fluorescence polarization spectra. The fluorescence excitation and emission spectra for the various protein adducts are shown in Figures 1-6. The excitation spectra agree with the absorption spectra (data not shown) as expected. The essential spectral features for the various labeled adducts are summarized in Table 1.

The labeled adducts all show similar spectral features since the fluorescence properties of eosin and erythrosin are mainly derived from the fluorescein skeleton structure (eosin is a tetrabromo of fluorescein while erythrosin is a tetraiodo derivative). However, minor differences do exist among the nine different labeled adducts shown in Table 1. N-acetyl cysteine adducts in general has emission maximum more in the blue region, in consistence with the notion that the fluorophore is exposed to the hydrophylic solvent environment. Also noticible is the difference in the UV excitation peak between the actin and tropomyosin adducts, in actin the peak appears around 305 nm whereas it appears near 256 nm in tropomyosin with twice the fluorescence intensity.

The phosphorescence decay kinetics were investigated using a pulsed nitrogen laser (Molectron Model UV1000, 1 megawatts @ 10 Hz., 10 ns pulse width) and a transient digitized oscilloscope (LeCroy Model 9400, 125 MHz random interleaved sampling rate). The instrument set-up is the same as that used in the experiments of VanderMeulen et al. (see Figure 9 of the report by VanderMeulen et al.)

The real time phosphorescence decay curves were analyzed by a curve-fitting technique using Asyst PC program (MacMillan Software) on an IBM AT PC. The phosphorescence decay curves were best characterized by a two-exponential fit. Typical decay curves are shown in Figures 1-12. The experimental data are shown as dots, the solid curves are the fitted curves using the exponential parameters listed in Table 2. The decay constants for erythrosin B iodoacetic acid labeled actin and eosin iodoacetic acid labeled N-acetyl cysteine and tropomyosin are summarized in Table 2.

An interesting and useful technique we have tried was to deoxygenate the labeled adducts with an enzyme oxygen scavenger. This technique was originally developed by Horie and Vanderkooi (1981). Glucose oxidase and substrate glucose were added to the sample, the enzyme reaction converted oxygen into hydrogen peroxide. The latter was converted to water by the addition of catalase. This scavenger system worked pretty well as evident by the data shown in Table 2. Oxygen is a well known fluorescence and phosphorescence quencher, in its presence the lifetime of eosin labeled proteins is much shorter. Thus, in undegassed samples, labeled N-acetylcysteine, actin and tropomyosin show short phosphorescence lifetimes, (two components) about 3.8 μs and 15 to 39 μs. In the presence of oxidase-catalase scavenger system, the deoxygenated samples show increased

The oxygen concentration dependent phosphorescence lifetime provides an effective and precise means for controlling the eosin and erythrosin probes such that they fall into the same time domain as that of the specific molecular motions of proteins or macromolecules being investigated.

Another interesting fluorescence property associated with the eosin and erythrosin probes, first observed by VanderMeulen et al (1988) in our laboratory, is the wavelength dependency of the polarization. The polarization excitation spectra for the various probes are shown in Figures 14-15. The maxima and minima polarization values for the various kinds of labeled proteins and N-acetylcysteine adducts are summarized in Table 3. As expected from the theory, the small cysteine adduct molecule has negligible polarization values and independent of excitation wavelength.

As explained in more details in the report of VanderMuelen et al, the importance of wavelength dependency of eosin fluorescence and phosphorescence is that it provides two independent means of probing the molecular motions of thin and thick filaments along two different axes. Our study is the first attempt in examining the hydrodynamic properties and flexibility of muscle filaments using dual wavelength approach. By constructing a molecular model in which various dimensions and shapes of the myosin or actin molecule are assumed, one can simulate the anisotropy decay curves predicted by the various models and compare then with the experimental data.

Conclusions and Future Planned Experiments

In summary, the present study is our first attempt to investigate the usefulness of eosin and erythrosin fluorescence-phosphorescence dual probes for investigating the various physical chemical properties of thin filament contractile proteins. From the data obtained so far, these probes seem to be ideal for what we planned for the project. Furthermore, we have also achieved an effective technique of conditioning phosphorescent lifetimes such that experiments can be targeted to perform in different time domains, e.g. from a few microseconds to a few hundred microseconds. Our next goal is to modify our instrument to incorporate polarizers and set the stage for fluorescence and phosphorescence anisotropy decay experiments.

References

Dowben, R.M. amd Lin T-I. 1983. In: Muscle and Cell Motility. (R.M. Dowben and J. Shay eds.), vol. IV. p. 179-206, Plenum, New York.

Dowben, R.M. and Lin, G. 1987. SPIE Proceedings 743:123-126.

Ebashi, S., Kodama, A., and Ebashi, F. 1968. J. Biochem. 64:465.

Eisenberg, E., and Keilley, W.W. 1974. J. Biol. Chem. 249:4742.

Hartshorne, D.J. and Mueller, H. 1969. Biochim. Biophys. Acta 175:301.

Horie and Vanderkooi. 1981.

Lin, T-I. and Dowben, R.M. 1983a. J. Biol. Chem. 258:5142.

Lin, T-I. and Dowben, R.M. 1983b. In: Excited States of Biopolymers. R.F. Stein ed., Chapter 3, p. 59-115. Plenum, New York.

Spudich, J. and Watt, S. 1971. J. Biol. Chem. 246:4866.

VanderMeulen, D.L., Nealon, D.G. and Jameson, D. 1988. Biophys. J. 53, 87.

Table 1. Fluorescence Excitation and Emission Spectral Characteristics for the Various Labeled Adducts

Sample	Excitation nm	Spectral Extrema Ratio	Emission nm
EryIaa-Tm	525	1.00	545
	493	0.39	
	346	0.066	
	306	0.136	
	256	0.205	
EosIaa-Tm	518	1.00	542
	486	0.34	
	346	0.05	
	301	0.097	
	253	0.219	
EosMal-Tm	526	1.00	545
	494	0.33	
	346	0.056	
	308	0.11	
	256	0.21	
EryIaa-Actin	528	1.00	542
	492	0.36	
	346	0.081	
	310	0.094	
EosIaa-Actin	520	1.00	542
	484	0.35	
	344	0.10	
	302	0.15	
EosMal-Actin	520	1.00	540
	486	0.35	
	346	0.072	
	300	0.132	
EryIaa-NaC	518	1.00	534
	486	0.35	
	302	0.13	
	254	0.18	
EodIaa-NaC	526	1.00	540
	491	0.32	
	311	0.076	
	257	0.14	
EosMal-NaC	518	1.00	539
	486	0.34	
	302	0.099	
	255	0.19	

EryIaa: Erythrosin Iodoacetic Acid. EosIaa: Eosin Iodoacetic Acid. EosMal: Eosin Maleimide. Tm: Tropomyosin. NaC: N-Acetyl Cysteine

Table 2. Phosphorescence Decay Lifetimes of Various Eosin and Erythrosin Labeled Adducts

Sample	τ_1	F_1	τ_1	F_1
EryIaa-Actin	3.69	0.13	38.3	0.87
EosIaa-NaC	3.78	0.36	23.5	0.64
EosIaa-NaC -O_2, 20 min.	5.11	0.09	75.1	0.91
EosIaa-NaC -O_2, 2 hr.	9.5	0.08	330.0	0.92
EosIaa-Tm	2.89	0.29	15.1	0.71
EosIaa-Tm -O_2, 20 min.	4.37	0.03	99.6	0.97
EosIaa-Tm -O_2, 1 hr.	6.53	0.03	131.1	0.97
EosIaa-Tm -O_2, 2 hr.	11.40	0.12	202.1	0.88

EryIaa: Erythrosin Iodoacetic Acid
EosIaa: Eosin Iodoacetic Acid
Tm: Tropomyosin
NaC: N-Acetyl Cysteine
-O_2: Deoxygenated samples were obtained by incubating the sample with an oxygen scavenger system consisting of 0.07 mg/ml glucose oxidase, 0.012 mg/ml catalase, and 0.3% glucose for the specified time.

Table 3. Fluorescence Polarization Characteristics of Labeled Tropomyosin and Actin

Sample	Wavelength nm	Polarization
EryIaa-Tm	492	0.295
	354	- 0.109
	304	- 0.114
EosIaa-Tm	488	0.376
	366	- 0.072
	316	- 0.105
EosMal-Tm	494	0.303
	356	- 0.104
	304	- 0.112
EryIaa-Actin	484	0.209
	366	- 0.018
	316	- 0.036
EosIaa-Actin	472	0.085
	366	- 0.026
	302	- 0.037
EosMal-Actin	466	0.082
	350	- 0.032
	304	- 0.034

EryIaa: Erythrosin B Iodoacetic Acid
EosIaa: Eosin Iodoacetic Acid
EosMal: Eosin Maleimide
Tm: Tropomyosin

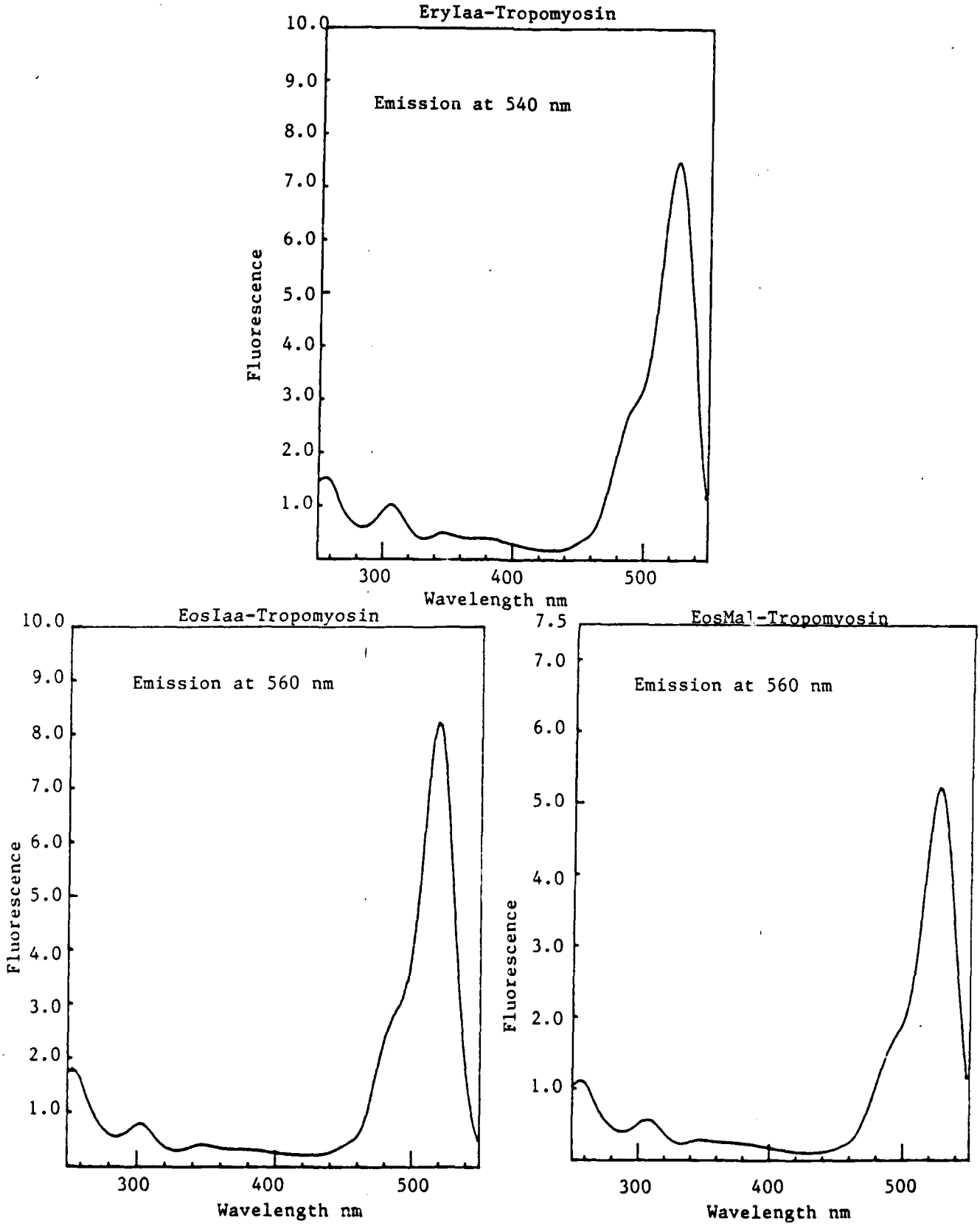

Figure 1. Fluorescence Excitation Spectra of Labeled Tropomyosin Adducts

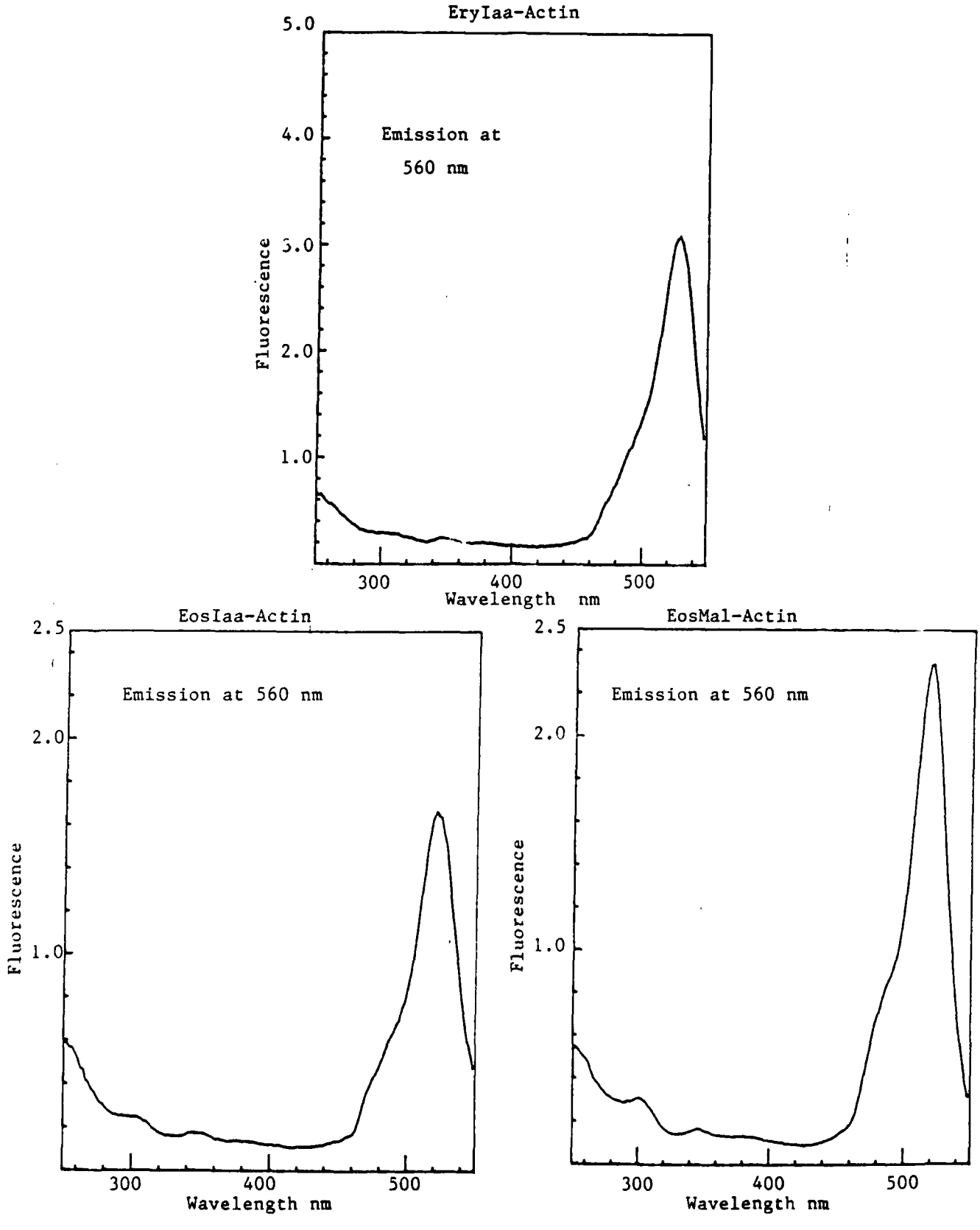

Figure 2. Fluorescence Excitation Spectra of Labeled Actin Adducts

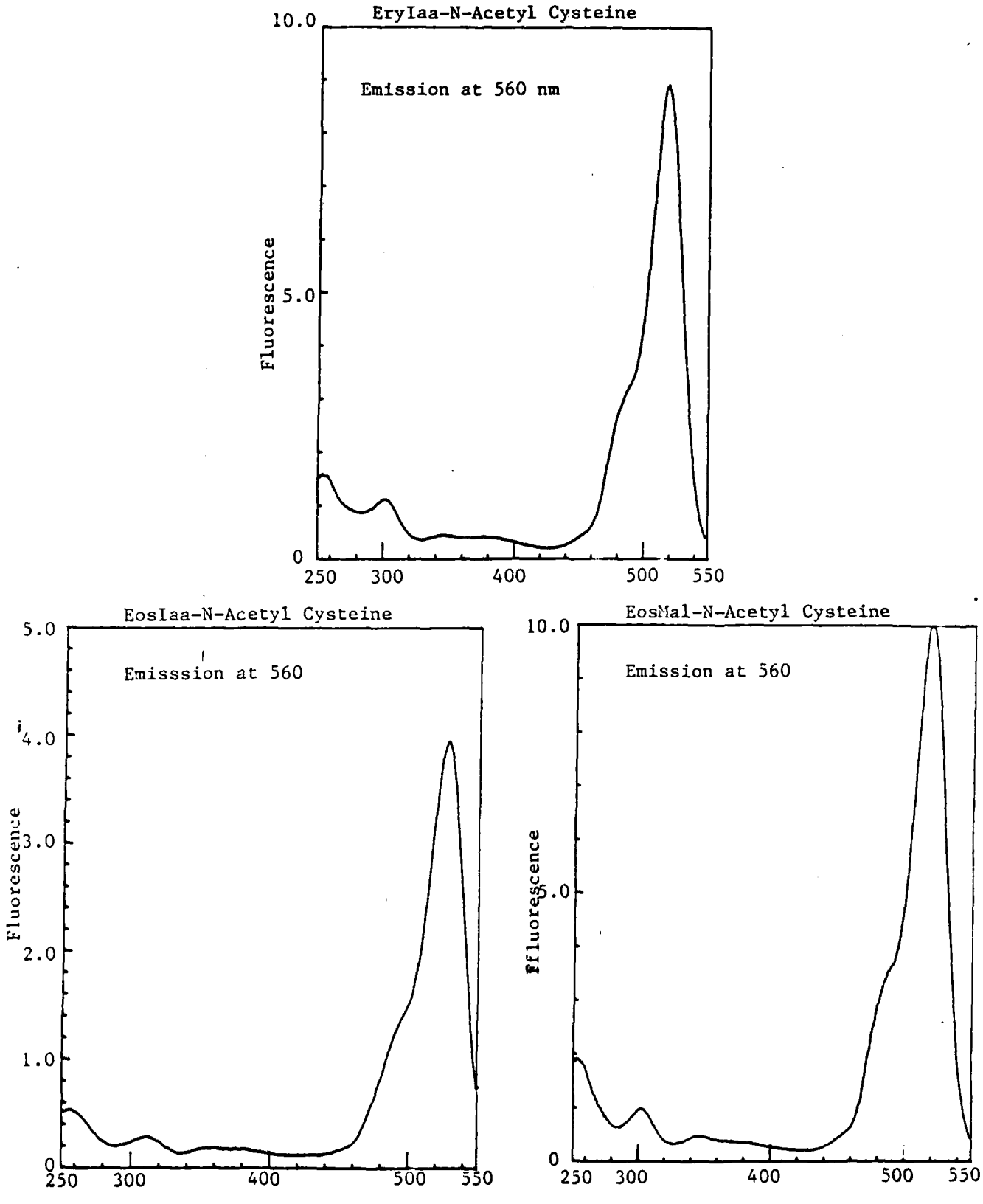

Figure 3. Fluorescence Excitation Spectra of Labeled N-acetyl cysteine Adducts

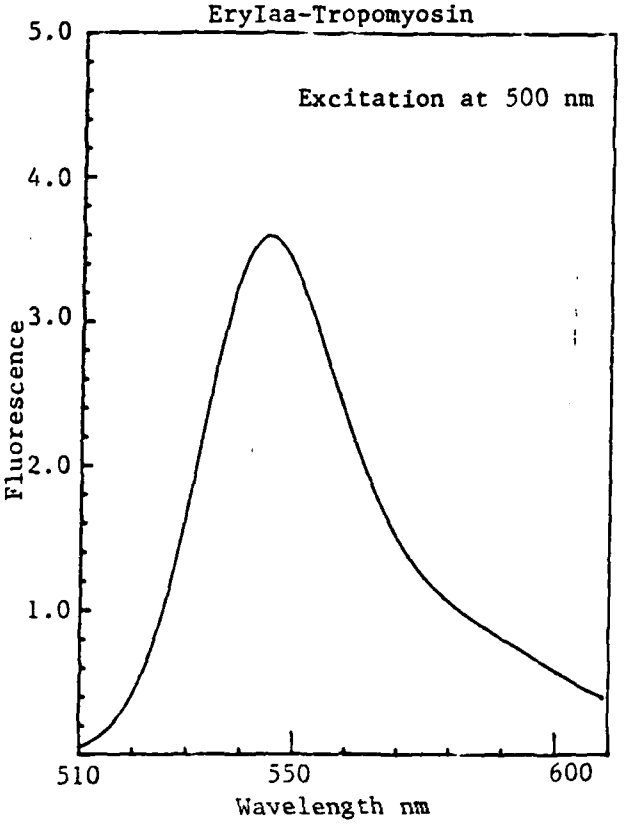
EryIaa-Tropomyosin
Excitation at 500 nm
5.0
4.0
3.0
2.0
1.0
Fluorescence
510
550
600
Wavelength nm

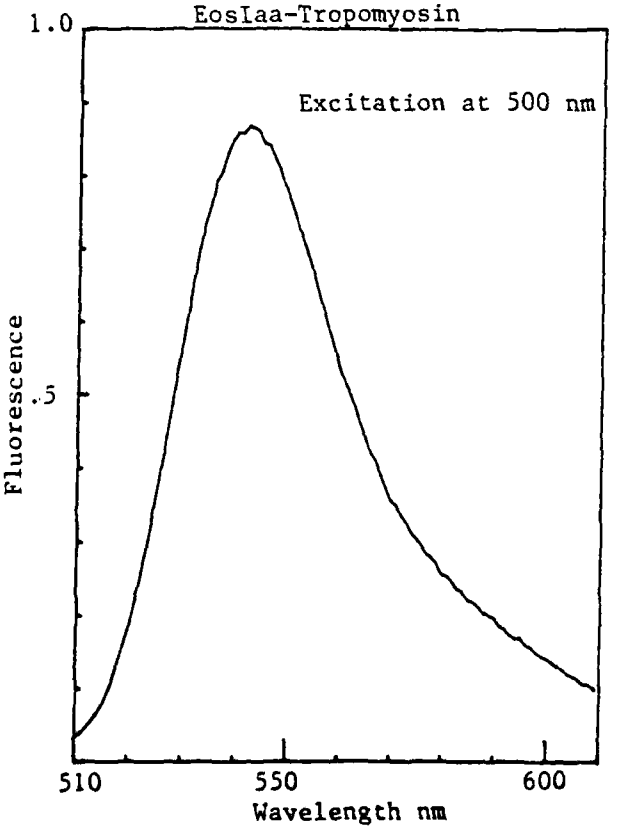
EosIaa-Tropomyosin
Excitation at 500 nm
1.0
.5
Fluorescence
510
550
600
Wavelength nm

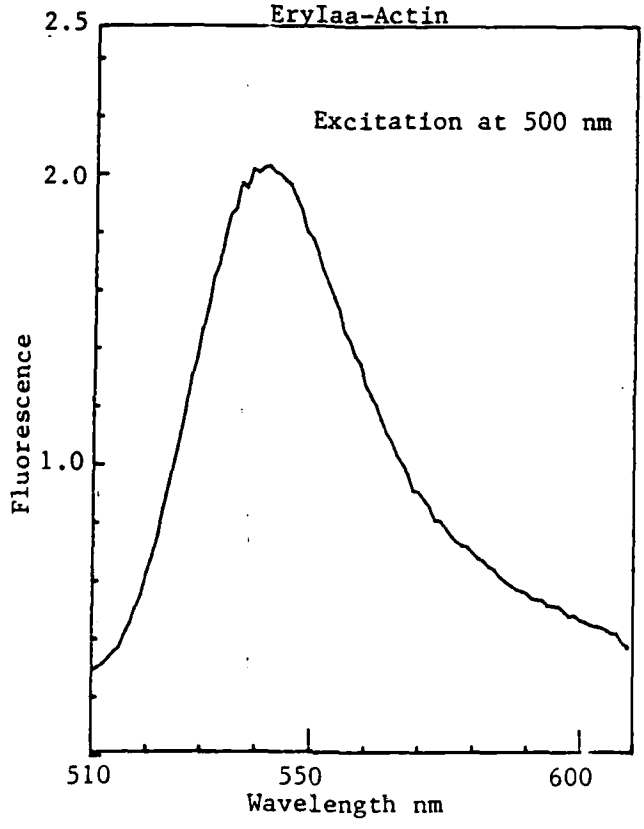
EryIaa-Actin
Excitation at 500 nm
2.5
2.0
1.0
Fluorescence
510
550
600
Wavelength nm

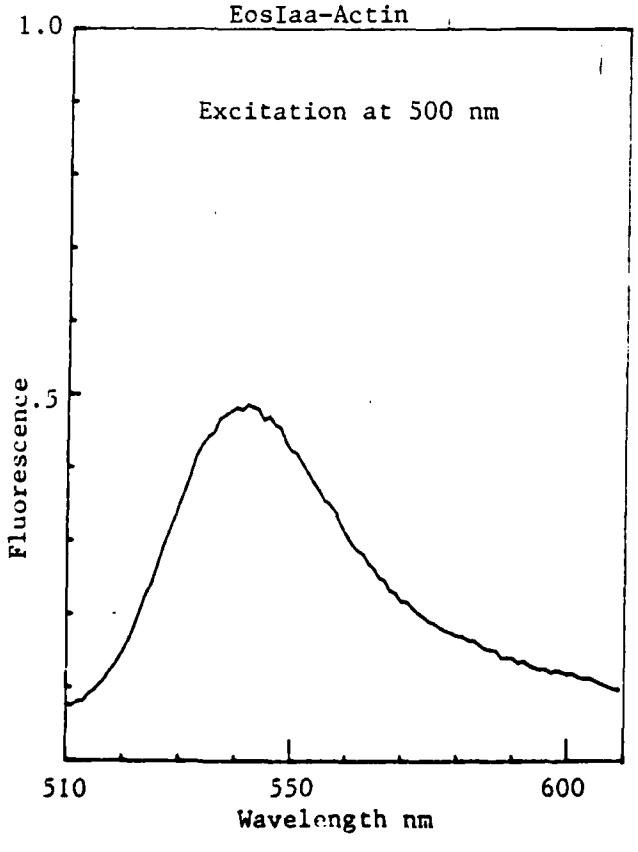
EosIaa-Actin
Excitation at 500 nm
1.0
.5
Fluorescence
510
550
600
Wavelength nm

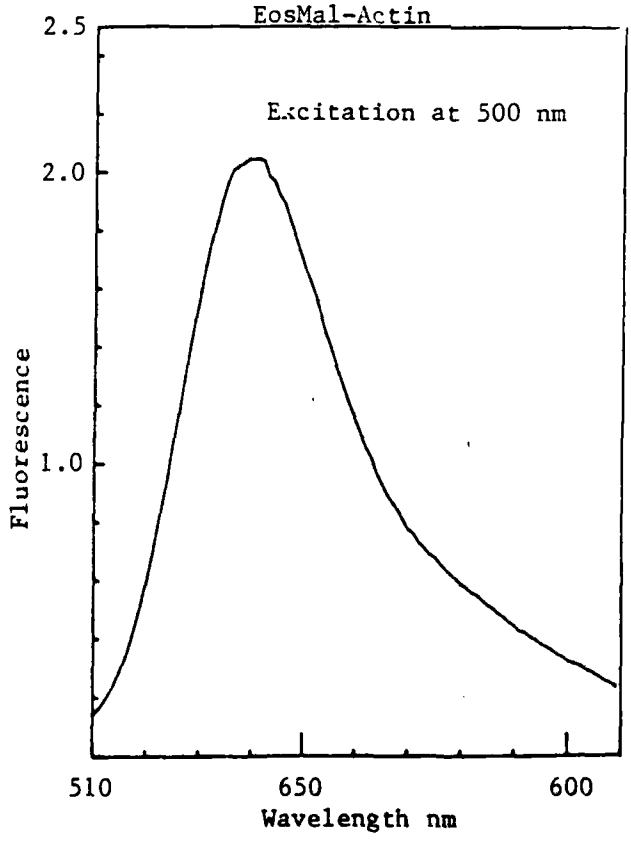
EosMal-Actin
Excitation at 500 nm
2.5
2.0
1.0
Fluorescence
510
650
600
Wavelength nm

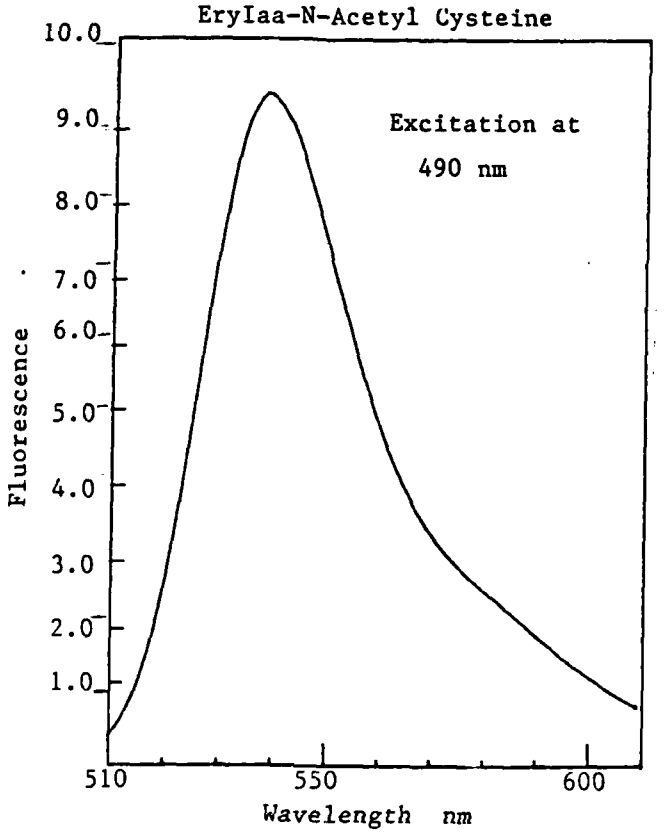
EryIaa-N-Acetyl Cysteine
Excitation at
490 nm
Fluorescence
10.0
9.0
8.0
7.0
6.0
5.0
4.0
3.0
2.0
1.0
510
550
600
Wavelength nm

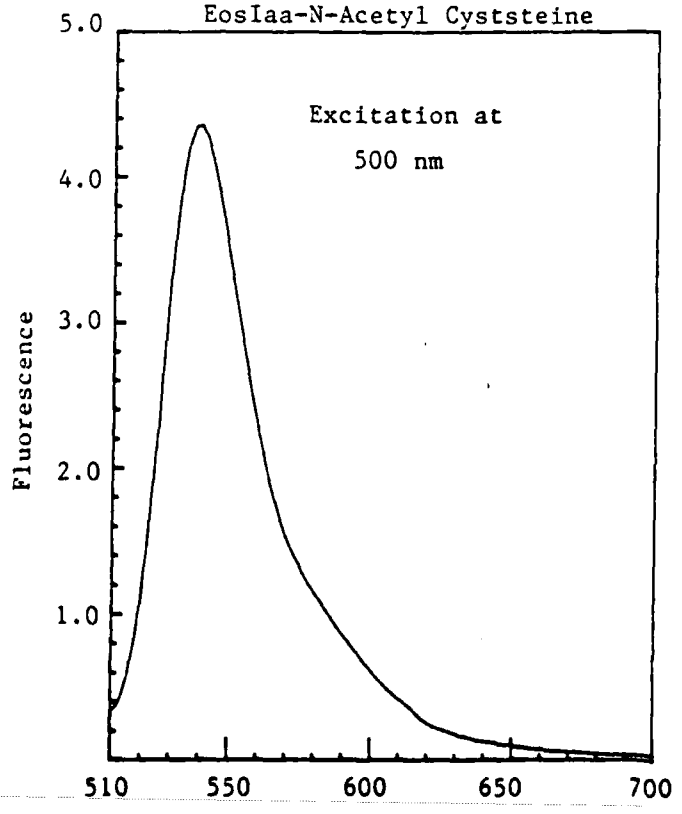
EosIaa-N-Acetyl Cyststeine
Excitation at
500 nm
Fluorescence
5.0
4.0
3.0
2.0
1.0
510
550
600
650
700

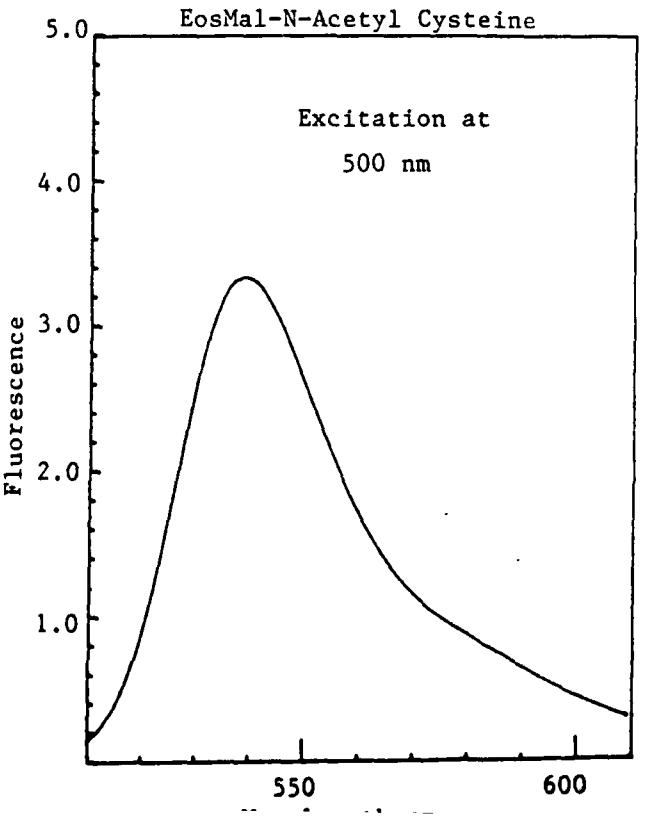
EosMal-N-Acetyl Cysteine
Excitation at
500 nm
Fluorescence
5.0
4.0
3.0
2.0
1.0
550
600

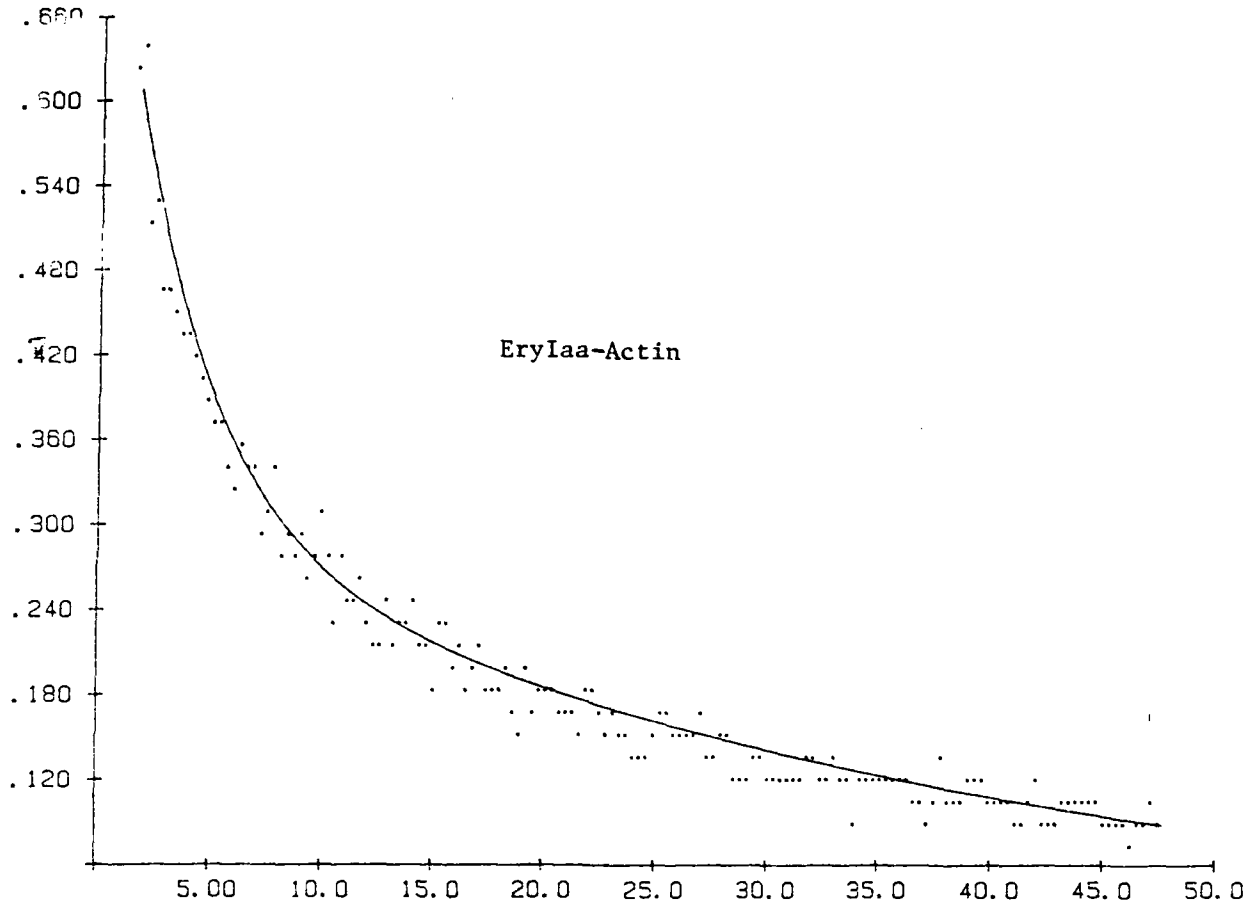
.660
.600
.540
.420
.420
.360
.300
.240
.180
.120
EryIaa-Actin
5.00
10.0
15.0
20.0
25.0
30.0
35.0
40.0
45.0
50.0

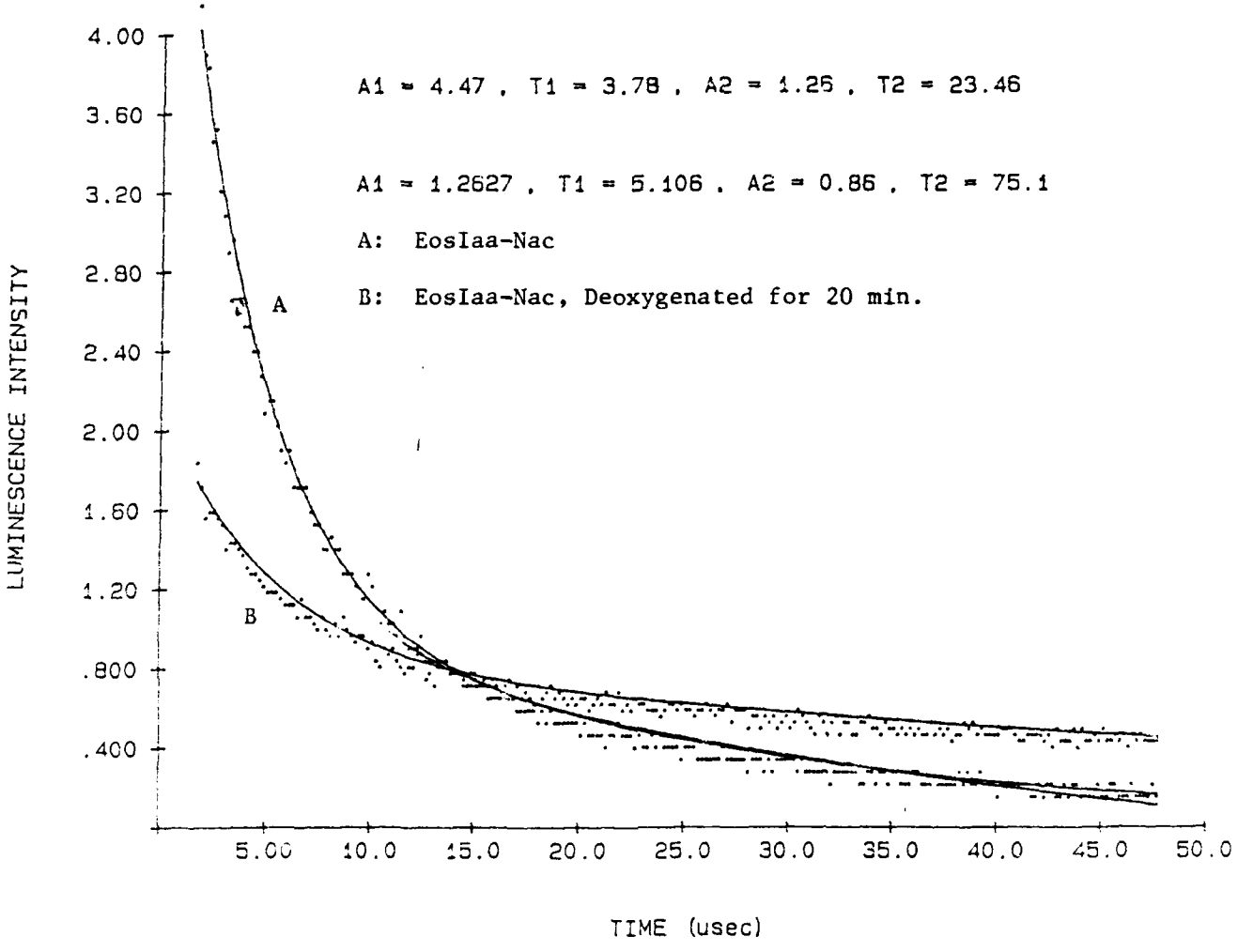
A1 = 4.47 , T1 = 3.78 , A2 = 1.25 , T2 = 23.46
A1 = 1.2627 , T1 = 5.106 , A2 = 0.86 , T2 = 75.1
A: EosIaa-Nac
B: EosIaa-Nac, Deoxygenated for 20 min.
A
B
LUMINESCENCE INTENSITY
4.00
3.60
3.20
2.80
2.40
2.00
1.60
1.20
.800
.400
5.00
10.0
15.0
20.0
25.0
30.0
35.0
40.0
45.0
50.0
TIME (usec)

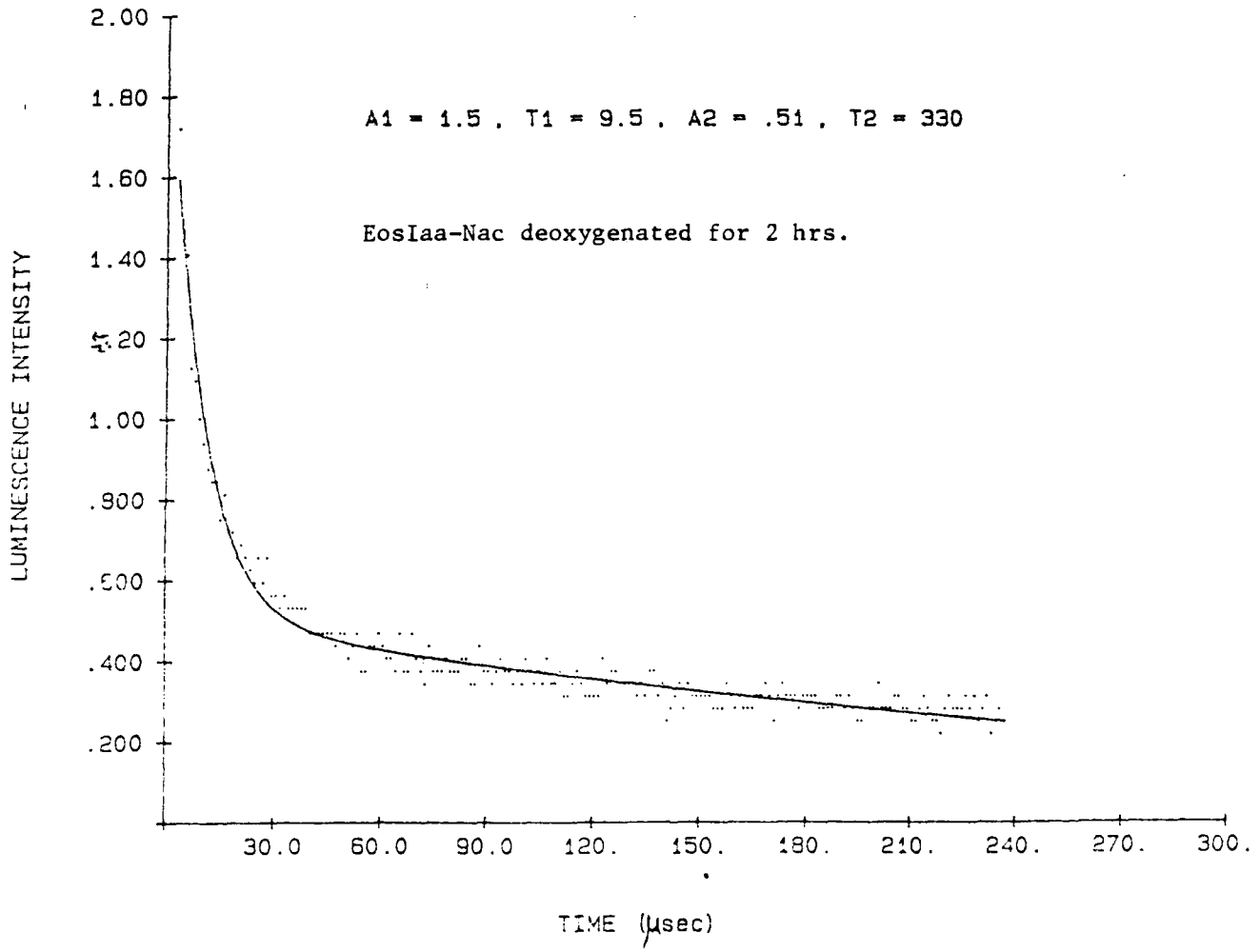

Figure 9. Phosphorescence Decay Curve

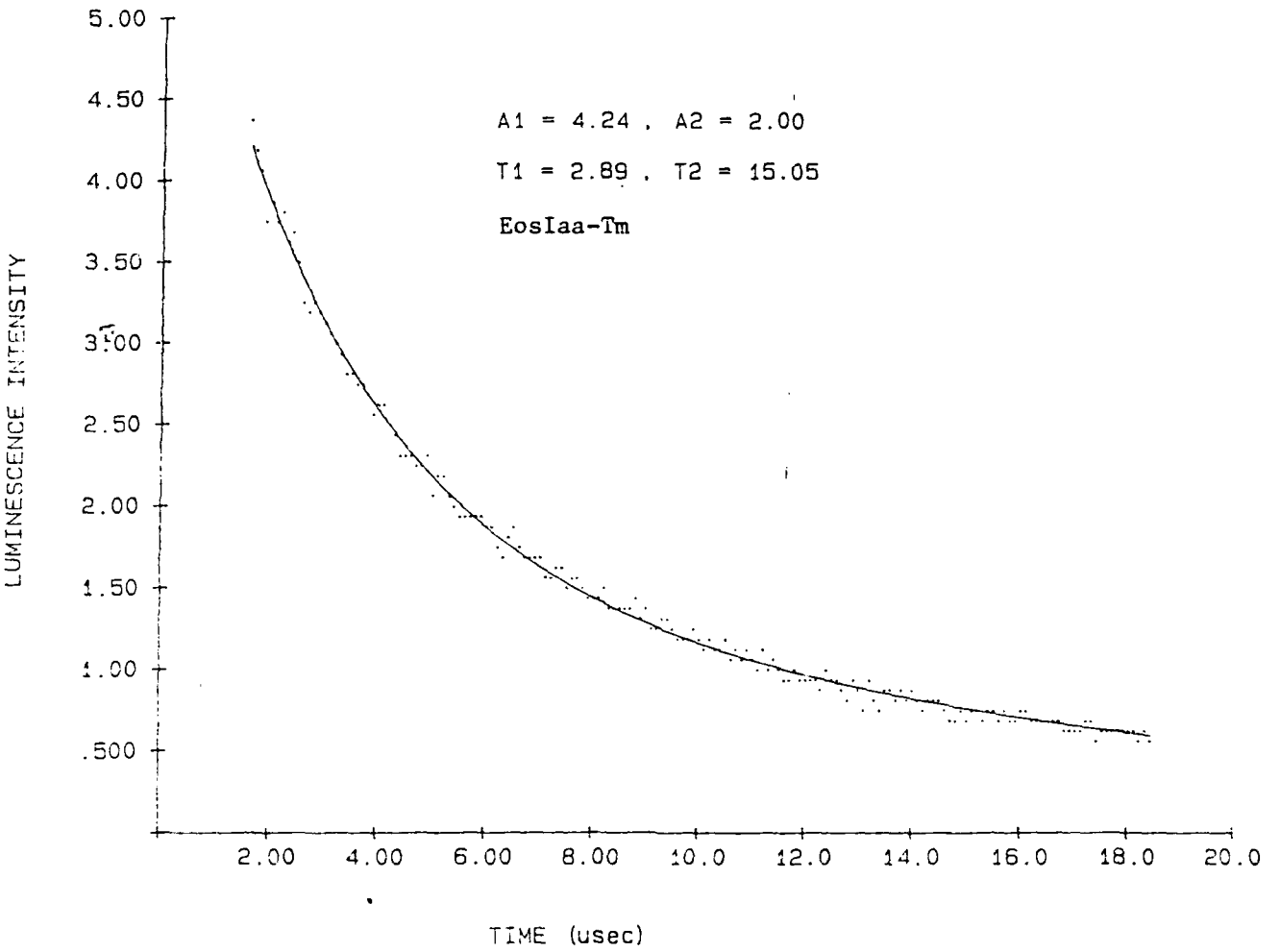
A1 = 4.24 , A2 = 2.00
T1 = 2.89 , T2 = 15.05
EosIaa-Tm
LUMINESCENCE INTENSITY
TIME (usec)
5.00
4.50
4.00
3.50
3.00
2.50
2.00
1.50
1.00
.500
2.00
4.00
6.00
8.00
10.0
12.0
14.0
16.0
18.0
20.0

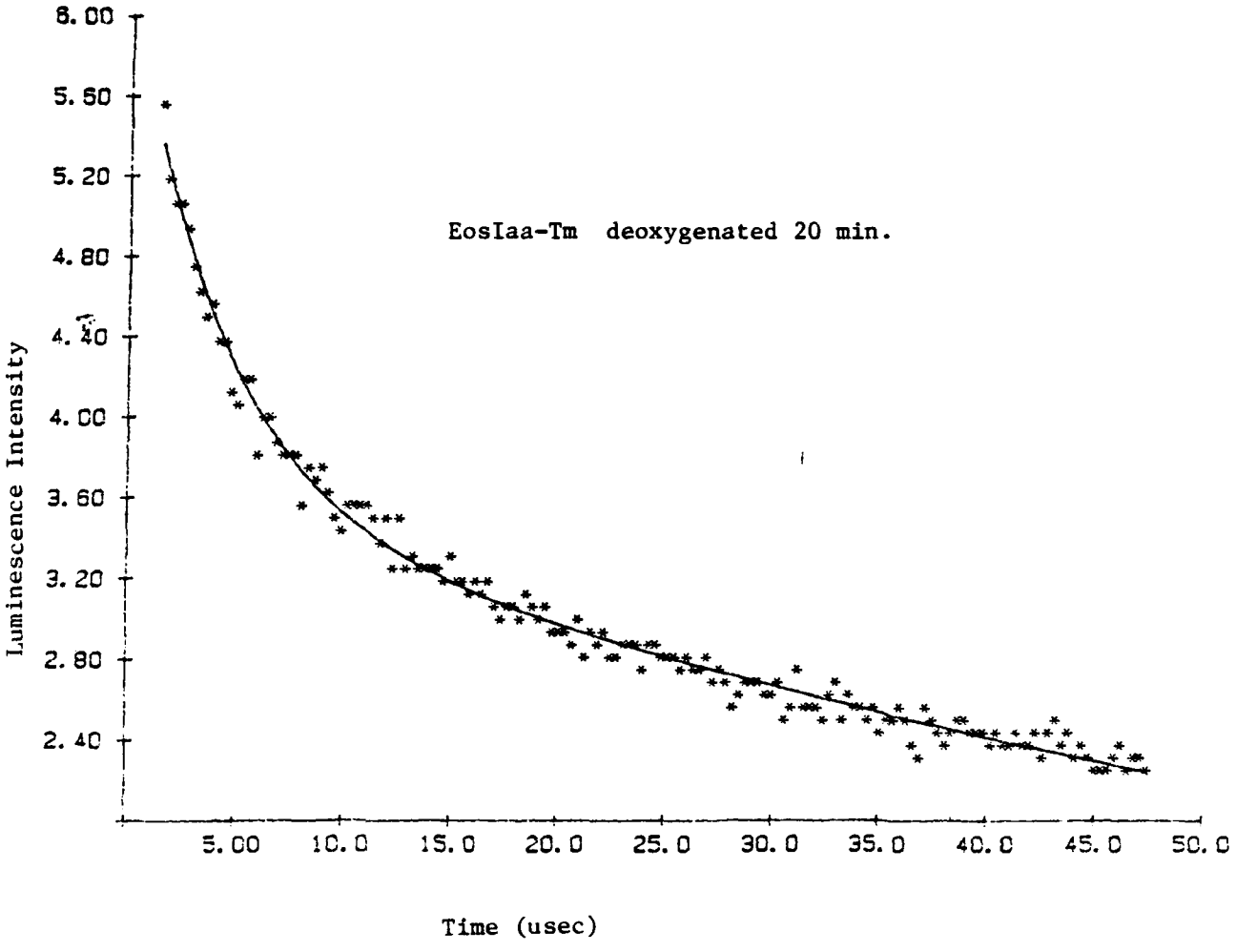

Figure 11. Phosphorescence Decay Curve

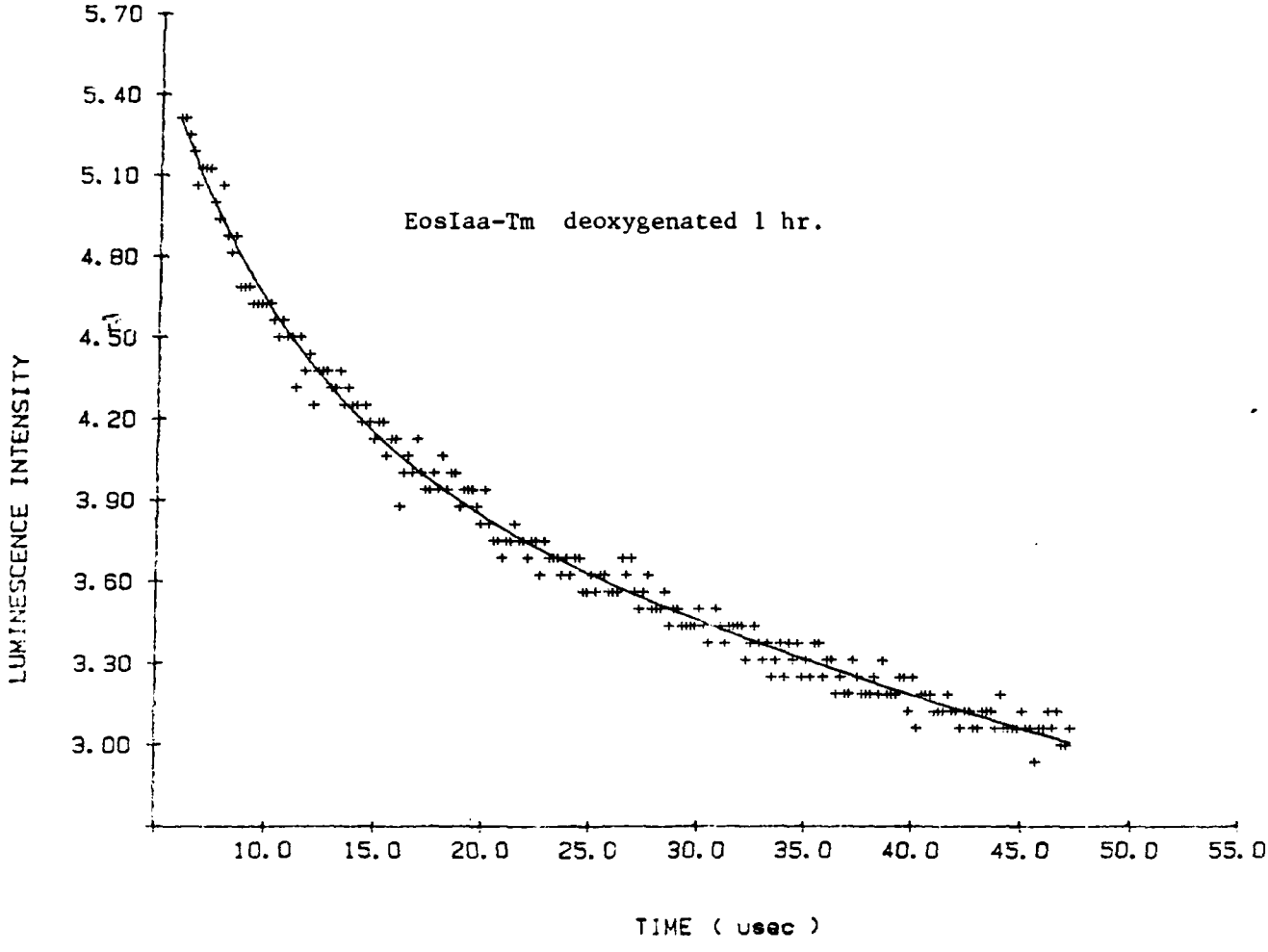

Figure 12. Phosphorescence Decay Curve

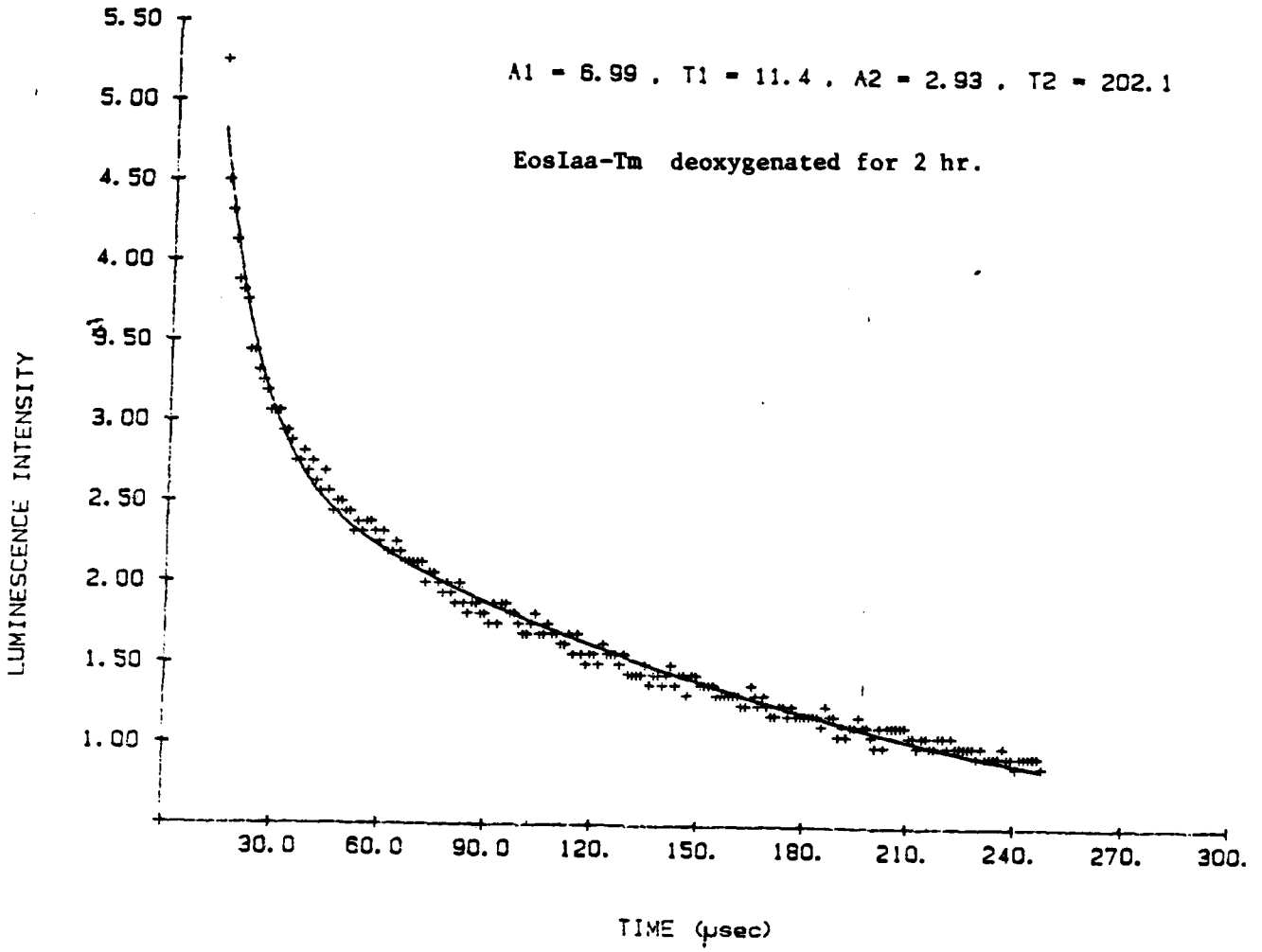

Figure 13. Phosphorescence Decay Curve

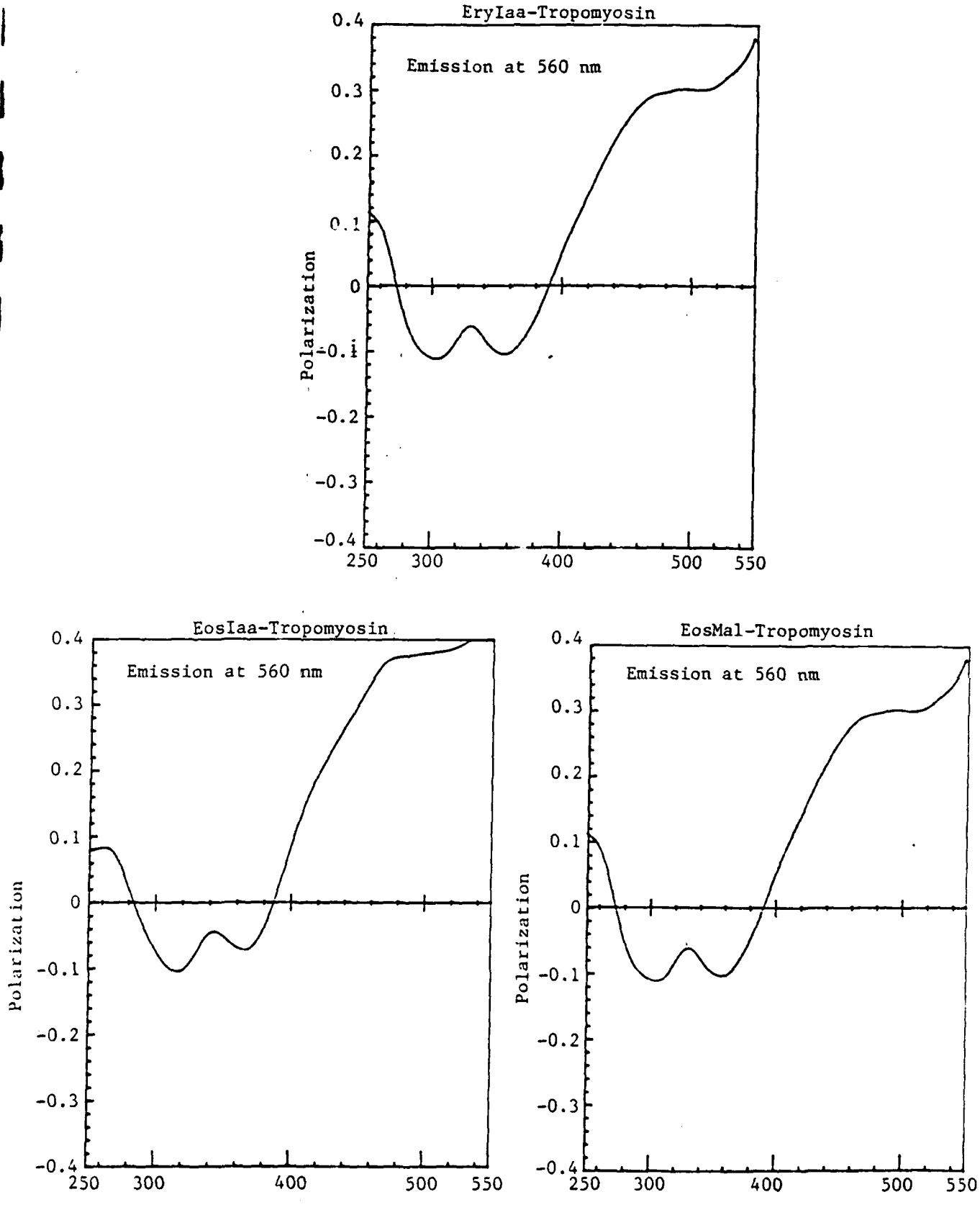

Figure 14. Fluorescence Polarization Excitation Spectra of Labeled Tropomyosin Adducts

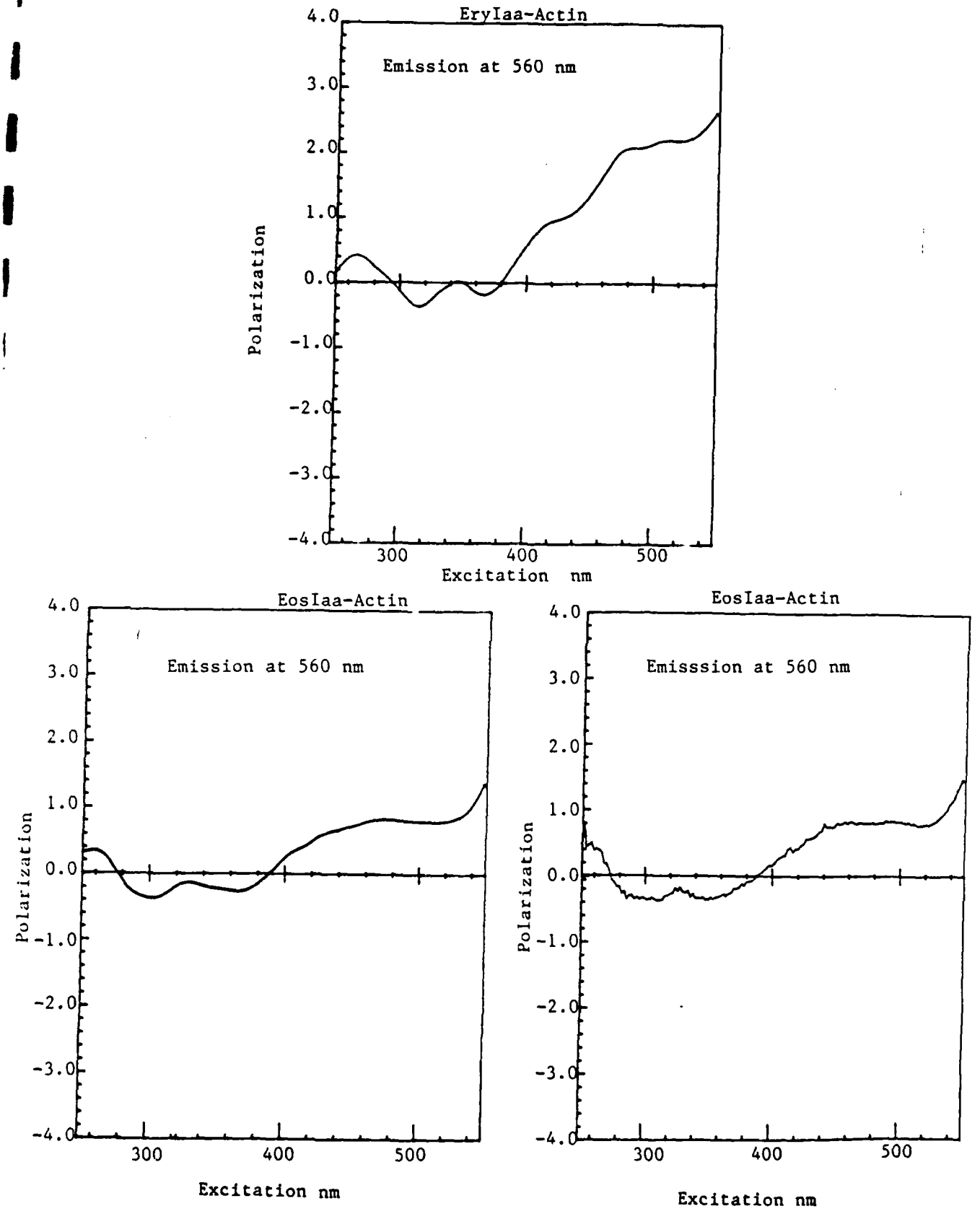

Figure 15. Fluorescence Polarization Excitation Spectra of Labeled Actin Adducts.

NEAR-ULTRAVIOLET EFFECTS ON CELLULAR TISSUE COMPONENTS: DIRECT PHOTOINDUCED CHANGES OF PROTEINS

Brief Summary

The potential role of light in the etiology of malignancy and a concern for the side-effects of current and proposed surgical uses of lasers make the study of photooxidative processes in tissue components a subject of biomedical interest. Moreover, studies of photoinduced changes in proteins could yield interesting insights into subtleties of structure, conformation, and dynamics important to biological function.

Using the protein lysozyme as a model, photoinduced oxidative changes were studied using near-UV irradiation, primarily with a nitrogen (337 nm) laser, with no specifically added sensitizing compounds. Near-UV irradiation of tryptophan alone (an amino acid component which is found in key positions in the structure of lysozyme) under similar conditions was also examined to extend the relevant background database, using HPLC, TLC, absorption and fluorescence spectrometry.

Near-UV irradiation of lysozyme, and tryptophan in solution, results in progressive loss of tryptophan, enzyme activity and production of "daughter products". The latter appear to include N-formyl-kynurenine, kynurenine, tryptamine, and anthranilic acid.

Enhancement of photochanges with deuterium oxide, compared to water as solvent, is consistent with a mechanism mediated by singlet oxygen. Involvement of peroxide and radicals have not been strictly ruled out. Exposures to laser light that resulted in 15% loss of tryptophan fluorescence produced no measurable loss in enzymatic activity. Fluorescence quenching experiments on irradiated lysozyme at low conversion percentages suggest that an exposed residue (Trp-62) is favored as an initial target of attack. Implications for enzyme mechanisms are discussed in the published article (preprint attached).

Background Perspective

Several questions arise in considering the health-related effects of near-UV radiation:

1) What are the possible or likely negative side effects of lasers of this spectral range that could be involved in new photodynamic and surgical techniques? Recently, use of near and mid-UV spectra in inactivation of viruses in blood has been reported (Prince, et al., 1983; Prodouz, et al., 1987). Potential for inducing photochemical reaction in blood products via endogeneous tryptophan, tryosine, and cysteine is present.
2) What is the role of light penetrating the ozone layer (UV-A, UV-B) in causing health problems involving, for example, the skin and eyes, including cancer, keratoses, aging and cataracts.
3) What are the side effects of any "toxic products" formed by the action of either natural abundance or man-made radiation? These secondary side effects could conceivable be expressed, for example, by autoimmune or malignancy reactions.
4) What are the primary mechanisms mediating these processes? Aside from yielding insights into structural and conformational aspects of cellular components of the body, such studies could lead to rational avenues of preventing or inhibiting deleterious consequences.

Examining the latter in detail, we studied the sub-cellular mechanisms of photochemical changes of proteins and amino acids, using the methods and instrumentation of analytical chemistry. Using the proteins lysozyme and its constituent amino acid tryptophan as

models, we followed changes induced by direct (no added exogenous sensitizer) irradiation with the nitrogen laser. Changes were assayed using customary methods germane to analytical and biological chemistry.

We have completed the first phase of this study and note that a manuscript based on this work has been accepted for publication and is in press with the journal Radiation and Environmental Biophysics. A preprint copy of this article is attached.

Projections

A. General Plan

Our results thus far (VanderMeulen and Judy, 1988) have demonstrated the development of an approach using the tools of spectroscopy and chromatography to monitor specific biochemical and structural effects caused by exposure of biological material to UV laser radiation. It will be difficult to generalize the observations made thus far without a study of a wider variety of proteins, and eventually other tissue components. Therefore, utilizing the detailed experience with the model protein lysozyme, we propose to broaden the scope of investigation to several proteins of interest. Special attention will be focused on those containing only one or two tryptophans, with known spatial locations (surface, exposed, buried), thus facilitating some aspects of interpretation. Since results thus far suggest mechanistic involvement of singlet oxygen and initial formation of NFK, we plan to do some comparative photooxidative studies with specifically added sensitizer (especially NFK). This will provide at least the following advantages: (1) exposure times are reduced, further minimizing potential contributions from long term exposure incubations and facilitating data throughput, and (2) questions of mechanism are more straightforward.

Outlined below are several favorable model components with selected characteristics highlighted. These will be exposed to UV irradiation under controlled conditions of oxygenation, pH, temperature and incident/absorbed flux. Samples are then analyzed as in previous portions of this study for lysozyme (VanderMeulen and Judy, 1988) to determine specific structural and functional changes.

At present, only two wavelengths have been used, 337 and 351 nm from the low power nitrogen and argon lasers, respectively. Availability of the free electron laser will not only offer the opportunity of using wavelength tunability to characterize the action spectrum of photochemical oxidation, but may also offer opportunity to study photochemical processes involving high concentrations of excited state species. The latter could be sustained by the very high peak power, high pulse repetition rate and long macropulse lengths. Additionally, if photochemical oxidation rates are found to be sensitive to attainment of high concentrations of excited state species, then the potential for photochemical reaction of endogenous species in proteins and for constructive or destructive clinical effects will have to be explored.

The great spectral diversity observed in proteins must reflect a diversity of interactions involving tryptophan. Table I lists some specific interactions observed in these molecular structures. In those structures which reveal details of the environment of individual indole moieties, there is a great variety of interactions, which may well account for the diversity of spectral parameters and quantum yields.

In considering how to separate the contributions of more than one tryptophyl residue, a useful procedure can be used to compare proteins obtained from different species in which there is a replacement of individual amino acids. The relative mutabilities of the aromatic amino acids are summarized in Table II. When distantly related sequences are compared,

tryptophan is altered about half of the time. Thus, pairs with one and two tryptophans in which one tryptophan is homologous are often found.

We will begin by considering specifically the following:

(l) Liver alcohol dehydrogenase (LADH): This enzyme catalyzes the oxidation of alcohols and the reduction of aldehydes and ketones in the presence of NAD and NADH, respectively. LADH is a dimer enzyme containing two tryptophans, one exposed to the solvent (Trp-15) and one buried at the dimer interface (Trp-314).

(2) Myoglobin: This protein contains one heme group and one polypeptide chain. The interaction of heme with the specific protein occurs at the fifth coordinate position of the iron and through additional bonds of the porphyrin with the polypeptide chain. The complex becomes able to bind molecular oxygen reversibly and its functional behavior appears to be essentially controlled by the "local environment" of the heme group in the protein. The property of forming a stable oxygenated derivative is lost on denaturation of the protein.

(a) tuna; contains one tryptophan at a surface (Trp-14), bonded to acid (E16), but with contact with an imidizole (H24)

(b) sperm whale; has an additional tryptophan (Trp-7), which is exposed

We anticipate that myoglobin will also be a subject of special interest in light of the additional chromophore contained within its structure and we plan to include Soret band excitation simultaneously with near-UV irradiation. This feature will potentially allow us to investigate if thermal vibration in the protein surrounding the heme group alters the rate of photochemical attack on Trp induced by near-UV radiation.

(3) Nuclease A: Micrococcal nuclease catalyzes cleavage of both DNA and RNA to yield 3'-nucleotides. It exhibits both exo- and endo-5-phosphodiesterase activities and catalyzed preferential endohydrolysis of the RNA and DNA at sites rich in adenylate or uridylate and deoxyadenylate or thymidylate (Alexander et al., 1961; Roberts et al., 1962; Rushisky et al., 1962). It contains one tryptophan (Trp-140), bonded to water, partially exposed at a surface and surrounded by charged residues, with maximum fluorescence at 325 mm and lacking fine structure; it may well be surrounded by waters forming a network of H-bonds.

(4) Superoxide dismutase: Superoxide dismutase catalyzes the destruction of the O_2 free radical to form O_2 and H_2O_2. The O_2 ion has been considered important in aging, lipid peroxidation and the peroxidative hemolysis of red blood cells (Fee and Teitelbamm, 1972) and is formed by the univalent reduction of O_2 during various enzymic reactions or by ionizing radiation. It may function in the protection of cells against the harmful effects of superoxide free-radicals (Fridovich, 1973; Lavelle, et al., 1973). Obtained from human red blood cells, it contains a single tryptophan residue.

(5) Subtilisin Carlsberg (protease, cleavage of peptide bonds): Both subtilisin Carlsberg and subtilisin inhibitor have a single tryptophyl residue with fluorescence maxima at 355 nm without structure; these residues are surrounded by several non-polar residues and exposed to solvent.

This list is by no means exhaustive in our consideration of useful models for study, and additional subjects for study can be included as needed. The choices we have listed are also appropriate as they are available commercially and have stability properties convenient

for travel to Stanford for experimentation. A discussion of interesting candidates in light of protein fluorescence characteristics is available (Longworth, 1983).

B. Experimental Details

We plan photoirradiation experiments utilizing frequency doubled FEL output. We anticipate the MKIII FEL facilities at Stanford to be available for these studies. For the MKIII facility two-three stages of frequency doubling will be required to achieve radiation in the range of 300-350 nm required for our studies. Since we anticipate using average power levels of up to 0.1 W in the near-UV, the FEL facility can deliver more than sufficient long wavelength power to meet our needs. We await the implementation of recent and "in progress" developments of crystals for use with the FEL before projecting site visits for this experimentation. Dr. S. Benson and others at Stanford have been advising us in this regard.

Irradiation will typically be done at 37°C, but additional experiments in the range 10-45°C can yield values for the activation energy from a standard "Arrhenius plot" [log rate vs. 1/T (K)]. The extinction coefficient of the samples at 337 nm would not result in any significant difference in intensity profile across the 1 cm pathlength. Both irradiated and dark control samples will be thermostated with a circulating water bath. Sample volume and geometry are adjusted so that the beam cross section essentially match that of the sample.

We plan to evaluate Trp photooxidation yields in the various proteins studied as a function of average power of each laser used in order to ascertain any effects of multiphonic absorption contributing to photosensitization (Borkman et al., 1986).

Lysozyme (hen egg white), equine liver alcohol dehydrogenase, sperm whale and tuna myoglobin, nuclease A from Staphlococcus aureus, human RBC superoxide dismutase subtilisin Carlsberg (protease) from Bacillus subtilis and subtilisin inhibitor, tryptophan, sodium azide, casein, D_2O, methanol and L-kynurenine (KYN) are purchased in the highest available grade from Sigma Chemical Co. HPLC grade ultrapure water is obtained from Alfa Products. Ultrapure sodium phosphate (mono- and di-basic) purchased from Aldrich; this was included in our protocol after HPLC analysis in early experiments revealed the presence of trace buffer impurities during chromatographic analysis of tryptophan and related compounds in buffer. Unless otherwise indicated, solutions of lysozyme (2.4 mg/ml, which is a ca. 1 mM in Trp) and tryptophan (1 mM) will be prepared in 0.07 M sodium phosphate, pH 7.4. N-formyl-kynurenine (NFK) has been synthesized according to a published procedure (Auerbach and Knox, 1957) and separated chromatographically from any remaining starting material. Chromatography of tryptophan and irradiated "daughter products" of photooxidation has been done in our lab with a Hewlett Packard 1090M HPLC, using published separation conditions with minor modifications (Yong and Lau, 1979), and in some cases using standard silica gel TLC procedures (e.g., Borkman et al., 1986). In addition, chromatography and analysis of the other amino acids of proteins can also be performed with this HPLC, for example, with phenylthiocarbamate derivitization on reverse phase column, multiple step gradient with a NaOAc-triethylamine buffer (pH 6.4) and 60% acetonitrile and 50°C and 1.5-2.0 ml/min. Acrylamide gel of proteins will be done to check protein purity with a Pharmacia Phast gel system and scanned with a Biomed SL2D-UV laser densitometer.

The enzymatic activity of lysozyme is assayed with a suspension of Micrococcus luteus (formerly M.lysodeikticus) cells as substrate (based on original procedure of Shugar, 1952). Typically, 0.5μg enzyme is added to a 0.2 mg/ml cell suspension in 0.066 M

potassium phosphate buffer (pH 6.25, 25°C) and the decrease in apparent absorbance at 450 nm followed; the rate is calculated from the linear region, after 0.3-0.5 minutes: Units/mg = (A_{450}/min X 1000)/mg enzyme. A concentration curve of specific activity vs. amount added enzyme showed that the activity per mg was constant between at least 0.1 - 0.9 µg and thus the assay parameters are not in an enzyme limited range.

Equine liver alcohol dehydrogenase reaction velocity is determined by the method of Vallee and Hoch (1955) in which the change in absorbance at 340 nm resulting from reduction of NAD is measured. One unit reduces one micromole of NAD per minute at 25°C under the specified conditions: (1) Immediately prior to use, enzymes are diluted to a concentration of 0.05-0.25 units/ml in 0.01 M phosphate buffer, pH 7.5 containing 0.1% gelatin; (2) for liver enzymes mg/ml = A_{280} X 2.2 with enzyme dissolved in 0.1 M phosphate buffer, pH 7.5; (3) pipette into each cuvette 1.5 ml 0.032 M pyrophosphate buffer, 0.5 ml 2.0 M ethanol, and 1.0 ml 0.025 M NAD; (4) incubate in spectrophotometer for 3-4 minutes at 25°C to achieve equilibrium and establish blank rate (if any); (5) at zero time, add 0.1 ml of appropriately diluted enzyme to the cuvette and record A_{340} for 3-4 minutes; (6) calculate ΔA_{340} from the linear portion of the curve.

Myoglobin (Mb) function is followed by measuring the oxygen dissociation-saturation properties. The percentage of $Mb0_2$ is calculated from:

$$Mb0_2\ \% = [A(o) - A(Mb)]/[A(MbO_2) - A(Mb)] \times 100$$

[where A = absorbance: o = at the oxygen partial pressure under examination; Mb = at complete deoxygenation; Mb02 = at complete oxygenation]. Mb absorbs maximally at 560 nm; Mb02 at 580 and 542 nm. Spectrophotometric readings are taken at concentrations of pigment between 0.2 and 1% and 2 mm light path at 460, 510, 560 and 580 nm; for higher concentrations readings can be taken at 600 and 800 nm, for lower concentrations at 410 and 430 nm. The reading at 510 nm (isosbestic point between Mb and $Mb0_2$) is taken in order to control the potential formation of Mb^+ and denaturation of the pigment. The formula is applied to readings obtained at the various wavelengths and the average of values obtained is used to plot the O_2-dissociation curve.

Further aspects of the function of myoglobin and hemaglobin have been thoroughly discussed (Antonini, 1965).

We assay micrococcal nuclease essentially with the procedure as described by Heins et al., 1967, based on the release of acid soluble oligonucleotides following nuclease digestion of DNA. One unit corresponds to a change in optical density of 1.0 at 260 nm at 37°C and pH 8.0 under those specified conditions.

Our assay method for superoxide dismutase is essentially that of Winterbourn et al., 1975, and is based on the ability of superoxide dismutase to inhibit the reduction of nitrobule tetrazolium (NBT) by superoxide. One unit is defined as that amount of enzyme causing half the maximum inhibition of NBT reduction. The reaction velocity will depend on assay conditions such as light intensity and reaction temperature and therefore is calibrated for comparative purposes.

The peptide cleaving ability of the protease can be measured by following the digestion of a reference compound such as casein. One unit will hydrolyze casein to produce color equivalent to 1.0 µmole (181 µg) of tyrosine per minute at pH 7.5 at 37°C (color by Folin-Ciocalteu reagent). Alternately, one unit is that amount of enzyme which liberates acid

soluble fragments equivalent to 0.001 A_{280} per minute at 37°C and pH 7.8 under the defined conditions; since casein lots may vary it is often necessary to calibrate with a reference enzyme or compare sample with control.

Absorbance spectra are recorded on a Perkin-Elmer UV/VIS 552A spectrophotomer. Fluorescence spectra are measured at 25°C with a SLM 500-SPF-C fluorescence spectrometer which affords state-of-the-art data collection and processing. Excitation and emission slits for recording spectra are usually set at 2 nm. Proteins and tryptophan are diluted with buffer where necessary to insure that spectroscopic measurements were in the linear range; e.g for excitation at 290 nm, this is 0.2 mg/ml for lysozyme and 0.1 mM for tryptophan.

Fluorescence quenching experiments are done at 25°C using fresh concentrated solutions of acrylamide (8 M) and sodium iodide (7 M), the latter with ca. 0.1 mM sodium thiosulfate added to prevent I_3^- formation. NaCl is used to account for ionic strength effects. Iodide quenching curves are analyzed to obtain the fluorescence fraction (F_{ex}) of relatively exposed Trp residues of the protein as described (Edwards and Silva, 1986) using plots of $F_O(F_O\text{-}F)$ vs. $1/[Q]$ from the Lehrer equation (Lehrer, 1971). The intercept is taken as $1/F_{ex}$, where F_O and F are the fluorescence intensities in the absence and presence of quencher Q, respectively. The excitation wavelength is usually 295 nm with emission measured at the appropriate wavelength for a given protein, using 1 and 5 nm slits, respectively.

References

Alexander, M., Heppel, L.A. and Hurwitz, J. (1961) J. Biol. Chem. 236, 3014.

Antonini, E. (1965) Physiol. Rev. 45, 123-170.

Auerbach, V.H. and Knox, W.E. (1957) Methods in Enzymol. 3, 620-623.

Borkman, R.F., Hibbard, L.B. and Dillon, J. (1986) Photochem. Photobiol. 43, 13-19.

Donoso, L.A. and Spikes, J.D. (1980) Enzyme 25, 111-117.

Edwards, A.M. and Silva, E. (1986) Radiat. Environ. Biophys. 25, 113-122.

Fee, J.A. and Teitelbaum, H.D. (1972) Biochem. Biophys. Res. Comm. 49, 150.

Fridovich, I. (1973) Biochem. Soc. Trans. 1, 48.

Grossweiner, L. (1976) Int. J. Rad. Biol. 29, 1-16.

Hayashi, K.,Imoto, T., and Funatsu, M. (1965) J. Biochem. (Tokyo) 58, 227-235.

Heins, J.N., Suriano, J.R., Taniuchi, H. and Anfinsen, C.B. (1967) J. Biol. Chem. 242, 1016.

Jori, G., Galiazzo, G., Tamburro, A.M., Scoffone, E. (1970) J. Biol. Chem. 245, 3375-3383.

Lavelle, F., Michelson, A.M. and Dimitrijevic, L. (1973) Biochem. Biophys. Res. Comm. 55, 350.

Lehrer, S. (1971) Biochemistry 17, 3254-3263.

Longworth, J.W. (1983) In Time-Resolved Fluorescence Spectroscopy in Biochemistry and Biology (Cundall, R.B. and Dale, R.E., eds), pp. 651-725, Plenum Press, N.Y.

Mandel, K., Bose, S.K., Chakrabarti, B. (1986) Photochem. Photobiol. 43, 515-523.

McGrath, H., Wilson, W.A., and Scopelitis, E. (1986) Photochem. Photobiol. 43, 627 631.

McLaren, A.D. and Shugar, D. (1964) Photochemistry of Proteins and Nucleic Acids, pp. 110-161, Pergamon Press, Oxford.

Parrish, J., Jaenicke, K., and Anderson, R. (1982) Photochem. Photobiol. 36, 187-192.

Prince AM, Stephan W, Brotman B. B-propiolactone/ultraviolet irradiation: a review of its effectiveness for inactivation of viruses in blood derivatives. (1983) Rev Infect Dis 5,92-107.

Prodouz KN, Fratantoni JC, Boone EJ, Booner RF. Use of laser-UV for inactivation of

Roberts, W.K., Dekker, C.A., Rushisky, G.W., and Knight, C.A. (1962) Biochem. Biophys. Acta 55, 664.

Rushisky, G.W., Knight, C.A., Roberts,W.K., and Dekker, C.A. (1962) Biochim. Biophys. Acta 55, 674.

Spikes, J.D. and Straight, R. (1967) Ann. Rev. Phys. Chem. 18, 409-436.

Shugar, D. (1952) Biochem. Biophys. Acta 8, 302-310.

Srinivasan, R. (1986) Science 234, 559-565.

Vallee, B.L. and Hoch, F.L. (1955) Proc. Nat. Acad. Sci. Usa 41, 327.

VanderMeulen, D.L. and Judy, M. (1988) Photooxidative Changes of Lysozyme with 337.1 mm Laser Radiation. Radiation Environ. Biophys., In press.

Walrant, P. and Santus, R. (1974) Photochem. Photobiol. 20, 455-460.

Winterbourn, C.C., Hawkins, R.E., Brian, M., and Carrel, R.W. (1975) J. Lab. Clin. Med. 85, 337.

Yong, S. and Lau, S. (1979) J. Chromatog. 175, 343-346.

TABLE I

Interactions of Tryptophan in Protein Structure

Buried		
No hydrogen bond	Azurin	W48
Bonded to peptide link	Lysozyme	W108-L56 peptide
	Serine protease	W141-F71 peptide
Bonded to alcohol	Globin (bloodworm)	W131-T13
Bonded to acid	Immunoglobulin	W35-HOH
	Prealbumin	W79-HOH
Bonded to acid	Cytochrome c	W59-Haem propionic acid
	Actinidin	W178-D121
Surface		
Bonded to water	Nuclease A	W140-HOH
	Chymotrypsin	W51-HOH
Bonded to amide	Globin, beta	W38-Q101
Bonded to acid	Lysozyme	W111-E27
	Myoglobin	W14-E16
	Glyceraldehyde-3-phosphate dehydrogenase	W310-D293

TABLE II

Mutational Changes of Aromatic Amino Acid

Normalized Mutability: Trp 0.01, Tyr 0.03, Phe 0.04

Mutation to closely related species

Trp → [Arg, Ser, Leu] > Phe > Tyr

Tyr → Phe > [His, Asn, Cys] > Trp

Phe → Tyr > [Leu, Ileu, Ser] > Trp

Mutation to distantly related species

Trp → [Arg, Leu, Lys] > Phe > Tyr

Tyr → Phe > Leu [Val, Ser, Cys, Ala] > Trp

Phe → Tyr > [Leu, Val, Ileu] > Trp

FIGURE LEGENDS

Figure 1. Fluorescence spectra of lysozyme after 2.5 hr irradiation at 25° with 337.1 nm laser radiation in buffer made with H_2O (O) or D_2O (Δ); compared to dark control (□). Excitation at 290 nm.

Figure 2A. Fluorescence spectra of lysozyme after 2.5 hr irradiation at 25° with 337.1 nm laser radiation in buffer made with D_2O (Δ), compared to dark control (□). Excitation at 360 nm.

Figure 2B. Fluorescence difference spectra (irradiated minus dark) of lysozyme after 2.5 hr of 337.1 nm irradiation at 25° in buffer made with D_2O (Δ) or H_2O (O), and of tryptophan with H_2O (+). The spectrum of chemical mixture of NFK + KYN (ca. 3:1 molar ratio) is presented for comparison (*). Excitation at 360 nm.

Figure 3. Fluorescence spectra of lysozyme (O) and tryptophan (+) after 3.5 hr irradiation with 337.1 nm laser radiation at 25°. Excitation at 322 nm. Inset: Difference absorption spectra (irradiated vs. dark control) for lysozyme (D_2O buffer) exposed to 2.5 hr 337.1 nm radiation, measured at 0.2 mg/ml (10x dilution of concentration used for irradiation).

Figure 4. Changes in lysozyme fluorescence (closed symbols, excitation at 290-295 nm) and enzyme activity (open symbols), expressed as percent of control, resulting from exposure to 337.1 nm laser radiation. Square: 37°C; triangle: 16°C.

Figure 5A. Stern-Volmer plot for acrylamide quenching of the fluorescence of lysozyme exposed for 1.5 hr to 337.1 nm radiation (O), and of dark control (□). Excitation at 295 nm.

Figure 5B. Modified Stern-Volmer plot for iodide quenching of the fluorescence of lysozyme exposed for 1.0 hr to 337.1 nm radiation (O), and of dark control (□). Excitation at 295 nm.

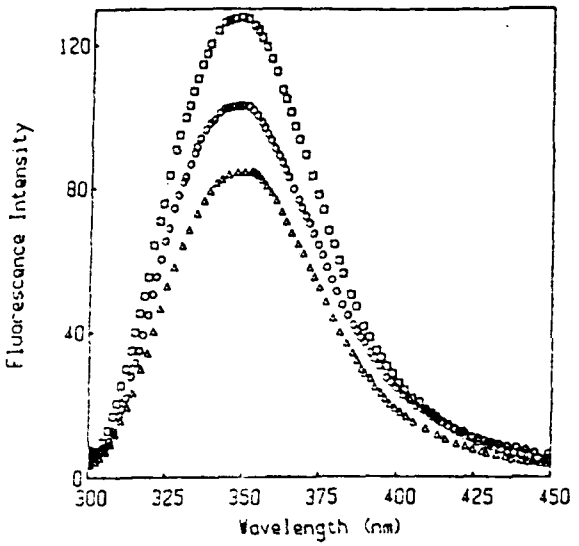
Fluorescence Intensity
120
80
40
0
300
325
350
375
400
425
450
Wavelength (nm)

FIG. 1

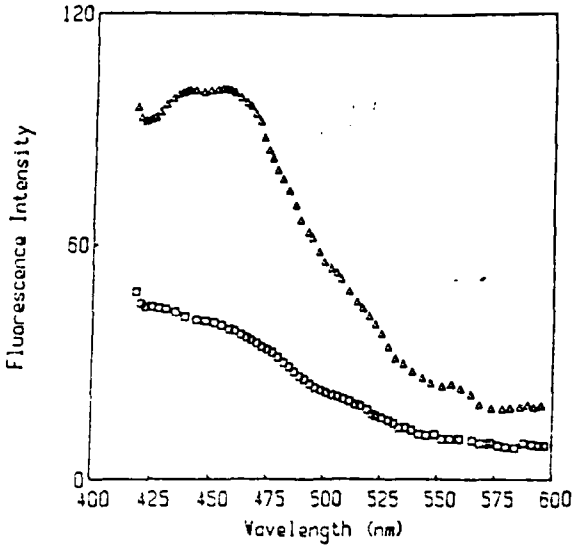
120
60
0
Fluorescence Intensity
400 425 450 475 500 525 550 575 600
Wavelength (nm)

FIG. 2A

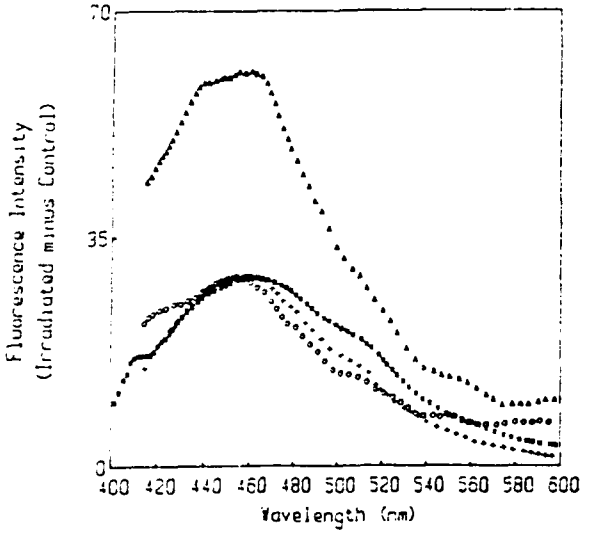
70
35
0
Fluorescence Intensity
(Irradiated minus Control)
400 420 440 460 480 500 520 540 560 580 600
Wavelength (nm)

FIG. 2B

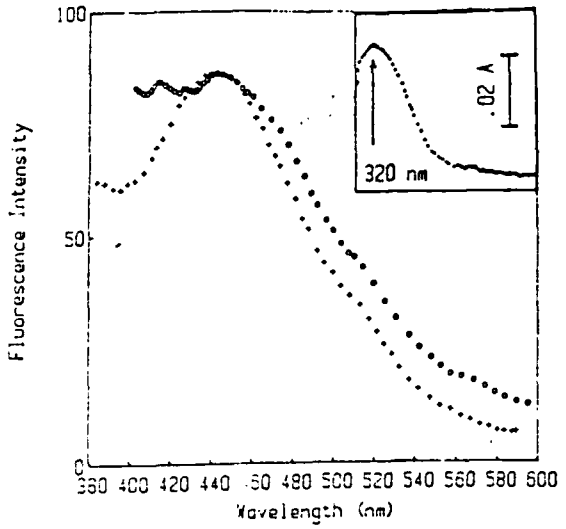
100
50
0
Fluorescence Intensity
320 nm
.02 A
380 400 420 440 460 480 500 520 540 560 580 600
Wavelength (nm)

FIG. 3

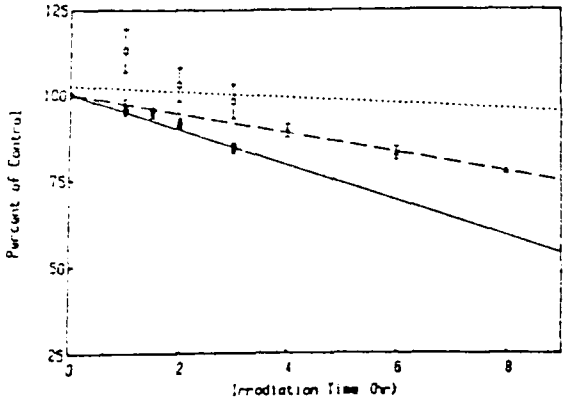
125
100
75
50
25
Percent of Control
0
2
4
6
8
Irradiation Time (hr)

FIG. 4

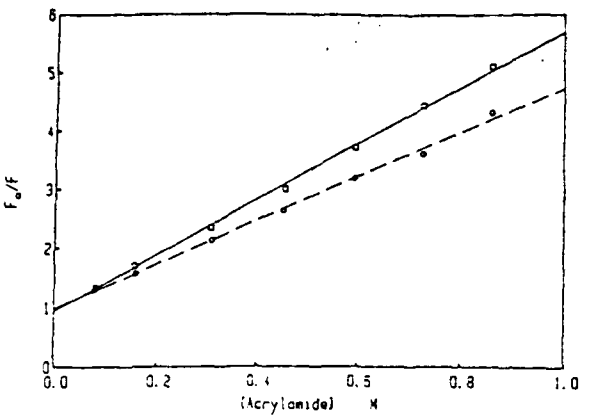
F_o/F
0
1
2
3
4
5
6
0.0
0.2
0.4
0.6
0.8
1.0
[Acrylamide] M

FIG. 5A

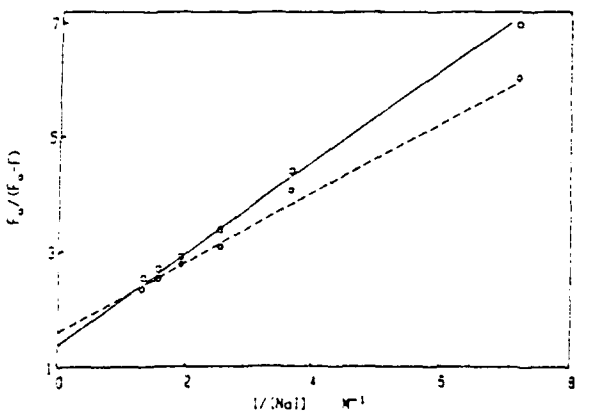
$F_o/(F_o-F)$
1
3
5
7
0
2
4
6
8
1/[NaI] M^{-1}

FIG. 5B

Radiat Environ Biophys (1988) 27: ■-■

Radiation and Environmental Biophysics

Photooxidative changes of lysozyme with 337.1 nm laser radiation

D.L. VanderMeulen and M.M. Judy
Baylor Research Foundation, 3500 Gaston Avenue, Dallas, TX 75246, USA

Received August 31, 1987 / Accepted in revised form March 6, 1988

Summary. Initial photoinduced oxidative changes in the protein lysozyme were studied using the 337.1 nm radiation from a pulsed nitrogen laser without exogenous sensitizing compounds. Irradiation of lysozyme and tryptophan in aerated solution results in the temperature and solvent dependent loss of tryptophan absorption and fluorescence, and the appearance of fluorescent "daughter products", primarily N-formyl-kynurenine and kynurenine. Exposures that resulted in 15% loss of tryptophan fluorescence produced no measurable loss in enzymatic activity. Fluorescence quenching experiments on irradiated lysozyme at low conversion percentage suggest that an exposed residue (Trp-62) is favored as an initial target of attack.

Introduction

Studies of the photodynamic and photochemical modifications of proteins and amino acids have been done 1) to selectively modify certain amino acids for mechanistic studies of biological action (Spikes 1977; Donoso and Spikes 1980; Straight and Spikes 1985), 2) to structurally map protein residues including degree of exposure (Ray and Koshland 1962; Jori et al. 1970; Ferrer and Silva 1981), and 3) to study the role of ultraviolet radiation in lens protein damage (Mandal et al. 1986 and references therein) and other biological effects involving enzyme inactivation, skin disease, aging, and tumors (McLaren and Shugar 1964; Grossweiner 1976; Parrish et al. 1982; McGarth et al. 1986). In addition, interest in the surgical uses of near-UV lasers makes the study of photooxidative processes in tissue components a subject of biomedical interest.

Such studies are generally of two types: 1) dye-sensitized photooxidation with added sensitizers and excitation at wavelengths longer than 320 nm (e.g., Edwards and Silva 1985; Ferrer and Silva 1981), or 2) direct photooxidation using wavelengths usually below 300 nm where tryptophan or other chromophore absorbs strongly (e.g., Shugar 1952; Walrant and Santus 1974).

2

Recently it was demonstrated that 337.1 nm radiation from a pulsed nitrogen laser was effective in the aerobic photooxidation of L-tryptophan in aqueous solution with no specifically added sensitizer (Borkman et al. 1986). We were able to confirm their results and extend this to a study of the photoinduced changes of the well-characterized protein lysozyme, also using the nitrogen laser.

Egg white lysozyme is a small, relatively stable and well-characterized enzyme molecule composed of a single polypeptide chain with 129 amino acid residues, cross-linked by four disulfide bridges. It is a compact prolate spheroid with a cleft on one side that forms the reactive enzymatic site. On the basis of a comparison of X-ray crystallographic data and high resolution proton NMR data, there is a good correlation between the conformation of the crystalline state and that of the protein in solution (Blake et al. 1978).

There are six tryptophan residues, numbered 28, 62, 63, 108, 111, and 123. Tryptophans 28, 111, and 123 are buried in the hydrophobic core of the protein. Residues 62, 63, and 108 are in the active site region. Fluorescence from the three tyrosine residues is negligible. Most of the intrinsic lysozyme fluorescence is due to Trp-62 and Trp-108. The three inaccessible Trp residues and Trp-63 together contribute about 10% or less to the total fluorescence (Imoto et al. 1971; Formoso and Forster 1975).

Materials and methods

Lysozyme, tryptophan, D_2O, methanol, and L-kynurenine (KYN) were purchased in the highest available grade from Sigma Chemical Co. Lysozyme of various lot numbers was used to minimize the possibility of any effect arising from a spurious preparation-specific impurity. HPLC grade ultrapure water was from Alfa Products. Ultrapure sodium mono- and di-basic phosphate (purchased from Aldrich) were used after HPLC analysis revealed the presence of trace buffer impurities during chromatographic analysis of tryptophan and related compounds in buffer. Unless otherwise indicated, solutions of lysozyme (2.4 mg/ml, which is ca. 1 mM in Trp) and tryptophan (1 mM) were prepared in 0.07 M sodium phosphate, pH 7.4. N-formyl-kynurenine (NFK) was synthesized according to a published procedure (Auerbach and Knox 1957) and separated chromatographically from any remaining starting material. Chromatography of tryptophan and irradiation "daughter products" of photooxidation was done with a Hewlett Packard 1090M HPLC, using published separation conditions with minor modifications (Yong and Lau 1979), and in some cases using standard silica gel TLC procedures (e.g., Borkman et al. 1986). Acrylamide gels of proteins were done to assess protein purity with a Pharmacia Phast gel system and scanned with a Biomed Instruments SL2D-UV laser densitometer.

Photoirradiation was generally done with a Molectron UV-1000 nitrogen laser operating at 20 kv and 20 Hz whose average incident power levels were 0.045 ± 0.005 W for 16 and 37° C experiments, and 0.1 W for 25° C experiments. Irradiation was at 37° C unless noted otherwise. The extinction

coefficient of the samples at 337.1 nm would not result in any significant differences in intensity profile across the 1 cm path length. Both irradiated and dark control samples were maintained at constant temperature in a thermostated circulating water bath (within ±0.5 deg.). Sample volume and geometry were adjusted so that the beam cross section essentially matched that of the sample. Borkman and co-workers (1986) showed that multiphoton events did not contribute to photooxidation of tryptophan during irradiaton with a pulsed nitrogen laser operating at power levels similar to those used in this work. The enzymatic activity of lysozyme was assayed with a suspension of *Micrococcus luteus* (formerly *M. lysodeikticus*) cells as substrate (based on original procedure of Shugar 1952). Typically, 0.5 µg enzyme was added to a 0.2 mg/ml cell suspension in 0.066 M potassium phosphate buffer (pH 6.25, 25° C) and the decrease in apparent absorbance at 450 nm followed; the rate was calculated from the linear region, after 0.3–0.5 *min*; *units/mg* = $(\Delta A_{450}/min \times 1000)/mg$ enzyme. A concentration curve of specific activity vs. amount added enzyme showed that the activity per mg was constant between at least 0.1–0.9 µg, and thus the assay parameters were not in an enzyme limited range.

Absorbance spectra were recorded on a Perkin-Elmer UV/VIS 552A spectrophotometer. Fluorescence spectra were measured at 25° C with a Farrand MKI fluorescence spectrometer which we have interfaced to a microcomputer for recording and mathematical or graphical processing of data; in addition, direct digital or analog readout of intensities could also be made. Excitation and emission slites for recording spectra were usually set at 5 and 2.5 nm, respectively. Lysozyme and tryptophan were diluted with buffer where necessary to ensure that spectroscopic measurements were in the linear range; for excitation at 290 nm, this was usually 0.2 mg/ml for lysozyme and 0.1 mM for tryptophan. Fluorescence lifetime measurements were recorded on a phase fluorometer using an argon laser excitation source (351 nm) modulated with a Pockels cell as described by Gratton et al. (1984).

Fluorescence quenching experiments were done at 25° C using fresh concentrated solutions of acrylamide (8 M) and sodium iodide (7 M), the latter with ca. 0.1 mM sodium thiosulfate added to prevent I_3-formation. NaCl was used in controls to account for ionic strength effects . Iodide quenching curves were analyzed to obtain the fluorescence fraction (F_{ex}) of relatively exposed Trp residues of the protein as described (Edwards and Silva 1986) using plots of $F_o/(F_o\text{-}F)$ vs. $1/[Q]$ from the Lehrer equation (Lehrer 1971). The intercept is taken as $1/F_{ex}$, where F_o and F are the fluorescence intensities in the absence and presence of quencher Q, respectively. The excitation wavelength was usually 295 nm with emission measured at 345 nm, using 1 and 5 nm slits, respectively.

Results and discussion

The normal metabolic degradation of tryptophan involves first an oxidative cleavage of the indole ring by molecular oxygen to form N-formyl-kynuren-

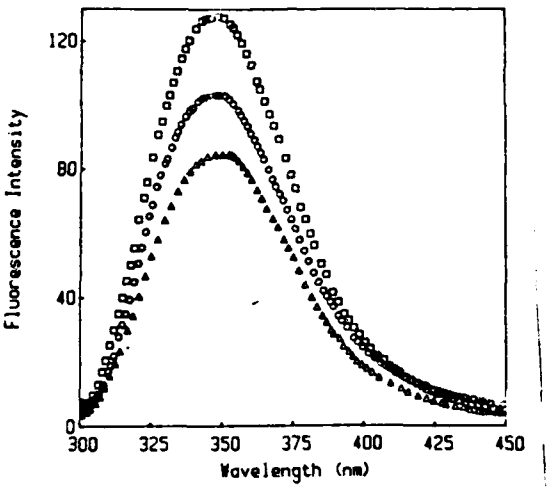

Fig. 1. Fluorescence spectra of lysozyme after 2.5 h irradiation at 25° with 337.1 nm laser radiation in buffer made with H_2O (O) or D_2O (Δ); compared to dark control (□). Excitation at 290 nm

ine, a reaction catalyzed by the enzyme tryptophan oxygenase. This is in turn converted to L-kynurenine. Some of the kynurenine is utilized for the synthesis of NAD but most is further degraded to anthranilic acid. It has been suggested that the photooxidation of tryptophan under our experimental conditions is not a direct photolysis but rather involved singlet oxygen generated under aerobic conditions (e.g., Borkman et al. 1986). The lifetime of singlet oxygen is longer in D_2O than in ordinary H_2O. Therefore, if this hypothesis is correct, photodegradation of tryptophan should be accelerated in D_2O; we investigated this as follows.

When lysozyme is irradiatd with the nitrogen laser at 337.1 nm, a decrease in the characteristic fluorescence of tryptophan is observed, indicating alteration of tryptophan (Fig. 1). (We also observed the progressive loss of absorbance and fluorescence as tryptophan in aqueous solution is photolyzed, as originally reported by Borkman et al. 1986.) If the irradiation buffer is made with D_2O instead of H_2O, the losses are considerably enhanced (ca. two-fold, Fig. 1; this is essentially due to the enhancement of the photooxidation rate of tryptophan in solution, cf. Borkman et al. 1986). A concomitant decrease in absorbance in the 250–300 nm band upon irradiation with approximately a two-fold greater decrease in the presence of D_2O is also seen. If singlet oxygen were involved, this result would be consistent with its longer lifetime in D_2O.

Additional evidence for oxygen involvement was obtained by comparing a normally irradiated sample (air in solution) with irradiated lysozyme in a solution which was contained within an evacuated and sealed cuvette. The tryptophan fluorescence decrease caused by irradiation was essentially suppressed compared to control. In a study of the 337.1 nm photolysis of tryptophan solutions (Borkman et al. 1986), degassing produced a very large reduction in the rate (< 1% of aerated rate).

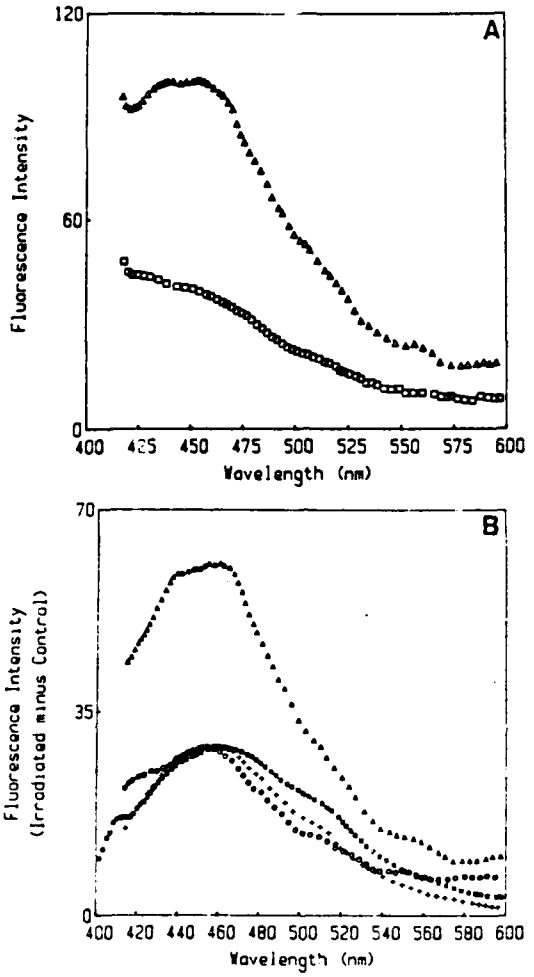

Fig. 2. A Fluorescence spectra of lysozyme after 2.5 h irradiation at 25° with 337.1 nm laser radiation in buffer made with D_2O (△), compared to dark control (□). Excitation at 360 nm. **B** Fluorescence difference spectra (irradiated minus dark) of lysozyme after 2.5 h of 337.1 nm irradiation at 25° in buffer made with D_2O (△) or H_2O (○), and of tryptophan with H_2O (+). The spectrum of chemical mixture of NFK + KYN (ca. 3:1 molar ratio) is presented for comparison (■). Excitation at 360 nm

Concomitant with the loss of tryptophan in lysozyme is the appearance of fluorescent photoproducts with emission maxima in the 440–480 nm range, with a shoulder near 510–520 nm (Fig. 2a). There is also an increase in absorbance in the 300–400 nm range due to absorbance by photochemically-generated products (Fig. 3, inset); maximum in the difference absorption spectrum of irradiated vs. dark control was typically 310–320 nm. It is known, for example, that NFK and KYN absorb with maxima at about 318 and 360 nm, respectively. Fluorescence difference spectra demonstrate enhancement of daughter product formation of D_2O (Fig. 2b). For comparison, the spectrum of photoproducts formed by irradiation of tryptophan in solution, and the spectrum of a mixture of NFK and KYN are presented by normalizing to the maxima at 460 nm where the molar extinction is

6

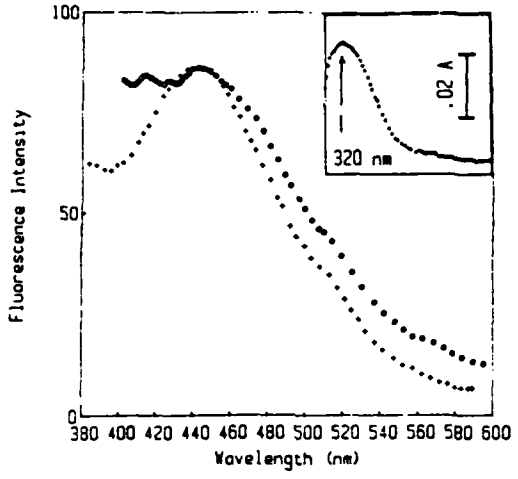

Fig. 3. Fluorescence spectra of lysozyme (O) and tryptophan (+) after 3.5 h irradiation with 337.1 nm laser radiation at 25°. Excitation at 322 nm. Inset: Difference absorption spectra (irradiated vs. dark control) for lysozyme (D_2O buffer) exposed to 2.5 h 337.1 nm radiation, measured at 0.2 mg.ml (10 × dilution of concentration used for irradiation)

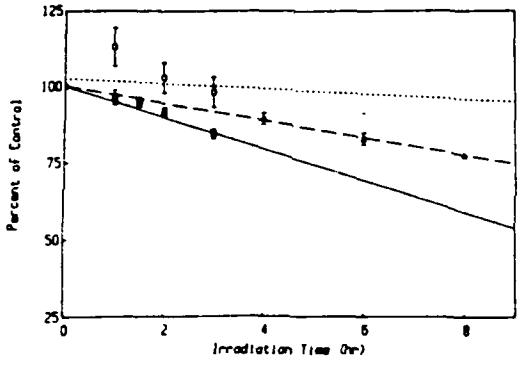

Fig. 4. Changes in lysozyme fluorescence (closed symbols, excitation at 290–295 nm) and enzyme activity (open symbols), expressed as percent of control, resulting from exposure to 337.1 nm laser radiation. Square: 37° C; triangle: 16° C

ca. 8000 for both. Under these excitation conditions (360 nm), kynurenine emission would, if anything, be favored, suggesting that the ratio of NFK to KYN in the irradiated lysozyme may be even higher. Excitation at 320 nm results in an emission maximum of 440 nm, close to that of NFK in solution and the spectrum of an irradiated tryptophan solution (Fig. 3). Examining the time dependence of the loss of tryptophan fluorescence in lysozyme with irradiation, the rate was found to increase ca. two-fold at 37° C compared to 16° C, perhaps reflecting the effect on a diffusing reactive species (Fig. 4). The rate reported for photooxidation of tryptophan in solution was about three times faster at 50° C compared to 25° C; photoionization was not believed to be responsible, though not strictly ruled out (Borkman et al. 1986). Regarding mechanism, the results for 337.1 nm irradiation of tryptophan (Borkman et al. 1986) point to either *1*) initial absorption by a long wavelength absorption tail of tryptophan itself which results in photoproduct-sensitizer formation, or *2*) absorption by an "impurity" sensitizer which could not be purified or detected by HPLC. Our own HPLC data

for tryptophan were consistent with both possibilities. Our detection limits were ca. 10^{-6} M for the case of NFK or KYN; when NFK is specifically added as a photosensitizer, it is generally ca. 2×10^{-4} M (e.g., Walrant and Santus 1974). Measurement of the absorption of 10 mM Trp in HPLC grade H_2O using a 10 cm quartz cuvette showed absorption at least to 340–350 nm, although it was indeed very weak ($\varepsilon_m < 10$). We did not attempt any further characterization of the primary mechanism.

It has been noted that the action of singlet oxygen is more efficient for protein residues relatively exposed and accessible to the solvent (Edwards and Silva 1985, references therein). Trp-62 is well exposed, while the Trp-108 is well buried in the protein core; also it is well known that 85–90% or more of the fluorescence of lysozyme arises from Trp-62 and Trp-108 (Imoto et al. 1971; Formoso and Forster 1975).

Using fluorescence quenching techniques (Eftink and Ghiron 1981), we analyzed lysozyme samples which had been photoirradiated for short times in an effort to determine if any of these fluorescent Trp residues were favored as targets of attack. With acrylamide as quencher, the Stern-Volmer constant was reduced from 4.8 M^{-1} (dark control) to 3.7 M^{-1} (Fig. 5a, calculated from the slope of F_o/F vs. [quencher], where F_o is the initial unquenched intensity of Trp fluorescence). Acrylamide is an efficient quencher and is able to penetrate to the interior of most proteins. If all fluorescent Trp residues were photooxidized uniformly, then only the initial unquenched intensity would be altered, not the quenching curve or Stern-Volmer constant. Thus, observation of a reduced quenching constant is consistent with the preferential loss of accessible residue.

To further investigate the relative participation of the Trp residues in photooxidation, quenching by sodium iodide was also utilized, since it has been demonstrated to preferentially suppress only the fluorescence of relatively exposed tryptophan residues of proteins (Lehrer 1971; Edwards and Silva 1986). When the Stern-Volmer data for iodide quenching are replotted according to the so-called Lehrer Equ. ($F_o/(F_o-F)$ vs. 1 [NaI], the reciprocal of the Y-intercept is interpreted as the fluorescence fraction of the exposed residue(s). The data of Fig. 5b show that the lysozyme sample irradiated for 1 h at 37° C has a reduced fluorescence fraction compared to dark control. The average of 5 such plots yields at $13 \pm 3\%$ decrease. Since Trp-62 is well exposed and Trp-108 is deeply buried in the protein, it seems reasonable to assign the former as the primary initial site of attack of 337.1 nm photooxidation. Singlet oxygen attack would also be favored at exterior sites. We observed a decided enhancement of photooxidation rate in D_2O, a factor consistent with, though not proving, such a mechanism. If the 13% fractional decrease in fluorescence calculated from iodide quenching data is related to Trp-62 and if this residue is assumed as a first estimate to account for approximately 40–45% of the total lysozyme fluorescence ($1.2 \times 85\%$, for Trp-62 + Trp-108), then this translates to a 5–6% decrease of total fluorescence after one hour ($0.13 \times 45\%$). This compares well with the value for total fluorescence loss of ca. 5% after one hour shown in Fig. 4.

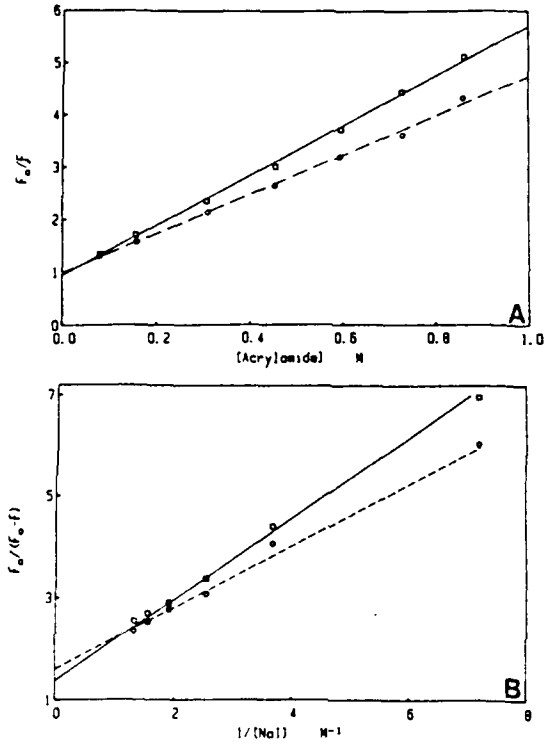

Fig. 5. A Stern-Volmer plot for acrylamide quenching of the fluorescence of lysozyme exposed for 1.5 h to 337.1 nm radiation (O), and of dark control (□). Excitation at 295 nm. B Modified Stern-Volmer plot for iodide quenching of the fluorescence of lysozyme exposed for 1.0 h to 337.1 nm radiation (O), and of dark control (□). Excitation at 295 nm

Using absorption data (e.g., Fig. 3, inset) and the molar extinction coefficient of NFK ($\varepsilon_{313} = 3{,}180\ M^{-1}cm^{-1}$; Walrant and Santus 1974), an approximate upper limit to the molar ratio of "daughter product" to lysozyme was always < 1. This assumes, as the spectra suggest, that a significant proportion of the product is NFK. Even for the 2.5 h D_2O sample, the value was ≤ 0.5. This of course does not by itself certify that only one specific Trp is altered, but a very much larger value would have inconsistent with this.

Since it appeared that Trp was photoconverted to NFK and KYN and since our dialysis and forced dialysis experiments indicated that the "daughter products" remain associated with the protein, we were interested in performing similar fluorescence experiments to see if quenching data were consistent with an external site for these species as well. However, this proved to be unfeasible as we did not observe any significant quenching of KYN alone in solution. Measurements of the fluorescence lifetime (τ) of NFK and KYN using a phase and modulation fluorometer indicated that a major lifetime component for each of these compounds is too short ($\tau \leq 0.1$ ns; cf. tryptophan, $\tau = 3$ ns) to be effectively quenched.

Measurements of enzymatic activity indicated essentially no change during irradiation at 37° C, even with exposure times producing significant

loss in tryptophan fluorescence (at least up to 3 h at 37° C, Fig. 4, open symbols). We did not attempt analysis of longer term effects as the scope of our study was limited to photoinduced effects present under low conversion percentage conditions. As indicated above, the 337.1 nm irradiation appears to initially affect primarily the more exposed Trp-62 residue. When Trp-62 is radically and rapidly oxidized by N-bromosuccinimide to the oxindole (Hayashi et al. 1965), enzyme activity is reduced to very low levels. As X-ray crystal data suggest, apparently Trp-62 decidedly moves to somehow block the active site groove but still allows inhibitor binding (Blake et al. 1978). However, under our conditions, the more limited photooxidation of Trp proceeds in large part only as far as the NFK stage, apparently less disturbing to the structural or charge configuration of the active site. The apparent initial increase in enzymatic activity (Fig. 4) may reflect a structural alteration near the active site (perhaps due to Trp 62 to NFK conversion and/or limited unfolding) leading to increased access to the substrate. Further study of this could be productive.

Acknowledgements. Thanks are due to R. Boriack, R. Goodson and Daryl Ussery for expert technical assistance, to Dr. D. Jameson for use of his fluorescence lifetime instrument, and Drs. R. Dowben and D. Nealon for valuable discussions. This work was supported by ONR FEL Contract N0014-86-K-0186.

References

Auerbach VH, Knox WE (1957) L-kynurenine and N-formyl-L-kynurenine. Methods Enzymol 3:620–623

Blake CCF, Grace DEP, Johnson LN, Perkins SJ, Phillips DC, Cassels R, Dobson CM, Poulsen FM, Williams RJP (1978) Physical and chemical properties of lysozyme. In: Porter R, Fitzsimons DW (eds) Molecular interactions and activity in proteins. Excerpta Medica, Amsterdam

Borkman RF, Hibbard LB, Dillon J (1986) The photolysis of tryptophan with 337.1 nm laser radiation. Photochem Photobiol 42:13–19

Donoso LA, Spikes JD (1980) Sheep liver β-N-acetylhexosaminidase: partial purification, characterization and photodynamic inactivation. Enzyme 25:111–117

Edwards AM, Silva E (1985) Photochemical reactivity of the homologous proteins α-lactalbumin and lysozyme. Radiat Environ Biophys 24:141–148

Edwards AM, Silva E (1986) Exposure of tryptophanyl residues in α-lactalbumin and lysozyme. Radiat Environ Biophys 25:113–122

Eftink MR, Ghiron CA (1981) Fluorescence quenching studies with proteins. Anal Biochem 114:199–227

Ferrer I, Silva E (1981) Isolation and photo-oxidation of lysozyme fragments. Radiat Environ Biophys 20:67–77

Formoso C, Forster LS (1975) Tryptophan fluorescence lifetimes in lysozyme. J Biol Chem 250:3738–3745

Gratton E, Jameson DM, Hall RD (1984) Multifrequency phase and modulation fluorometry. Ann Rev Biophys Bioeng 13:105–124

Grossweiner L (1976) Flash photolysis of enzymes. Int J Radiat Biol 29:1–16

Hayashi K, Imoto T, Funatsu M (1965) The position of the active tryptophan residue in lysozyme. J Biochem (Tokyo) 58:227–235

Imoto T, Forster LS, Rupley JA, Tanaka R (1971) Fluorescence of lysozyme: emissions from tryptophan residues 62 and 108 and energy migration. Proc Natl Acad Sci USA 69:1151–1155

Jori G, Galiazzo G, Tamburro AM, Scoffone E (1970) Dye-sensitized photooxidation as a

tool for determining the degree of exposure of amino acid residues in proteins. J Biol Chem 245:3375–3383

Lehrer S (1971) Solute perturbation of protein fluorescence. Biochemistry 17:3254–3263

McGarth H, Wilson WA, Scopelitis E (1986) Acute effects of low-fluence ultraviolet light on human T-lymphocyte subsets. Photochem Photobiol 43:627–631

McLaren AD, Shugar D (1964) Photochemistry of proteins and nucleic acids. Pergamon Press, Oxford, pp 110–161

Mandal K, Bose SK, Chakrabarti B (1986) Sensitizer-induced conformational changes in lens crystallin-I. Photodynamic action of methylene blue and N-formyl kynurenine on bovine α-crystallin. Photochem Photobiol 43:515–523

Parrish J, Jaenicke K, Anderson R (1982) Erythema and melanogenesis action spectra of normal human skin. Photochem Photobiol 36:187–192

Ray WJ, Koshland DE (1962) Identification of amino acids involved in phosphogluconitase action. J Biol Chem 237:2493–2505

Shugar D (1952) The measurement of lysozyme activity and the ultra-violet inactivation of lysozyme. Biochim Biophys Acta 8:302–310

Spikes JD (1977) Photosensitization. In: Smith KC (ed) The science of photobiology. Plenum Press, New York, pp 87–112

Straight R, Spikes JD (1985) Photosensitized oxidation of biomolecules. In: Frimer AA (ed) Singlet oxygen, Vol IV. CRC Press, Boca Raton, pp 91–143

Walrant P, Santus R (1974) Ultraviolet and N-formyl-kynurenine-sensitized photoinactivation of bovine carbonic anhydrase: An internal photodynamic effect. Photochem Photobiol 20:455–460

Yong S, Lau S (1979) Rapid separation of tryptophan, kynurenines, and indoles using reversed-phase high-performance liquid chromatography. J Chromatogr 175:343–346

LASER SPECTROSCOPIC STUDIES OF PROTEIN STRUCTURE AND FLEXIBILITY

Introduction

The most recent evidence on myosin reinforces the fundamental importance of the 'head' region of this protein in contractile function (Hynes et al., 1987). It appears that the flexibility and relative dynamic motional properties of the major structural 'subdomains' are functional in the contractile process. Thus, experiments have been undertaken with myosin labeled with specifically attached probes capable of monitoring (1) rather fast, 'localized' motions, as well as (2) relatively slower, 'global' rotations. Spectroscopically, these could be related to singlet-state (fluorescence) and triplet-state (phosphorescence) luminescence measurements. The photophysical properties of the probe eosin have been shown to be useful for both types.

Time-resolved biophysical studies have demonstrated that myosin heads are segmentally flexible about a swivel-like connection to the filamentous tail (Morales et al., 1982; Thomas et al., 1975). More localized 'internal' motions of the head region and any relationship to the enzymatic and contractile function as yet are not fully characterized but their existence is supported by proton NMR and transient electrical birefringence data (Highsmith et al., 1979; Highsmith and Eden, 1986).

As oxygen quenching and other data have shown, local 'internal' motions of the protein structure are not uncommon. Thus, they cannot always be accurately represented as a rigid hydrodynamic ellipsoid (Weber, 1976). Depending on the time scale monitored, the motions of the fluorophore, its 'environment', and the protein as a whole need to be incorporated into what has been termed a 'restricted flexible model' (Wahl and Weber, 1967).

We have initiated fluorescence anisotropy measurements of myosin labeled at specific sites with a probe of relatively short excited singlet lifetime in an effort to acquire additional information on the dynamics of such motions. Steady-state and time-resolved measurements were carried out at different excitation wavelengths in order to increase the information available on the probe's rotational modalities by photoselecting transition dipole moments exhibiting significantly different orientations (Wegener, 1985; VanderMeulen and Wegener, 1985; VanderMeulen et al., 1986). A portion of this work was presented recently (VanderMeulen et al., 1988) and an additional manuscript is in preparation.

Materials and Methods

Myosin was prepared from rabbit skeletal muscle according to the method of Tonomura et al., 1966 with minor modifications. Since it appeared that small amounts of other muscle proteins may be present in this preparation, and since fluorescence polarization results for myosin would be sensitive to the presence of non-specifically labeled low molecular weight impurities, we investigated ways to improve the preparation. It was found that pure myosin could be isolated using DEAE-cellulose ion exchange chromatography or an agarose-ADP affinity gel (P & L Biochemicals). Preparation purity was checked by SDS gel electrophoresis using the Pharmacia Phast-gel system and Coomassie blue staining of protein bands. Myosin ATPase activity was monitored by pH STAT measurements (White, 1982). With 0.1 mg myosin in 2.0 ml reaction mixture at 25°C (1 mM Tris-

maleate, 10 mM $CaCl_2$, 2mM ATP, pH 8) control activity was typically ca. 0.9 μmoles/min/mg.

Eosin Y lactone and eosin-5-maleimide (and related covalent thiol probes) were purchased from Aldrich and Molecular probes, respectively. Eosin was conjugated to myosin using the procedure of Kinosita et al., 1984. Unreacted probe (eosin) was removed by a 10 cm Sephadex G-25 "desalting" column or extensive dialysis against 0.5 M KC1, 5 mM MOPS (pH 7), and 0.1 mM EDTA. Myosin is soluble in such high salt conditions. Protein concentrations were measured primarily using UV absorption methods.

Excitation polarization spectra were recorded on a T-format fluorescence spectrometer. Perrin plots (described below) of free fluorophore or dye-protein conjugates were recorded by varying temperature in a 70% glycerol solution or varying viscosity with sucrose additions at 5°C.

Time-resolved fluorescence measurements were carried out using a multifrequency phase fluorometer based on the Gratton design (Gratton et al., 1984), located in the laboratory of Dr. D.M. Jameson, UTHSC, Dallas. In this technique the intensity of the exciting light is modulated at variable frequencies and the phase shift (P) and relative modulation (M) of the emitted light with respect to the excitation are determined. Phase and modulation lifetimes are calculated by:

$$\tan(P) = \omega\tau^{P} \qquad M = [1 + (\omega\tau^{M})^{2}]^{-\frac{1}{2}}$$

The data may be analyzed assuming a series of exponentials; the goodness of the fit is judged by the reduced chi-square defined as:

$$\chi^2 = \frac{1}{(2n - f - 1)} \sum \left\{ \left[\frac{P_c - P_m}{\sigma^P} \right]^2 + \left[\frac{M_c - M_m}{\sigma^M} \right]^2 \right\}$$

In addition to fluorescence lifetime determinations, the multifrequency phase and modulation method permits characterization of the rotational modes of the system (Weber, 1977; Mantulin and Weber, 1977). In the time domain such information is obtained by differential polarized phase fluorometry (also known as dynamic polarization). In this approach, the sample is illuminated by parallel polarized light, the intensity of which is modulated at high frequencies. The phase decay between the parallel and perpendicular components of the emission $\varphi(\|)$, $\varphi(\perp)$ are determined and the differential tangent function ($\Delta\phi$) may be calculated as (Gratton et al., 1984):

$$\Delta\phi = \tan\phi(\|) - \tan\phi(\perp)$$

where

$$\Delta\Phi = \tan^{-1} \frac{3\omega rR}{[(k^2 + \omega^2)(1 + r - 2r^2) + R(R + 2k + kr)]}$$

where r is the limiting anisotropy, R the rotation rate, k the radiative decay rate ($1/\tau$) and ω the angular modulation frequency.

The corresponding expression for the differential modulation ratio is:

$$Y^2 = \frac{\left\{\left[k + \frac{6R}{(1-r)}\right]^2 + \omega^2\right\}}{\left\{\left[k + \frac{6R}{(1+2r)}\right]^2 + \omega^2\right\}}$$

where $Y = M_2/M_1$ and and M_2 and M_1 are the respective demodulation ratios for the parallel and perpendicular emitted components.

Analysis of the phase delay (or modulation ratio) versus frequency curves thus permits one to characterize the fluorophore's rotational parameters. The data can be fit to a range of rotator models including anisotropic rotators and combination of global and local rotations which have been demonstrated in a number of fluorophore-protein cases.

Results and Discussion

Excitation polarization spectra for fluorophores typically demonstrate wavelength dependence of the intrinsic polarization, P_0 (or limiting anisotropy, r_0). Excitation into the lowest energy absorption band typically yields high (positive) r_0 values, whereas absorption by higher energy bands with differing orientation of the transition dipole may produce negative values. Accordingly, Fig. 1 shows excitation polarization spectra with eosin-5-maleimide adducts of myosin and ('control') spectra with eosin linked to N-acetyl-cysteine. It is significant that the eosin probe retains the key features of wavelength dependence of dipole orientation upon binding to the protein. We have studied the anisotropic rotations of the myosin 'head' region utilizing the wavelength dependence of eosin conjugated to a specific binding sites on myosin (reactive SH_1 thiol, Fig. 2).

Rotational information from steady-state measurements was obtained using Perrin-Weber anisotropy plots obtained by varying solvent viscosity and/or temperature. Isothermal plots have the advantage of eliminating effects of activating thermal protein rotational modes. The data in Figs. 3 and 4 show the effects of varying solvent viscosity (n) on the fluorescence anisotropy eosin, presented in a format normalized to the value of r_0 (limiting value when dye motion is 100% restricted). Comparison of Figs. 3 and 4 shows that eosin in solution has isotropic photophysically-evidenced hydrodynamics (no detectable differences in rotational behavior even when markedly different orientations of absorption dipole are excited), whereas restricted motion and anisotropic rotations are exhibited by the protein bound probe.

Time-resolved measurements, including lifetime and dynamic polarization, were made using multifrequency phase and modulation fluorometry. Multiple excitation wavelengths were used (e.g., 514 and 351 nm for eosin), again corresponding to positive and negative limiting anisotropy. Data for measurement of fluorescence lifetimes are presented in Fig. 5. As expected, the lifetimes are essentially insensitive to changes in excitation wavelength for both free and protein bound dye (see summary of results in Table 1). We see only the typical lengthening of the lifetime upon binding (1.2 ns for free probe, 2.2 ns when bound to myosin). Thus, these control data show that any differences in rotational information based on wavelength-dependent fluorescence polarization data are not due to 'trivial' changes in excited state lifetime.

As with the steady-state anisotropy data (above), differential phase measurements (dynamic polarization data, see Materials and Methods) show clear wavelength-dependent differences in the apparent rotational modes of bound probe (Figs. 6 & 7). For 514 or 351 nm

excitation of free eosin, rotation is essentially isotropic, with a Debye rotational relaxation time of ca. 0.4 ns.

Bound to the SH_1 thiol of myosin, however, two components are evident for 514 nm and 351 nm; see Table 1 for data summary. The fractional weighting of the faster rate was much smaller for 351 nm (<10%) than for 514 nm (>40%), evidence for highly anisotropic rotation. For comparison, dynamic polarization data for eosin Y in 90% propylene glycol are shown in Fig. 8 and Table 1. As with aqueous buffer, the rotational behavior is essentially isotropic, with the rates of rotation for both excitation wavelengths slowed by a little more than an order of magnitude, from ca. 0.5 ns to 10-15 ns, as expected for the more viscous environment. Comparison with the eosin--myosin data suggests that when bound to myosin, restricted and anisotropic rotational modes are exhibited for this probe attached to the SH_1 thiol region. The apparent rotational rates are wavelengths dependent. Excitation with both 351 and 514 nm reveal a very slow rotational component (> 0.1 μs) no doubt due to the global motion of the large (MW ≈ 480,000) protein. In addition, excitation into the 514 nm dipole direction results in a relatively fast subnanosecond component, similar to the rate for freely rotating eosin in aqueous solution. On the other hand, excitation into the 351 nm dipole direction (approx. normal to the visible transition). reveals a somewhat slower restricted rotation of a few nanoseconds. For perspective, the latter can be compared to the ca. 10 ns rate measured for free eosin in viscous solution (Fig. 8).

Conclusions and Projections

1. The lifetime and apparent rotational relaxation times of eosin in aqueous solution are essentially invariant with excitation wavelength. In more viscous solvents such as propylene glycol/water mixtures the apparent rotational rates differ upon excitation in the regions of positive and negative anisotropy.

2. Using eosin attached to the SH_1 thiol of the myosin head, we have detected differing rotational modes of the bound probe dependent upon excitation wavelength. A rigorous model which accounts for all the steady-state and time-resolved observations may require a more complete global analysis. In addition, further comparative examination of eosin and help in relating spectroscopic data to specific structural and dynamic parameters.

3. We anticipate that application of this excitation wavelength dependent approach will provide additional information on the potential physiological relevance of such motions such as the effects of nucleotide and actin binding. As these motions are determined probes and additional labeling sites on myosin and its subfragments will also be examined.

4. FEL Measurements. As discussed in previous reports, we plan to utilize both in-house and FEL laser sources to implement the experimental program. The FEL source is to be used in conjunction with phosphorescence-type measurements studying the slower time base motions of the protein.

On October 9, 1987, a detailed site visit was made at the Stanford MKIII FEL. The current instrumental configuration, as well as specific optical parameters were analyzed to determine the most efficient way to interface to our experimental setup. Then, in November, Dr. G. Lin and Dr. D.L. VanderMeulen conducted an experimental site visit with several pieces of specialized instrumentation brought from our laboratory. Some data on the FEL pulse structure and our gating mechanism were taken. This visit was useful in helping determine the best strategy for acquiring luminescence data on an actual labeled protein sample on the next visit. The date of this experimental trip has been on hold

pending the outcome of certain instrumental modifications. Drs. G. Lin of Baylor and S. Benson of Stanford have been communicating in this regard.

We plan to make two types of time-resolved luminescence measurements in the microsecond-to-millisecond time range of myosin and myosin subfragments labeled specifically at the SH_1 thiol of the head region with eosin-5-maleimide, eosin-5-iodoacetamide, and erythrosin-5 iodoacetamide. (Measurement with more than one type of covalent linking group provides evidence concerning its influence, if any.) Later, additional sites of labeling on the myosin head (different sub-domain regions) can be examined.

(1) Phosphorescence

The labeled protein is excited with the 2 μs macropulses at 15 Hz, selecting the sixth harmonic with filters (ca. 500 nm, well within the absorption band of both eosin and erythrosin). Using the gated PMI instrumentation (Fig. 9), the phosphorescence decay is recorded. With proper selection of excitation and emission polarizer orientation, anisotropies of decay, hence corresponding macromolecule motions are thereby monitored.

(2) Fluorescence Recovery

In this measurement mode, the intense FEL macropulse at 500 nm is used to pulse the sample labeled with luminescence probe. Under conditions favorable for the stabilization of the triplet state, this results in the depletion of the ground singlet state population (which is responsible for any observed fluorescence when the sample is excited). Thus, immediately after the macropulse, if the sample is 'probed' with a steady-state light beam of moderate intensity (e.g., with small monochromator/xenon lamp unit), the resulting fluorescent signal is lower than it would be if there had been no macropulse stimulation. With time, the excited triplet state population declines, resulting in a gradual return of the ground state singlet levels to its pre-pulse level. This can be followed in a sensitive manner by monitoring the corresponding rise in fluorescence intensity. With the use of polarizers, the anisotropy of motion of the system can be measured. By following the return of fluorescence with excitation at both 350 and 500 nm (e.g., for eosin), a greater level of '3-D' dynamic information is recovered, since two transition dipoles of distinct physical orientation are utilized.

References

Gratton, E., Jameson, D.M. and Hall, R.D. (1984) Ann. Rev. Biophys. Bioeng. 13, 105.
Highsmith, S. and Eden, D. (1986) Biochemistry 25, 2237.
Highsmith, S., Akasaka, K., Konrad, M., Goody, R., Holmes, K., Wade-Jardetzky, N., and Jardetsky, O. (1979) Biochemistry 18, 4238.
Hynes, T.R., Block. S.M., White, B.T., and Spudich, J.A. (1987) Cell 48, 953.
Kinosita, K., Jr., Ishiwata, S., Yoshimura, H., Asai, H. and Ikegami, A. (1984) Biochemistry 24, 5963.
Mantulin, W.W. and Weber, G. (1977) J. Chem. Phys. 66, 4092.
Morales, M.F., Borejdo, J., Botts, J., Cooke, R., Mendelson, R.A. and Takashi, R. (1982) Ann. Rev. Phys. Chem. 33, 319.
Thomas, D.D., Seidel, J.C., Hyde, J.S. and Gergely, J. (1975) PNAS 72, 1724.
Tonomura, Y., Appel, P. and Morales, M. (1966) Biochemistry 5, 515.
VanderMeulen, D.L., Nealon, D.G. and Jameson, D.(1988) Biophys. J. 53, 87.
VanderMeulen, D.L. and Wegener, W.A. (1985) Biophys. J. 47, 467.

VanderMeulen, D.L., VanderMeer, B.W., Thomas, V. and Jameson, D.M. (1986) Biophys. J. 49, 334.
Wahl, P. and Weber, G. (1967) J. Mol. Biol. 30, 371.
Weber, G. (1976) in Excited States of Biological Molecules (Birks, J.B., ed.), Wiley, London, 363.
Weber, G. (1977) J. Chem. Phys. 66, 4081.
Wegener, W.A. (1984) Biophys. J. 46, 795.
White, H.D. (1982) Methods in Enzymol. 85B, 698.

SUMMARY OF LIFETIMES(τ) AND DEBYE ROTATIONAL RELAXATION TIMES(ρ) FOR EOSIN Y AND EMI-MYOSIN

	Excitation Wavelength (nm)							
	514				351			
Lifetimes (ns)	τ_1	f_1#	χ^2		τ_1	f_1#	χ^2	
Eosin Y:								
Buffer*	1.16	0.99	3.91		1.18	1.02	2.77	
Propylene Glycol/H_2O	2.47	1.00	2.65		2.41	1.02	6.94	
EMI-Myosin:								
Buffer*	2.16	0.99	1.13		2.25	1.01	2.19	
Debye Rotational Relaxation Times (ns)	ρ_1	a_1	ρ_2	a_2	ρ_1	a_1	ρ_2	a_2
Eosin Y:								
Buffer*	0.57	0.36	-	-	0.45	-0.125	-	-
Propylene Glycol/H_2O	15.6	0.36	-	-	10	-0.125	-	-
EMI-Myosin:								
Buffer*	390	0.21	0.42	0.15	150	-0.115	2.50	-0.010

* Buffer consisted of: 0.5M KCl, 10mM MOPS (pH 7.0), 0.2mM EDTA

In some cases a small scattering component was used with τ_2 fixed at 0.001 ns in order to improve the fit.

TABLE 1

EXCITATION POLARIZATION SPECTRA FOR EOSIN-5-MALEIMIDE ADDUCTS OF N-ACETYL-CYSTEINE AND MYOSIN AT 5 °C

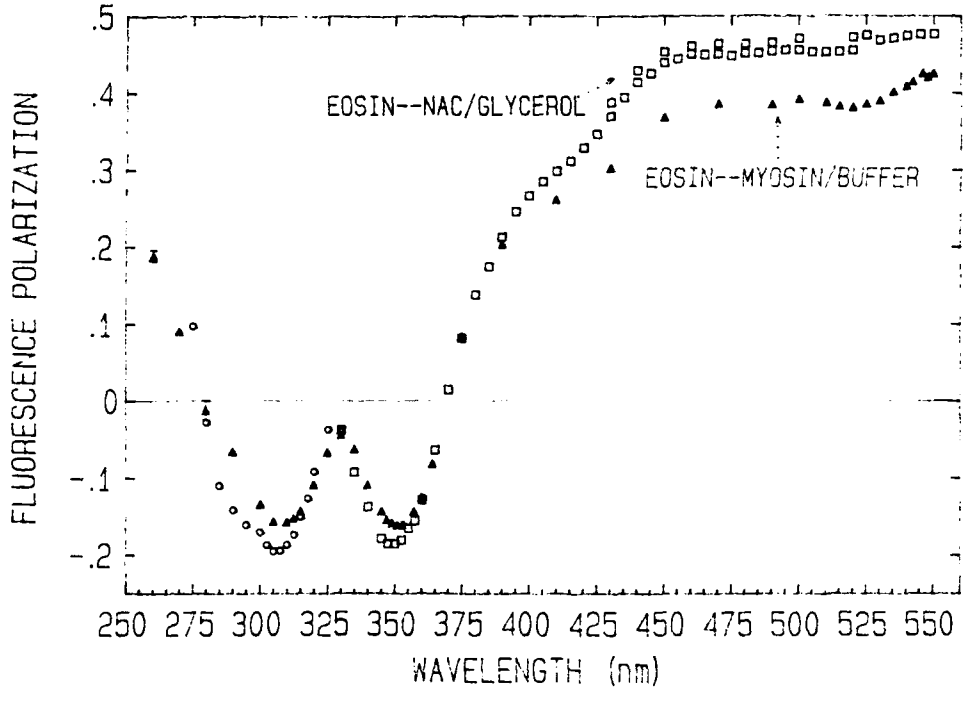

FIGURE 1

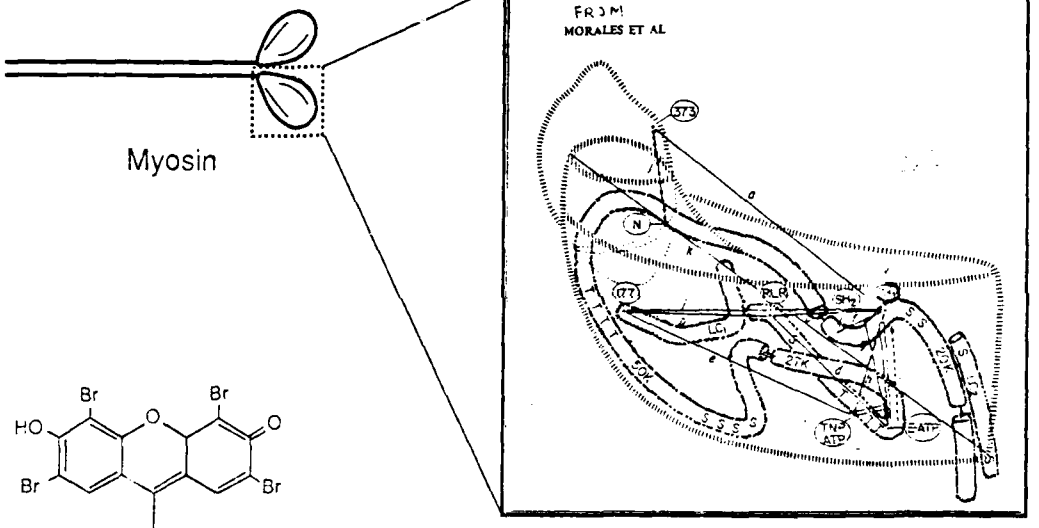

Expanded View of Myosin Head Region Containing the Eosin-Labelled SH_1

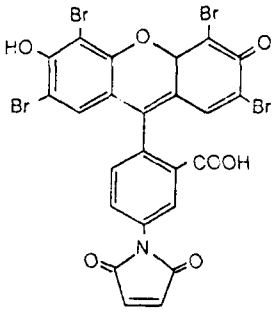

Eosin-5-Maleimide

FIGURE 2

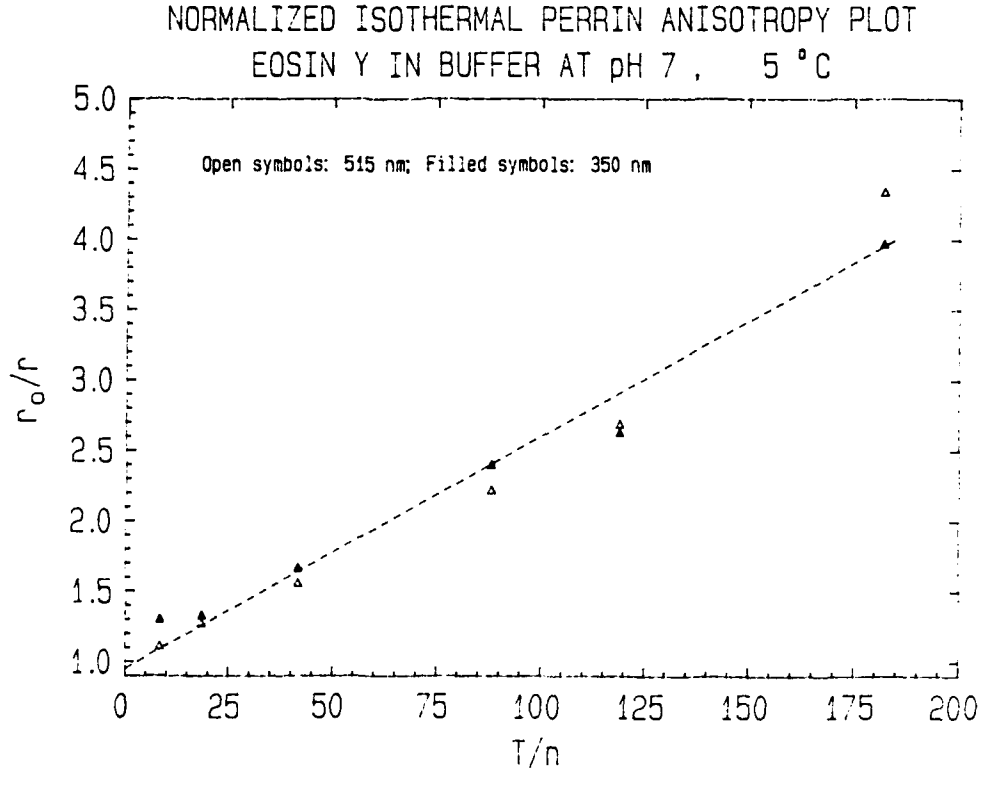
NORMALIZED ISOTHERMAL PERRIN ANISOTROPY PLOT
EOSIN Y IN BUFFER AT pH 7 , 5 °C
Open symbols: 515 nm; Filled symbols: 350 nm
r_o/r
5.0
4.5
4.0
3.5
3.0
2.5
2.0
1.5
1.0
0
25
50
75
100
125
150
175
200
T/n

FIGURE 3

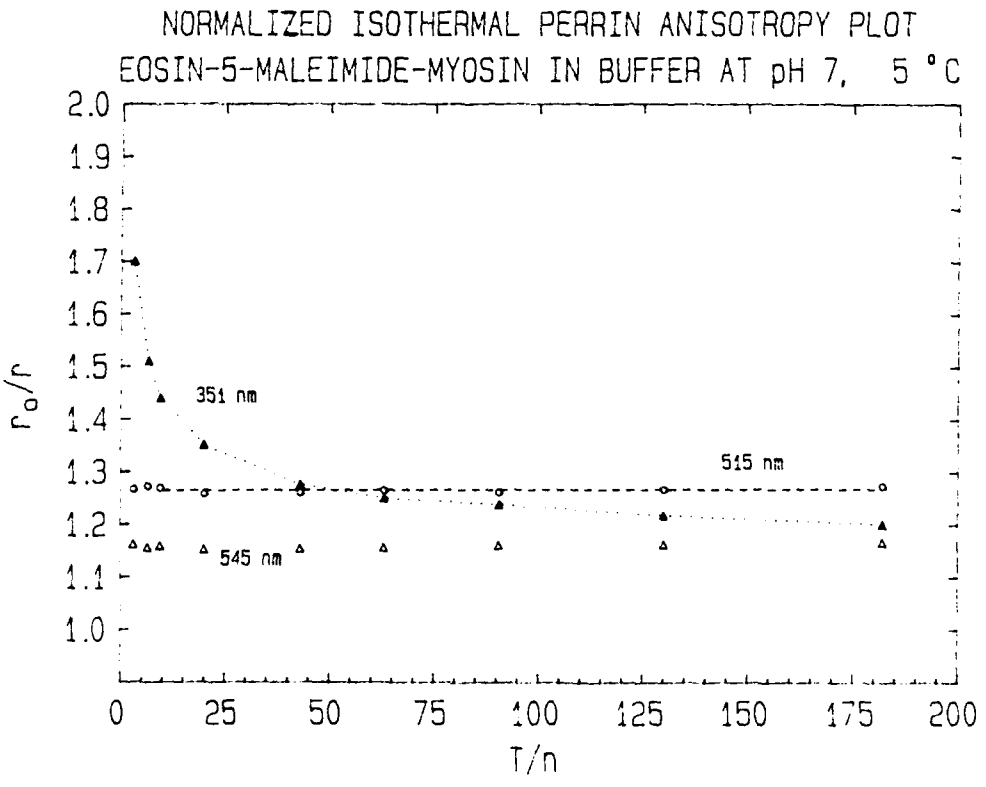
NORMALIZED ISOTHERMAL PERRIN ANISOTROPY PLOT
EOSIN-5-MALEIMIDE-MYOSIN IN BUFFER AT pH 7, 5 °C
2.0
1.9
1.8
1.7
1.6
1.5
1.4
1.3
1.2
1.1
1.0
r_o/r
351 nm
515 nm
545 nm
0
25
50
75
100
125
150
175
200
T/n

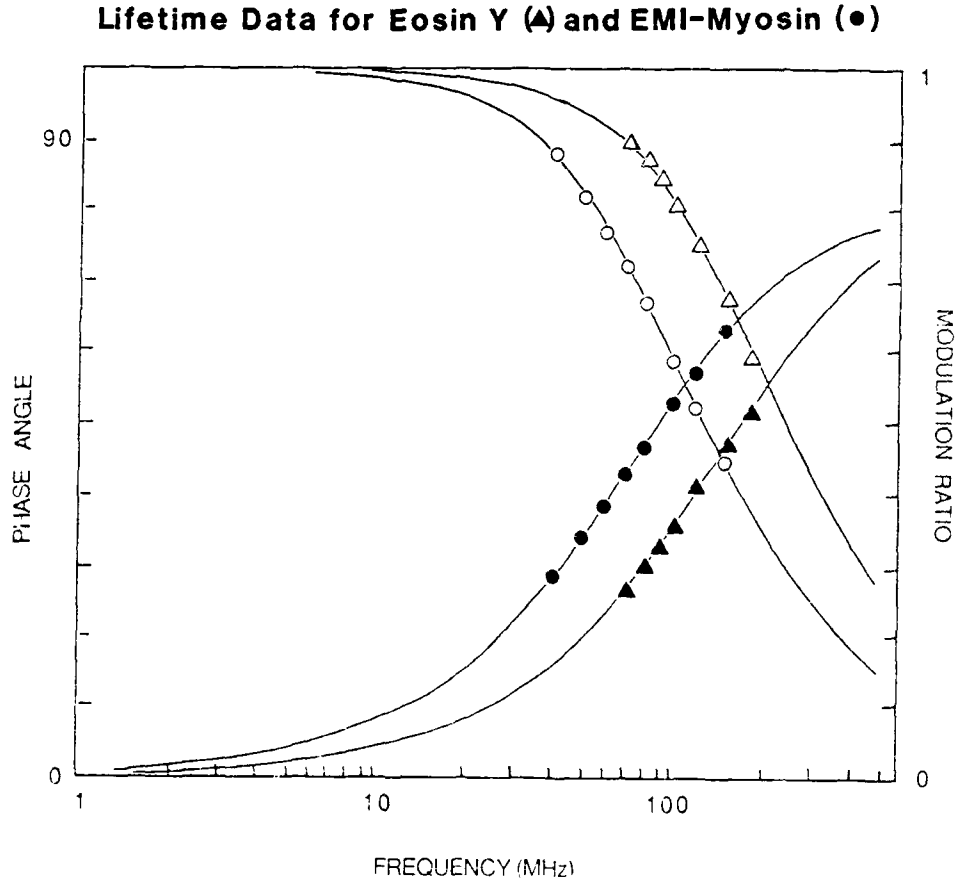
Lifetime Data for Eosin Y (▲) and EMI-Myosin (●)
90
0
PHASE ANGLE
1
0
MODULATION RATIO
1
10
100
FREQUENCY (MHz)

FIGURE 5

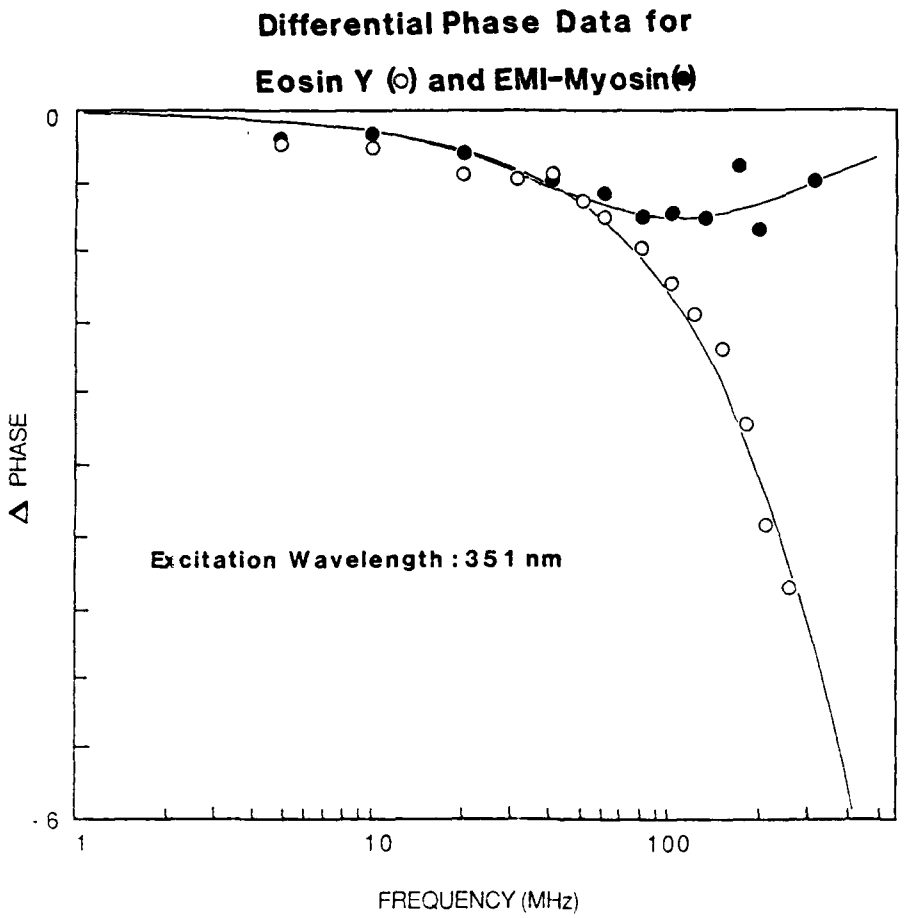
Differential Phase Data for
Eosin Y (o) and EMI-Myosin(●)
0
-6
Δ PHASE
Excitation Wavelength : 351 nm
1
10
100
FREQUENCY (MHz)

FIGURE 6

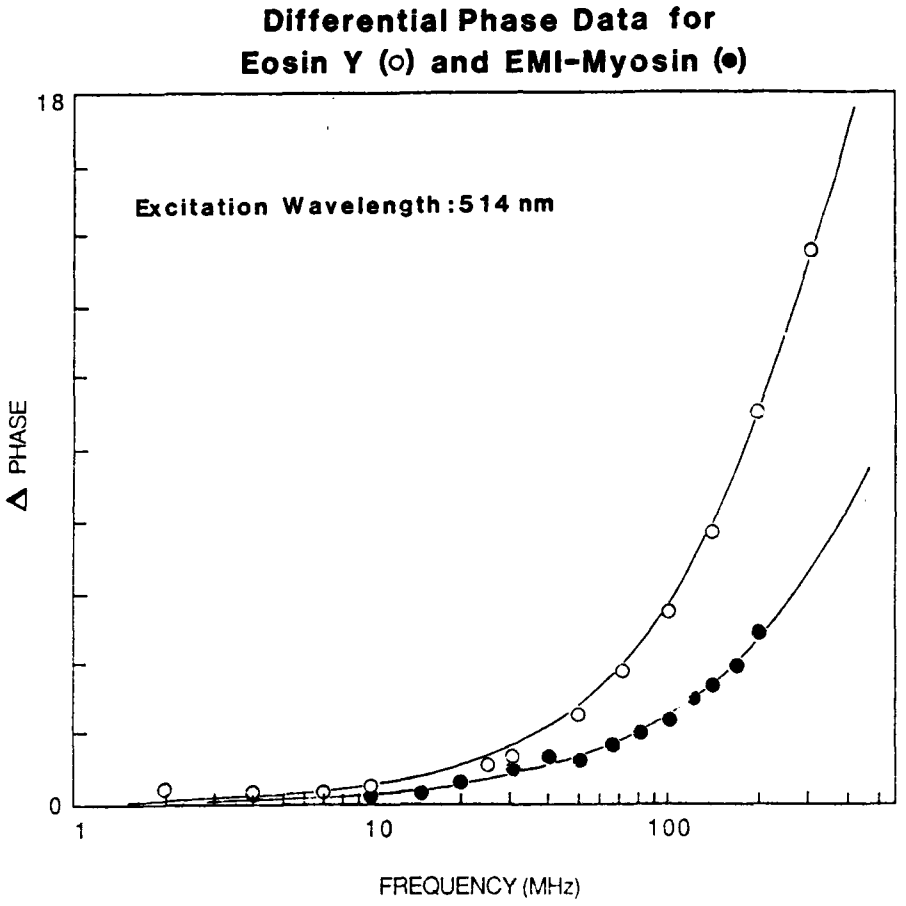
Differential Phase Data for
Eosin Y (o) and EMI-Myosin (•)
Excitation Wavelength : 514 nm
Δ PHASE
18
0
1
10
100
FREQUENCY (MHz)

FIGURE 7

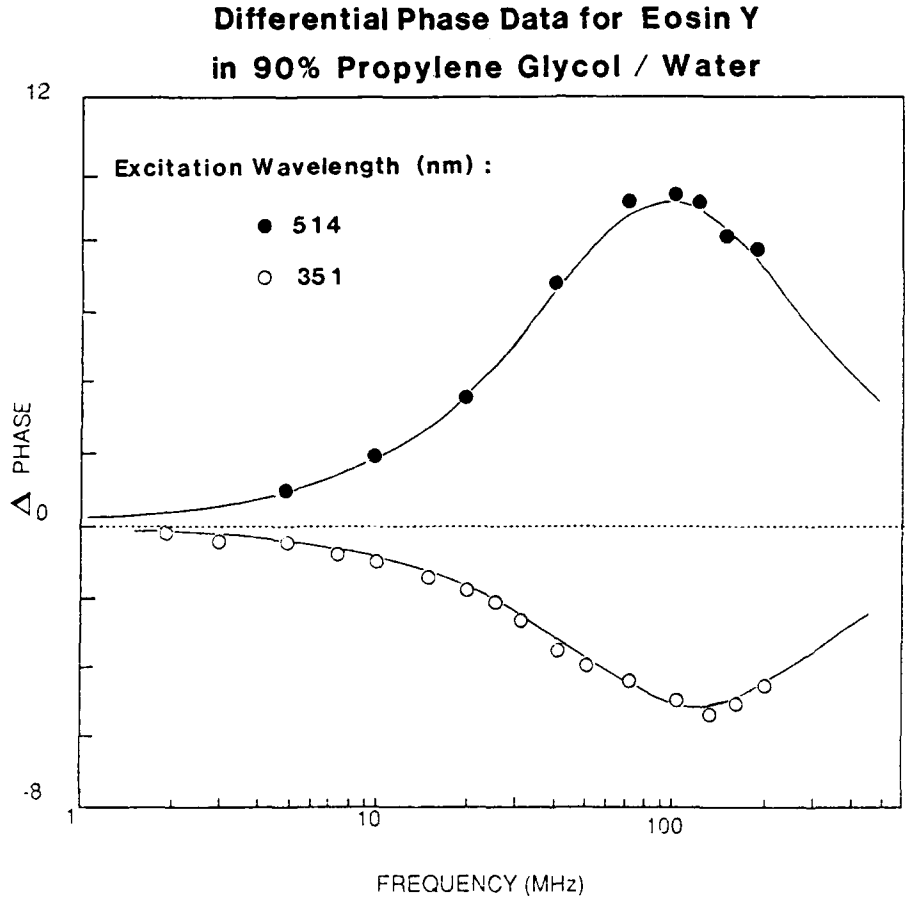
Differential Phase Data for Eosin Y
in 90% Propylene Glycol / Water
12
Excitation Wavelength (nm) :
514
351
Δ0 PHASE
-8
1
10
100
FREQUENCY (MHz)

FIGURE 8

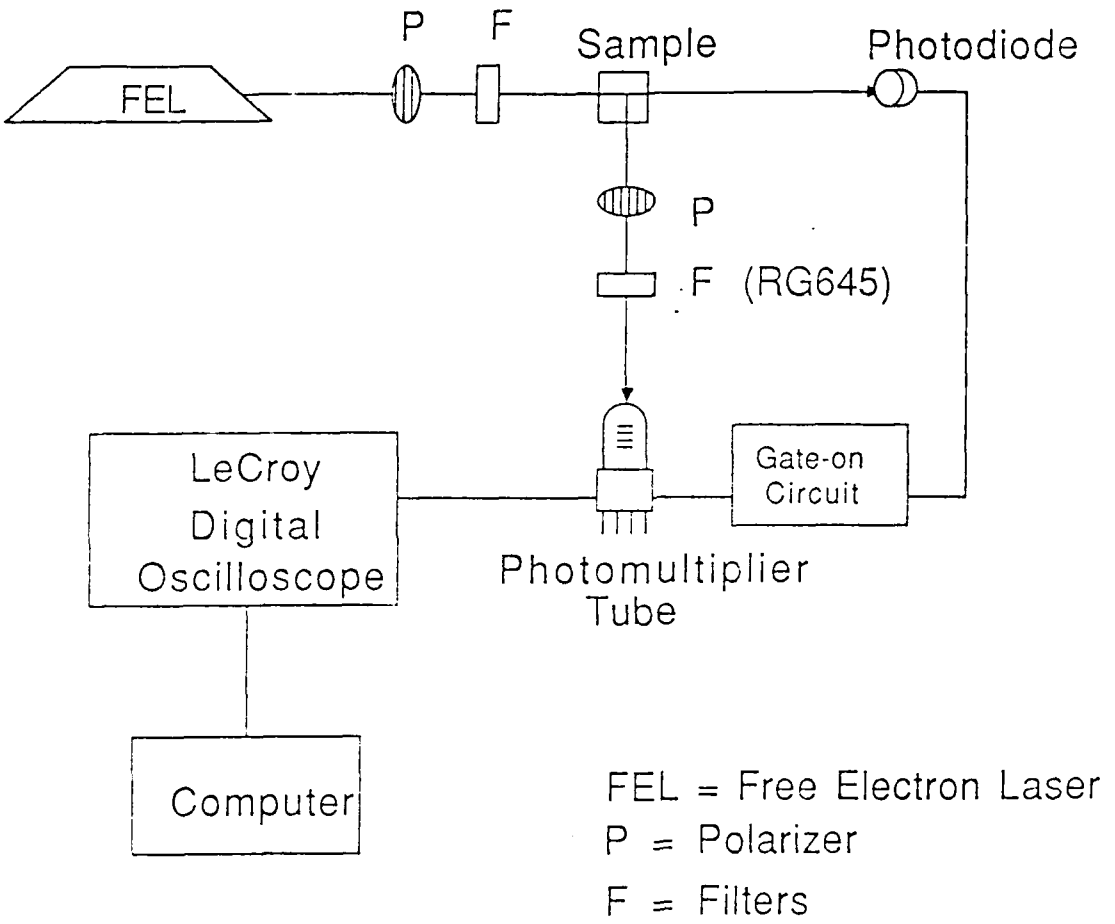
P
F
Sample
Photodiode
FEL
P
F (RG645)
LeCroy
Digital
Oscilloscope
Gate-on
Circuit
Photomultiplier
Tube
Computer
FEL = Free Electron Laser
P = Polarizer
F = Filters

FIGURE 9

SPECTROSCOPIC CHARACTERIZATION OF SIX NEW NOVEL FLUORESCENT PROBES

Objectives

Although quite a few organic dyes already exist which have been proved to be effective in photodynamic therapy for cancer cell kill, e.g., hematoporphyrin and its many derivatives, the existing compounds are mostly unpurified and the effective ingredient is not known. Some of these compounds have also proved to posses undesirable side effects. The search for better dyes with no or the least toxicity and more desirable spectral characteristics is an essential task that we are continuing to pursue.

We have recently synthesized more than a dozen new fluorescent probes in our laboratory. These probes fall in general to two groups: julolidino coumarin and pyrene sulfonyl derivatives, with a variety of functional groups substituted in various positions.

The objective in our synthetic strategy is to obtain probes that have longest red shift and high extinction coefficient for potential application in photodynamic therapy for killing tumor cells and cells infected by various pathogens. Obtaining dyes with long red shift is beneficial from clinical standpoint because it offers the deepest light penetration possible in the tissue.

The main purpose of the present study are (1) to characterize the absorption and fluorescence spectral properties of these novel probes; (2) to try correlating spectral characteristics with (a) the position of the substituents and (b) the type of functional groups; and (3) to investigate the potential application in photodynamic therapy as well as in hydrodynamic studies of protein macromolecular assembly.

Methods and Materials

Of the more than 20 dyes that have been synthesized thus far and their absorption and fluorescence spectral properties characterized, six compounds appear to be most promising. These six probes are (1) 1,3-diacetyloxy 6,8-dichlorosulfite pyrene; (2) 1,3-dihydroxyl 6,8 disodiumsulfonate pyrene; (3) 1,3-disodiumsulfonate pyrene; (4) 3-acetic acid 4-methyl [7-julolidino]coumarin; (5) 3-carboxylic acid 4-methyl [7-julolidino]coumarin; and (6) 3-methylcarboxylate [7-julolidino]coumarin. The chemical structure of these compounds are shown in Figure 1.
Of these six probes, the two disodiumsulfonate pyrene derivatives (compounds 2 & 3) and the 3-acetic acid coumarin derivative (compound 4) are water soluble. They were dissolved in 12.5 mM sodium phosphate buffer (pH 7.2) to a stock solution of 0.05 mM. For the rest three non-water soluble derivatives, they were dissolved in 100% dimethylforamide (DMF) in 0.1 mM concentration (the two coumarin derivatives, compounds 5 & 6) or 2.5 mM (pyrene compound 1). Compound 5 was further diluted 1:2 (two-fold dilution) with 25 mM phosphate buffer (pH adjusted to 7.2). Compound 6 was diluted 1:2 with pure ethanol. The absorption spectra all were measured at final concentration of 0.05 mM with the exception of compound 1 which was diluted 1:250 (from 2.5 mM) to a final of 0.01 mM.

Absorption spectra were scanned on a Perkin-Elmer Model 552 Spectrophotometer to better than 1 nm resolution using either 1 cm or 1 mm (for very high extinction compound, see Table 1) cuvettes. All spectra were scanned at 60 nm/min except for compound three, which has very fine vibronic structures, the scanning speed was set at 20 nm/min.

For fluorescence spectral studies, the samples prepared for the absorbance scans were further diluted either 1:100 or 1:1000 and put in 1 cm standard four-side quartz windows cell. The excitation and emission spectra were taken on a SLM-Aminco Model 500C spectrofluorimeter at ambient temperature. Fluorescence polarization excitation spectra were taken using the same instrument with a polarization accessory.

Results and Discussion

Absorption Spectral Characteristics

The absorption spectra for the three pyrene and the three [7-julolidino]coumarin derivatives were depicted in Figure 2 & 3 respectively and their spectral characteristics summarized in Table 1.

Among the pyrene compounds, only 1,3-disodiumsulfonate pyrene retains the very fine vibronic structure with multiple sharp peaks and valleys. The positions of these peaks change very little compared to the parent pyrene compound. On the other hand, the two other pyrene derivatives with additional substitutions to the 6 and 8 positions (the 6,8 positions are symmetrical to the 1,3 positions) show pronounced spectral changes. Both diacetyloxy and dihydroxyl derivatives exhibit large red shift and absorb strongly in the blue-green region. It seems that the additional electron rich oxygen atoms from the substituents cause these shifts. The difference seen in the UV region between the latter two compounds is probably due to the additional charges carried by the sulfonate salts in compound 2.

Among the three [7-julolidino]coumarin derivatives, the 3-acetic acid derivative differs very much from the other two in its absorption spectra. The former absorbs mostly in the UV, while the latter two have similar spectra and their absorption maxima shift about 150 nm compared to the former. The latter two compounds absorb quite strongly in the blue region.

Comparing the chemical structures for the three coumarin compounds, we suggest that in 3-acetic acid 4-methyl [7-julolidino]-coumarin the reason that there is no large absorption peak shift to the visible region is because the presence of the extra carbon atom of the acetic acid group. The extra carbon atom further separates the electron rich oxygen atoms of the side chain from the coumarin ring thus reducing the electron resonance.

Fluorescence Spectral Characteristics

The fluorescence excitation spectra for the pyrene and coumarin derivatives are depicted in Figures 4 and 5 respectively and their spectral features summarized in Table 2. The excitation spectra were corrected for the wavelength dependency of energy dispersion in the xenon lamp used in the spectrofluorometer. Therefore, in principle, the fluorescence excitation spectra for these compounds should be identical to their absorption spectra. However, in 1,3-diacetyloxy 6,8-dichlorosulfite pyrene we find there are some discrepancies between the absorption and excitation spectra. There are several possibilities for the cause of these discrepancies. One possibility is that there are more than one emission dipole. Second, the compound is not very soluble, thus there could be some aggregate forms which exhibit same absorbance characteristics as the monomer but different fluorescence properties. Another possibility is the compound may not be pure.

Comparing the absorption and the excitation spectra for the coumarin derivatives (shown in Figure 3 and 5 respectively), we find very negligible difference between the two as expected from the theory.

The fluorescence emission spectra for the pyrene and coumarin probes are displayed in Figures 6 and 7 respectively (see Table 2 also). For the pyrene derivatives, the two blue-green absorbing dyes emit in the green region (500-510 nm), making them the only class of pyrene compounds that emit in such long wavelength. Previously, only pyrene excimers have been found to emit in this wavelength region.

Of the three coumarin derivatives, only 3-acetic acid 4-methyl [7-julolidino]coumarin (which absorbs mainly in the UV region) does not emit in the visible region. The other two blue absorbing coumarin compounds fluoresce intensely in the green region.

We also made fluorescence polarization measurements (data not shown) for these compounds, the polarization values are all very low or negative as expected for small organic molecules free in solution. It remains to be seen whether or not binding of these probes to large protein molecules may bring a large polarization change, and whether or not binding of these probes to hydrophobic pockets on proteins can bring large intensity changes useful for probing protein-protein interaction.

Conclusions and Future Plan

We have successfully synthesized more than a dozen interesting fluorescent dyes and found two pyrene and two coumarin derivatives particularly attractive. All four compounds emit in the green and exhibit extremely high fluorescence yield.

One of our original objective set out in the beginning is to achieve wavelength shift as long as possible into the red region. Although so far we have only obtained dyes which absorb mainly in the blue-green region, we believe that by deductive reasoning and comparing spectra feature with the position and the chemical characteristics of the substituent in the coumarin and pyrene side chains we have grasped the key in synthesizing dyes that will have further wavelength shift into the red region.

Four dyes described in this paper are ideal for trial in photodynamic therapy using argon ion laser at either 488 nm or 518 nm lines. Experiments utilizing these probes are presently being planned and we definitely will also like to collaborate with other groups to further advance these applications.

Table 1. Absorption Spectral Characteristics of Coumarin and Pyrene Derivatives

Compound	Absorbance Extrema (nm)	Ext. Coeff. (10^4 M^{-1} cm^{-1})	O.D. Ratio
1. 1,3-Diacetyloxy	287 (m)	82.00	1.00
6,8-Chlorosulfite	396 (p)	65.00	0.79
Pyrene	369 (p)	60.00	0.73
	384 (s)	59.00	0.72
	450 (s)	32.00	0.39
2. 1,3-Dihydroxyl	245 (m)	1.48	1.00
6,8-Disodiumsulfonate	410 (p)	1.02	0.69
Pyrene	460 (p)	0.87	0.59
	285 (p)	0.85	0.57
	300 (s)	0.81	0.55
3. 1,3-Disodiumsulfonate	285 (m)	1.55	1.00
Pyrene	375 (p)	1.48	0.95
	244 (p)	1.37	0.88
	201 (p)	1.22	0.79
	236 (p)	1.10	0.71
	355 (p)	1.08	0.70
	272 (p)	0.80	0.52
	340 (p)	0.48	0.31
	262 (p)	0.30	0.19
	323 (s)	0.17	0.11
4. 3-Acetic Acid 4-Methyl	216 (m)	19.40	1.00
[7-Julolidino]	230 (s)	12.60	0.65
Coumarin	282 (p)	9.80	0.51
5. 3-Carboxylic Acid	425 (m)	24.40	1.00
4-Methyl[7-Julolidino]	265 (p)	7.00	0.29
Coumarin	296 (s)	3.20	0.13
6. 3-Methylcaboxylate	440 (m)	14.90	1.00
[7-Julolidino]	290 (p)	4.30	0.29
Coumarin	313 (s)	2.20	0.15

(m): Maximum (s): Shoulder (p): Peak

Table 2. Fluorescence Spectral Characteristics of Coumarin and Pyrene Derivatives

Compound	Emission Extrema (nm)	Excitation Extrema (nm)	Intensity Ratio
1. 1,3-Diacetyloxy 6,8-Chlorosulfite Pyrene	500	399 (m)	1.00
		467 (s)	0.77
		448 (p)	0.92
		384 (s)	0.83
		366 (s)	0.59
		288 (p)	0.78
2. 1,3-Dihydroxyl 6,8-Disodiumsulfonate Pyrene	497	469 (m)	1.00
		454 (p)	0.94
		404 (p)	0.87
		291 (p)	0.61
3. 1,3-Disodiumsulfonate Pyrene	403 (m)	375 (m)	1.00
	425 (s)	354 (p)	0.72
		338 (s)	0.31
		325 (s)	0.10
		282 (p)	0.78
		271 (p)	0.37
		262 (s)	0.14
4. 3-Acetic Acid 4-Methyl [7-Julolidino] Coumarin	360	278 (m)	1.00
		304 (s)	0.66
5. 3-Carboxylic Acid 4-Methyl[7-Julolidino] Coumarin	487	427 (m)	1.00
		296 (s)	0.12
		265 (p)	0.20
6. 3-Methylcaboxylate [7-Julolidino] Coumarin	503	452 (m)	1.00
		313 (s)	0.19
		289 (p)	0.27

(m): Maximum (s): Shoulder (p): Peak

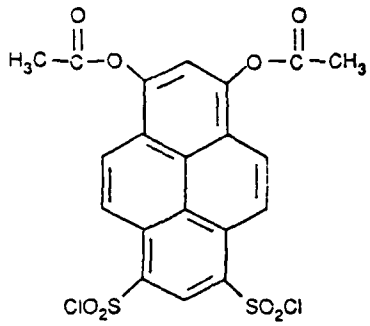

1. 1,3-Diacetyloxy 6,8-Dichlorosulfite Pyrene
   Mol. Wt. 514

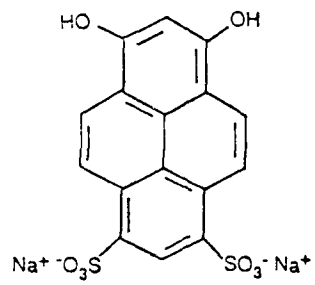

2. 1,3-Dihydroxy 6,8-Disodiumsulfonate Pyrene
   Mol. Wt. 438

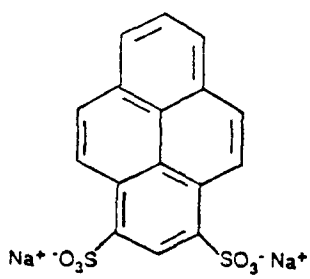

3. 1,3-Disodiumsulfonate Pyrene

   Mol. Wt. 406

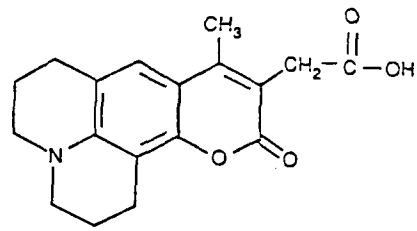

4. 3-Acetic Acid 4-Methyl [7-Julolidino] Coumarin
   Mol. Wt. 313

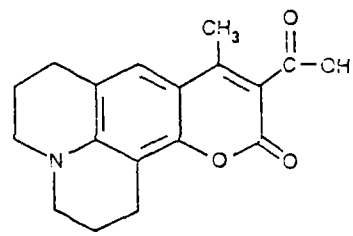

5. 3-Carboxylic Acid 4-Methyl [7-Julolidino] Coumarin
   Mol. Wt. 299

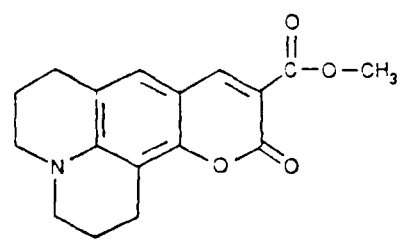

6. 3-Methylcarboxylate [7-Julolidino] Coumarin
   Mol. Wt. 299

Absorption Spectra for New Pyrene Derivatives

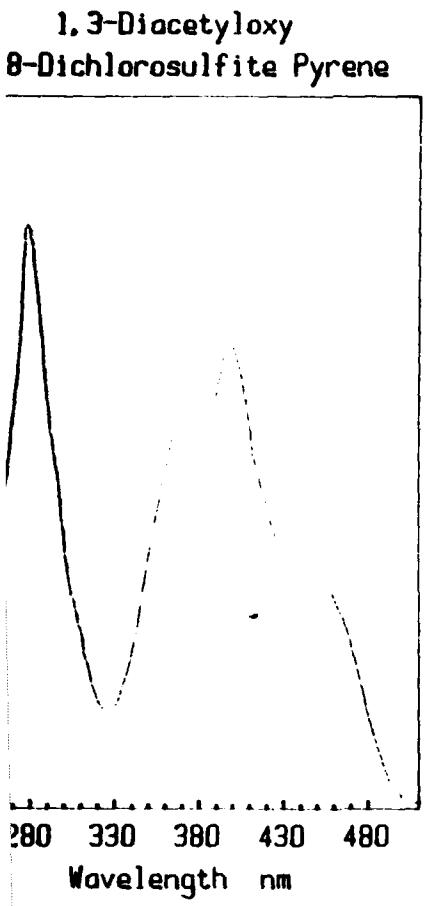

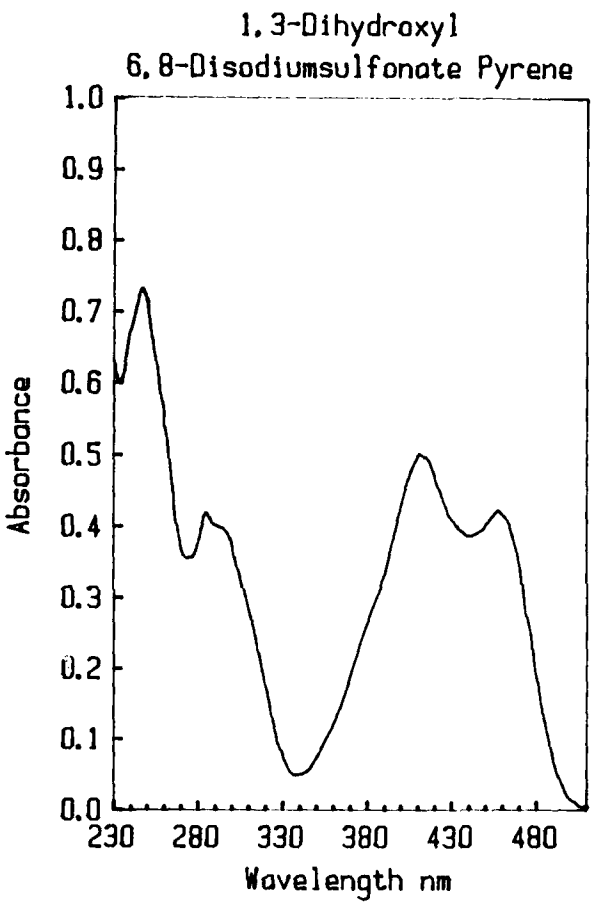

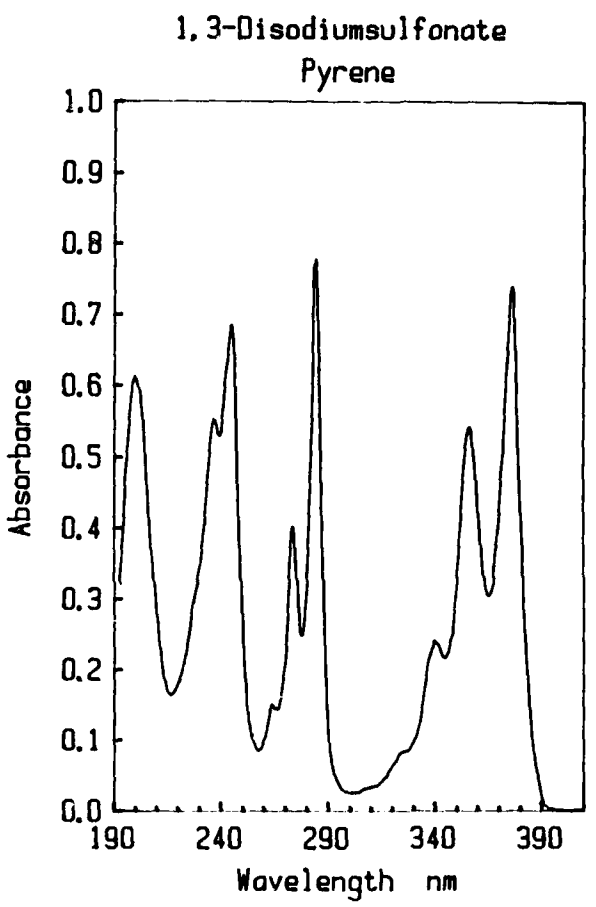

e 2.

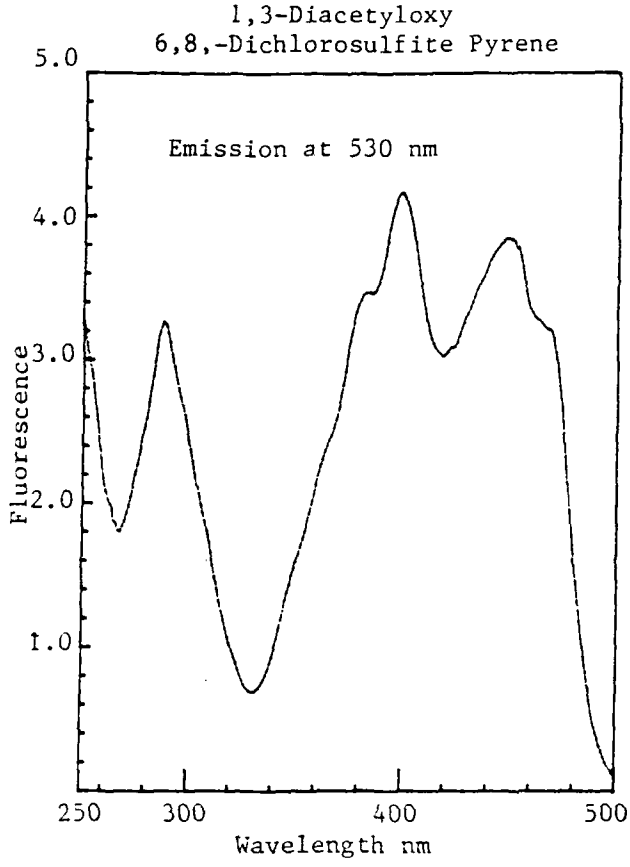
1,3-Diacetyloxy
6,8,-Dichlorosulfite Pyrene
Emission at 530 nm
5.0
4.0
3.0
2.0
1.0
Fluorescence
250
300
400
500
Wavelength nm

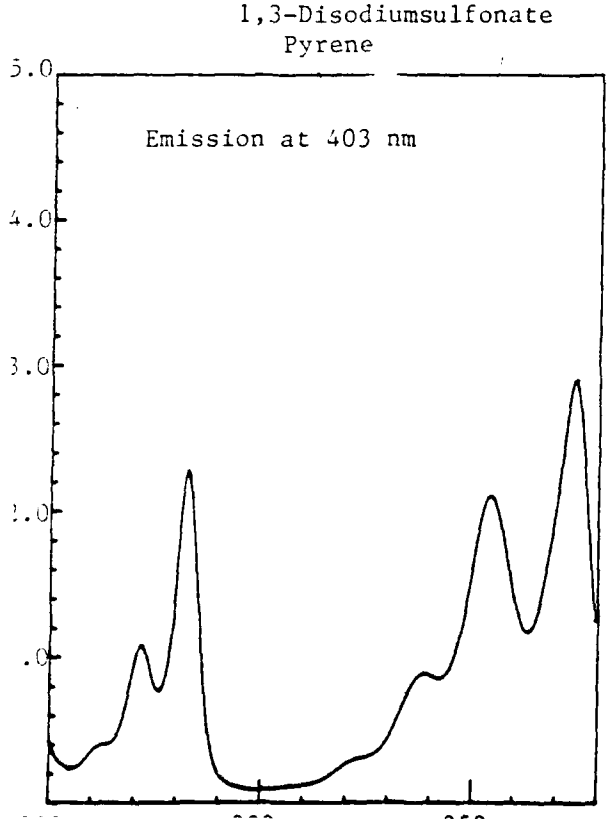
1,3-Disodiumsulfonate
Pyrene
Emission at 403 nm

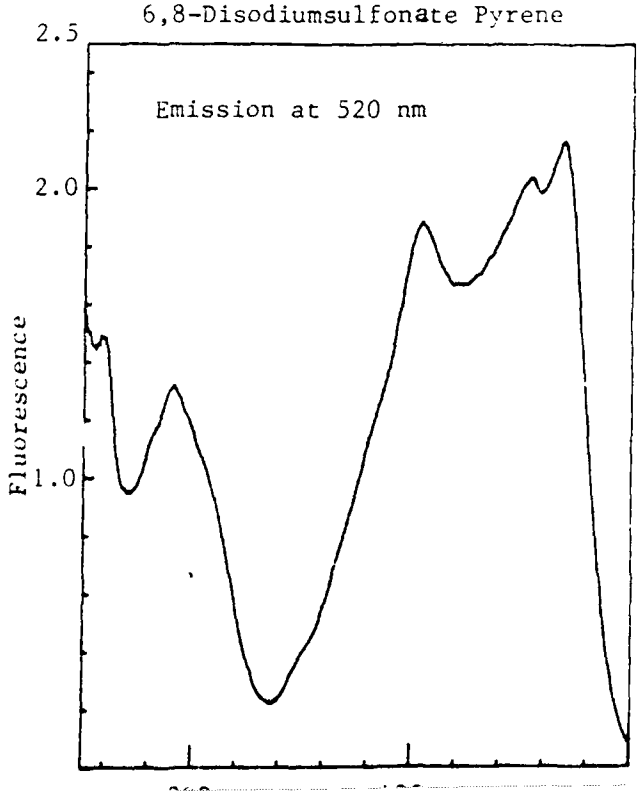
1,3-Dihydroxyl
6,8-Disodiumsulfonate Pyrene
Emission at 520 nm
2.5
2.0
1.0
Fluorescence

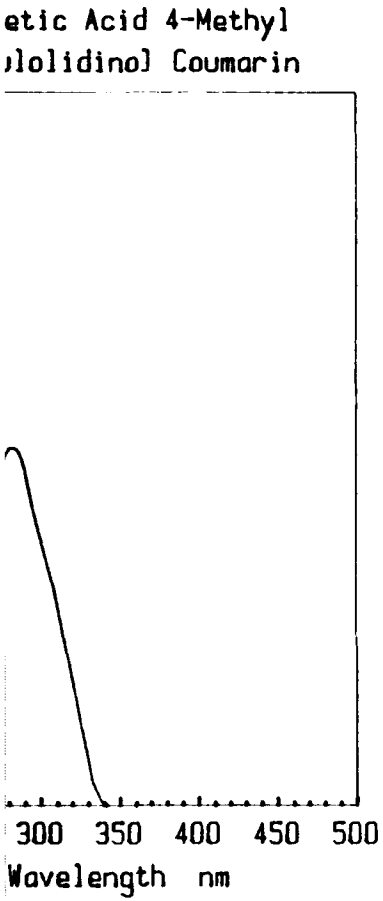
etic Acid 4-Methyl
ılolidino] Coumarin
300 350 400 450 500
Wavelength nm

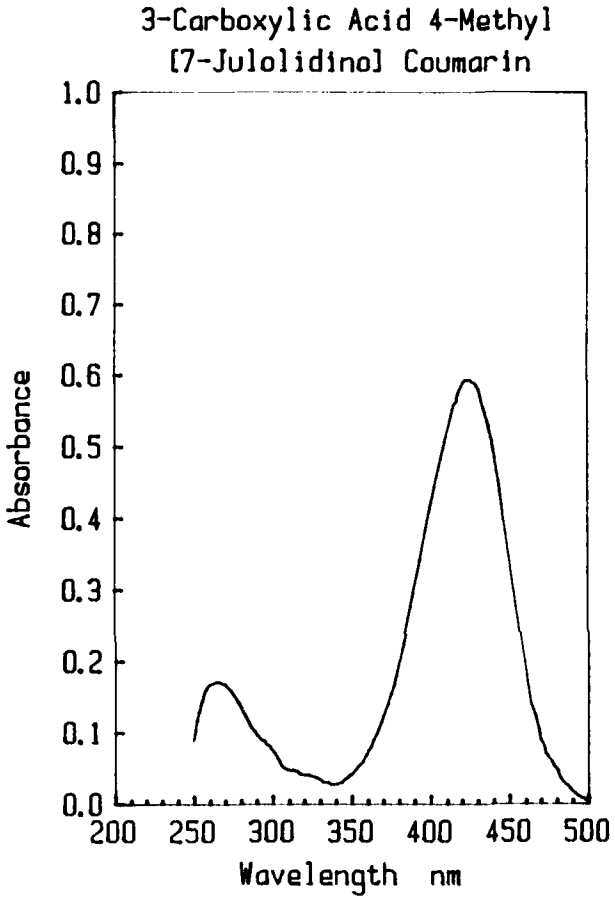
3-Carboxylic Acid 4-Methyl
[7-Julolidino] Coumarin
Absorbance
1.0
0.9
0.8
0.7
0.6
0.5
0.4
0.3
0.2
0.1
0.0
200 250 300 350 400 450 500
Wavelength nm

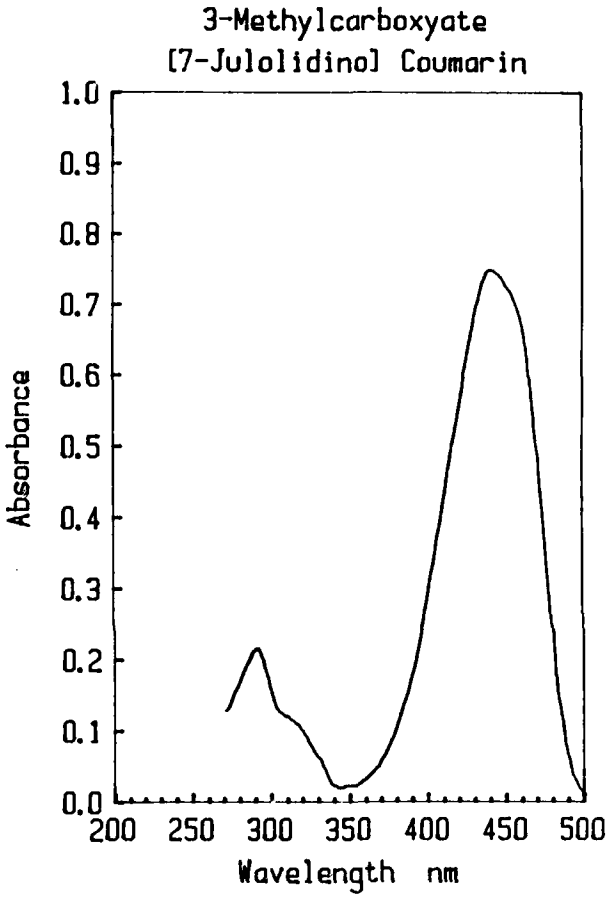
3-Methylcarboxyate
[7-Julolidino] Coumarin
Absorbance
1.0
0.9
0.8
0.7
0.6
0.5
0.4
0.3
0.2
0.1
0.0
200 250 300 350 400 450 500
Wavelength nm

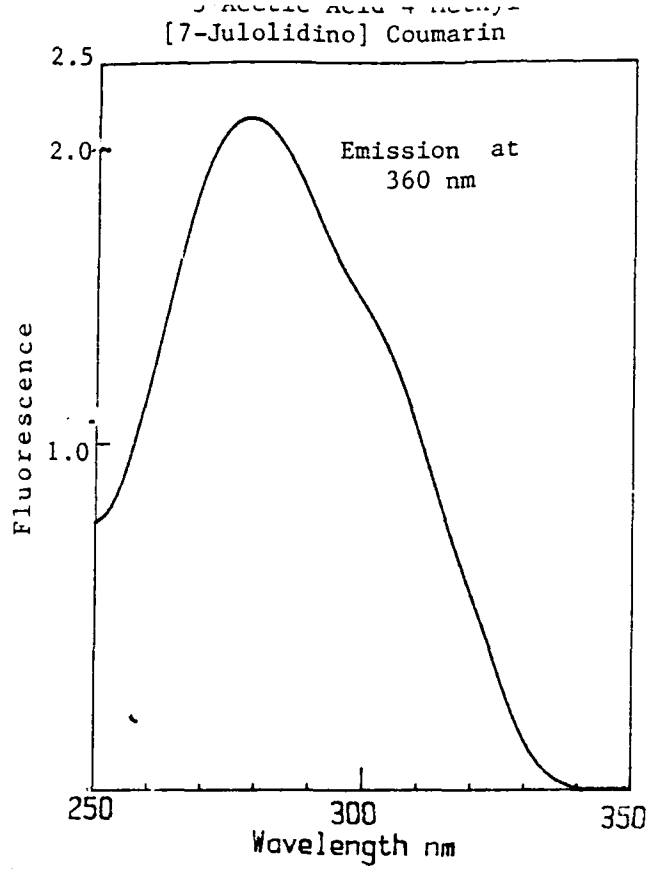
[7-Julolidino] Coumarin
2.5
2.0
1.0
Fluorescence
Emission at
360 nm
250
300
350
Wavelength nm

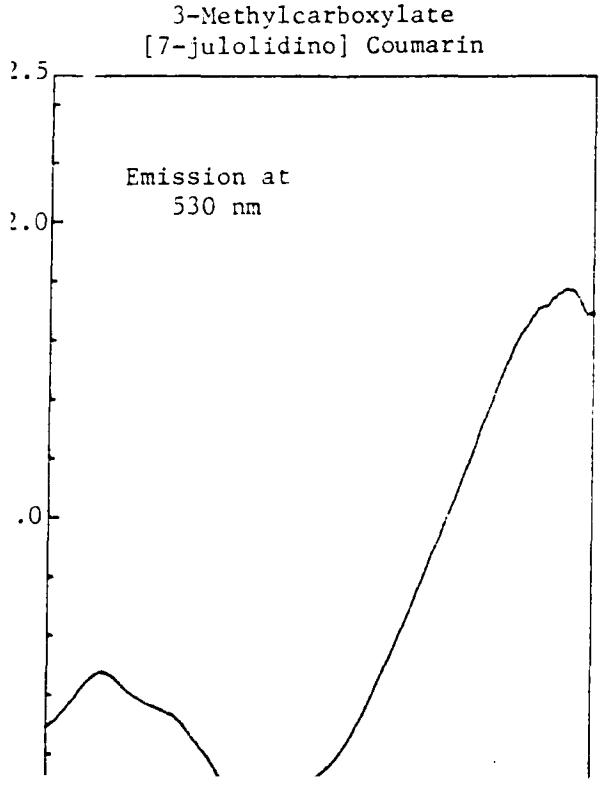
3-Methylcarboxylate
[7-julolidino] Coumarin
Emission at
530 nm

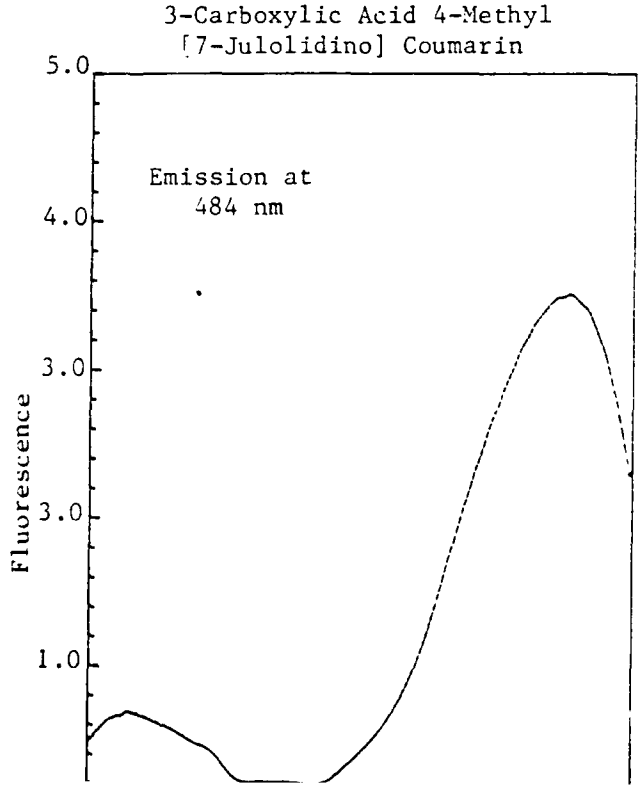
3-Carboxylic Acid 4-Methyl
[7-Julolidino] Coumarin
5.0
4.0
3.0
3.0
1.0
Fluorescence
Emission at
484 nm

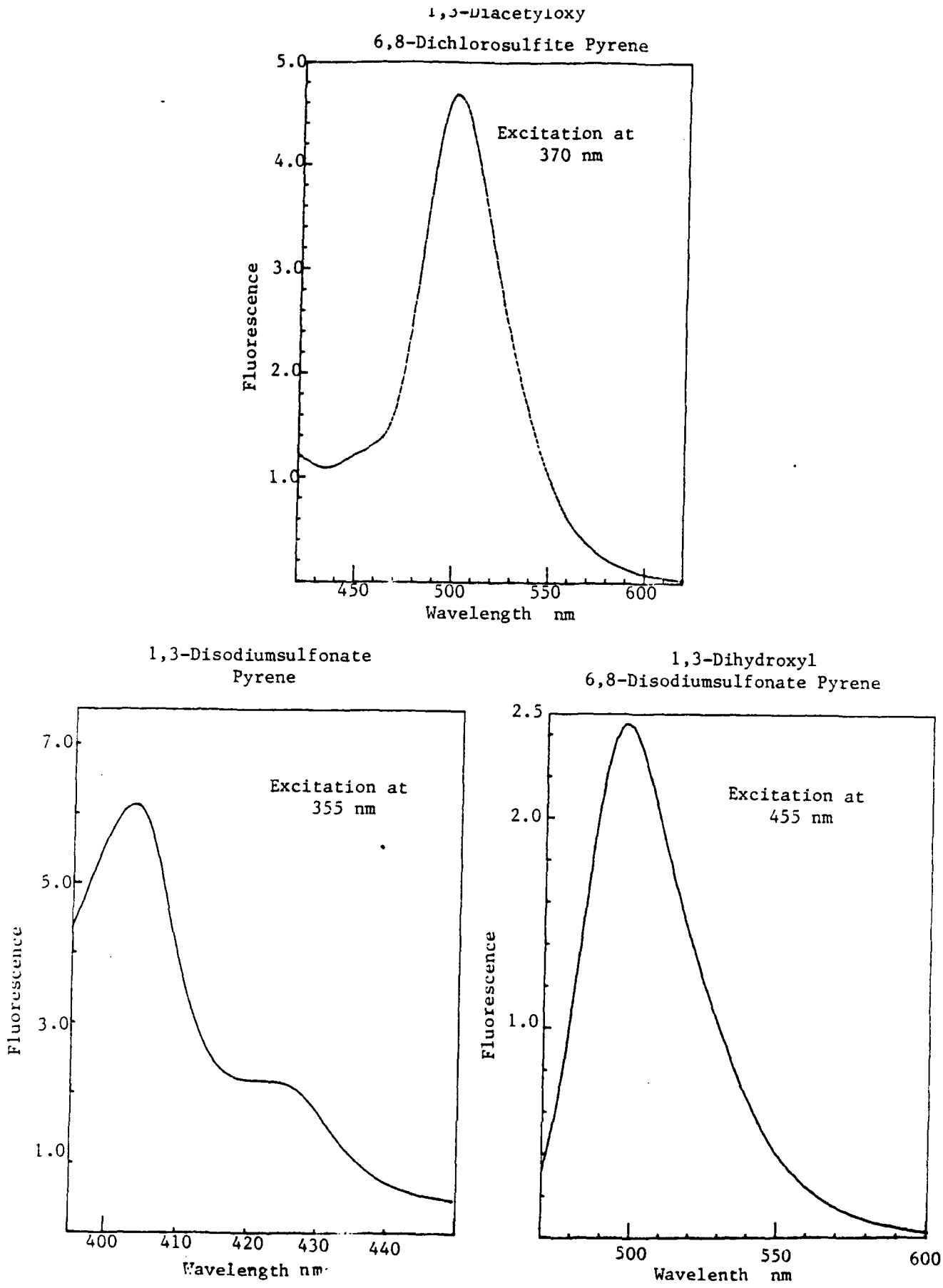

Figure 6. Fluorescence Emission Spectra of Pyrene Derivatives

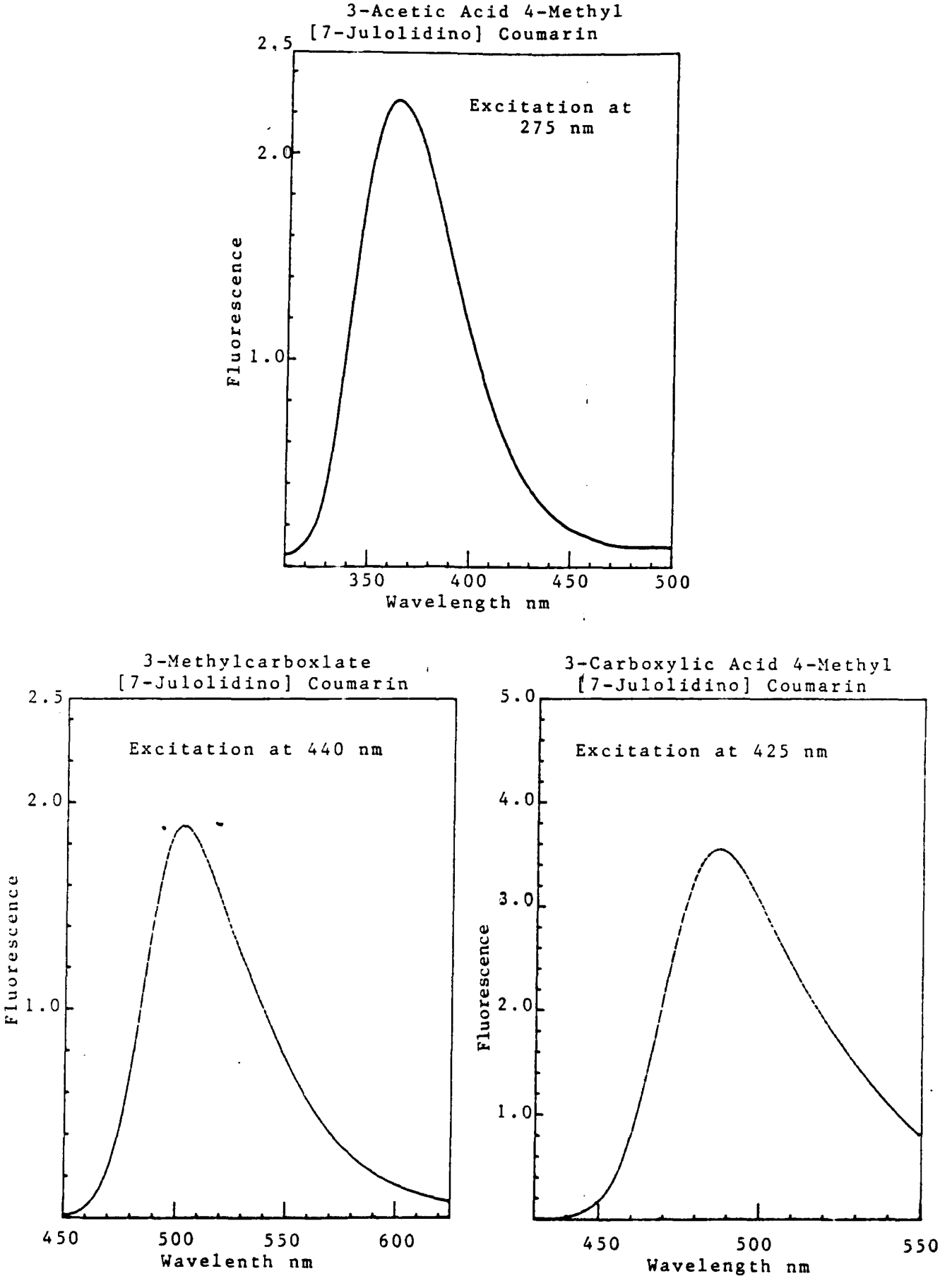

Figure 7. Fluoreasence Emission Spectra of Coumarin Derivatives

CURRENT STATE OF LEUKEMIA AND AUTOLOGOUS BONE MARROW PURGING

Ten percent of all cancers are leukemias and 24,000 cases are reported each year (Pendergrass, 1985). Thousands of persons die of leukemia every year in spite of major advances in patient management and chemotherapy. The use of highly toxic chemotherapy agents carries with it the potential for leukemia cell kill but because of its toxicity, it can also kill normal marrow cells that are essential for life. Thus, systems for protecting marrow cells during treatment are essential. One protective system involves removing the marrow cells prior to therapy and replacing them following therapy, a technique called autologous marrow transplantation. Autologous bone marrow transplantation in leukemia, lymphoma and small cell lung carcinoma involves patient selection, marrow aspiration, marrow storage with or without clean-up, treatment of patient with chemotherapy, reinfusion of marrow and supportive care. Ex-vivo purging of bone marrow is essential because transplantation with untreated marrow (Dicke et al; 1985), or marrow fractionated on albumin density gradients (Dicke et al; 1979), is associated with a high relapse rate suggesting some ex-vivo treatment ("purging") should be employed in an effort to eliminate occult tumor cells from marrow cell suspension. Bone marrow clean-up is usually done by cytotoxic antibodies (single or cocktails), antibody-toxin conjugates or cytotoxic drugs. The use of cytotoxic antibodies or antibody-toxin conjugates have severe limitations due to tumor associated antigen modulation and unpracticability of developing a tumor cell specific antibody for each patient. Chemotherapy with cytotoxic drugs have limitations due to toxicity to bone marrow cells. Drugs such as busulfan and nitrosourea are known to be toxic to stem cells and would be unsuitable for ex-vivo purging. Two agents 4-sulphoethylthiocyclophosphamide (mafosfamid) and 4-hydroperoxy-cyclophosphamide (4HC), have been used in clinical studies (Gorin et al; 1986). The efficacy of these drugs is affected by the magnitude of erythrocyte contamination in bone marrow cells to be purged. Erythrocytes contain aldehyde dehydrogenase which inactivates these congeners of cyclophosphamide. Therefore the effective concentration of these agents will be reduced in the presence of large amounts of erythrocytes resulting in a higher number of hematopoietic progenitor cells, but the lower drug concentration is also ineffective in complete killing of tumor cells. In contrast incubation of erythrocyte free marrow cells with these agents may subject normal stem cells to a toxic concentration of the drug. In clinical studies with these agents Gorin et al; 1986 have reported an actual relapse rate of 87% in patients with Acute Lymphocytic Leukemia and a 46 % relapse rate in patients with Acute Non-Lymphocytic Leukemia. Various explanations of relapse have to be considered. High among them is the possibility that living tumor cells were reinfused due to incomplete purging of marrow. Ciobanu et al; 1986 have reported that normal human marrow granulocyte-macrophage colony-forming cells are reduced to 7.4% and 3.6% of control values when incubated with 23.6 μg/ml or 44.2 μg/ml, respectively of etaposide. Several biochemical and immunochemical methods have been tried for the use in purging marrow. For example, antibody mediated bone marrow purging has been reported by Kersey et al; 1987, Kemshead et al; 1987. Bone marrow purging with 4-hydroxyclophosphamide and vincristine has been reported by Auber et al, 1987 for acute leukemia in second remission. Treatment of refractory tumor cells by veramapil in clonogenic leukemic cell line have been reported and a phase I study of cis-platinum, etaposide cyclophosphamide, and vincristine in pediatric tumors have been reported by Miale et al; 1987. These and several other studies on bone marrow purging were reported in the first international workshop on bone marrow purging and in recent advances in bone marrow transplantation (Gale, 1983, 1987). High dose chemotherapy in allogeneic marrow transplantation for malignant lymphoma has been reported by Phillip et al; 1986 and high doses of chemotherapy in autologous marrow transplantation for small cell lung

carcinoma has been reported by McVie, 1985. All these methodologies have been tried and some are being used in purging marrow with a high success rate of killing tumor cells. However, a good purging system selectively spares a majority of the normal cells. Unfortunately, the tumor effective chemotherapeutic agents used thus far have not been able to save more than 10% of the normal hematopoietic progenitor cells.

Photochemotherapy: Accomplishments and Studies in Progress

Photodynamic therapy can be simply defined as a chemical reaction activated by light. An ideal purging agent kills 100% of the tumor cells while 100% of the normal cells are spared. In an effort to approach these ideals, we have utilized Merocyanine 540 (MC 540) mediated, laser light induced photodynamic purging of bone marrow cells. Our early findings were very encouraging because we were able to attain a 99.999% kill of leukemic cells and survival of 55% of the normal marrow cells with 25% survival of normal hematopoietic progenitor cells, a significant improvement over the chemotherapeutic approach. More recently by using 0.25% human albumin instead of fetal bovine serum, we have been able to retain 99.9999% of leukemic cell killing efficiency while markedly extending the normal cell survival to 80% (Gulliya et al, 1987, 1988). Under these conditions, 40% of the granulocyte-macrophage colony forming cells also survived the treatment. It is important to note that the use of laser light has virtually eliminated the non-specific cytotoxicity observed by day light sources alone. Exposure to daylight source alone has been reported to kill 25% to 65% of cells (Sieber et al; 1986).

We have been successful in killing non-hodgkins lymphoma cells with the same efficiency. There was > 6 log reduction in clonogenic lymphoma stem cells while as much as 50% of the normal marrow CFU-GM cells survived the treatment. In these studies, the effect of recombinant interferon alpha (IFN) was also investigated. It was observed that the presence of low levels of IFN interferes with the complete elimination of leukemic cells but not lymphoma cells by photodynamic therapy. These results are of clinical importance because many leukemic and lymphoma patients are treated with IFN as well. At present, we are investigating the effect of photochemotherapy on the elimination of small cell lung carcinoma, adenocarcinoma and breast cancer cells.

Ongoing Long Term Studies

During the course of this study we asked ourselves a question. Why are leukemic cells more prone to MC 540 uptake and photodynamic kill? To answer this question we have to understand the mechanism of preferential MC 540 uptake and cell kill. Towards this end, we examined leukemia cell culture supernatant to see if we can find a factor(s) that will enhance the MC 540 uptake in normal cells. The rationale being that we can monitor and compare changes induced by the factor. We have identified at least one such factor. When normal cells are incubated with this factor, they behave like leukemic cells with regard to increased MC 540 uptake. This increase in uptake of MC 540 is not due to change in cell size or cell proliferation. Therefore it is very likely that the cell membrane architecture may have been altered by this factor in such a way that it enhances the uptake of MC 540 by the factor treated cell. Hence, this system provides us with a model where the continuous formation of a leukemic-like cell can be continuously monitored to really pin-point the site of and nature of alterations as they occur. Therefore, the aim of this study is to further purify and characterize the tumor cell factor followed by an examination of the alterations caused by tumor cell factor. The long term goal of this study is to understand the mechanisms involved in leukemic cell kill achieved by the photodynamic process.

Objectives

Using photodynamic therapy of leukemic cells with merocyanine 540 and laser light, we have been successful in killing 99.9999% (limit of detection) of leukemic cells while 80% of the normal cells and 40% of the granulocyte-macrophage bone marrow precusor cells survived the treatment. There are several reasons for the success of this project. The main reason is the selective uptake of MC 540 by leukemic cells. This raises two very important questions: 1) Why the leukemic cells are able to sequester MC 540 more than the normal cells?; and 2) Is there a factor produced by leukemic cells that can make the normal cells behave like leukemic cells? The answer to the second question is yes, because we have identified at least one such factor. One objective of this study is to purify and characterize the factor to understand the mechanism(s) involved in the increased uptake of MC 540 by leukemic cells which upon exposure to light kills them. Photodynamic therapy is a relatively new treatment modality that depends upon selective killing of abnormal but not normal cells. Several different explanations have been offered to explain the selectivity of the dye systems. Among these explanations are: 1) enhanced retention of dye by tumor cell; 2) enhanced uptake of dye (active vs passive); 3) differences in cell surface glycoproteins dye binding affinities; 4) differences in membrane charge; and 5) variation in pinocytotic activity, etc. To date, no unifying concensus has been reached which motivates a basis of understanding on which new dyes can be rationally developed. The second objective will be to evaluate what effects the leukemic cell derived factor has on pinocytosis, binding affinity, surface charge, and for dye transport. The leukemia cell model will be used to understand the mechanism(s) maintained above. The knowledge gained from these studies will be applied to other tumor cells.

Research Plan (1988 - 1990)

1. Purification and characterization of tumor cell factor. The factor will be purified by conventional protein sizing method followed by high pressure liquid chromatography using size separation and ion-exchange columns. Biological activity will be tested on each fraction collected. This partially purified factor will then be further analyzed and purified by isoelectric focusing and sodium dodecylsulphate gel electrophoresis.

2. The highly purified protein from electrophoretic separation will be used to prepare polyclonal and/or monoclonal antibodies. These antibodies will be used for further purification of factor and cell surface receptor identification purposes. The amino acid analysis and amino acid sequencing will be done if a homogenous band of pure protein is obtainable by the above process.

3. The membranes of normal cells, factor treated cells and tumor cells will be analyzed to determine the differences in lipids and proteins of the cell membranes. Differences in the membrane function will be analyzed by membrane transport studies.These comparisons may indicate the nature of alteration caused by tumor cell factor that makes the normal cells behave like leukemic cells in terms of MC 540 uptake and cell kill.

4. The effect of purified factor on MC 540 uptake will be determined by fluorimetric method using SLM spectrofluorimeter and the site of binding will be determined with the help of monoclonal antibodies and a fluorescence microscope equipped with image analyzer. The alterations in membrane charge will be determined by potential sensitive dyes.

5. Use of free electron laser on new dyes evaluating pulse properties.

6. The direction of further investigation will depend upon the results obtained in step 1, 2 and 3.

Significance for Leukemia Research

The understanding of the mechanism(s) at molecular level involved in the alteration of a normal cell to behave like leukemic cells (such as those caused by tumor cell factor) may provide the key to the knowledge of how a normal cell becomes leukemic. Moreover, this knowledge may open novel ways of treatment for leukemia on the basis of the understanding of the mechanism.

References

1. Auber, M., Horwitz, L., Spitzer, G., Khorana, S., Jagannath, S., McCredie, K., and Dicke, K.
Proc. of First Int. Workshop on bone marrow purging, 1987, 2:120
2. Ciobanu, N., Paietta, E., Andreef, M., Papenhausen, P., Wiernik, P.H.
Exp. Hematol. 1986, 14:626-35
3. Dicke, K.A., Zander, A., Spitzer, G., Verma, D.S., Peters, L., Vellekoop, L., McCredie, K.B., Hester, J.
Lancet 1979, 1:514-7
4. Dicke, K.A., Jagganath, S., Vellekoop, L., Horwitz, L., Culbert, S., Spitzer, G., Zander, A.
Int. J. Cell clon. 1985, 3:240
5. Gale, R.P. editor, "Recent Advances in Bone Marrow Transplantation", Alan R. Liss, Inc., N.Y., 1983
6. Gale, R.P. editor, "Proc. of First Int. Workshop on Bone Marrow Purging", Bone Marrow Transplant., Vol. 2, 1987
7. Gorin, N.C., Douay, L., Laporte, J.P., Lopez, M., Mary, J.Y., Nahman, A., Salmon, C., Aegerter, P., Stachowiak, J., David, R., Pene, F., Kautor, G., Deloux, J., Duhamel, E., Akker, J.V., Gerota, J., Parlier, Y., Duhamel, G.
Blood 1986, 67:1367-76
8. Gulliya, K.S., Pervaiz, S., Matthews, J.L., Fay, J., Dowben, R.M.
Proc. Soc. Exp. Biol. Med. (S.W. Section), Vol. 9, 1987 (Abst.)
9. Gulliya, K.S., Matthews, J.L., Fay, J., Dowben, R.M.
New Directions in Photodynamic Therapy, Douglas Neckers, ed., Proc. SPIE 847. 163-165 (1987)
10. Gulliya, K.S., Fay, J.W., Dowben, R.M., Berkholder, S., Matthews, J.L.
Cancer Chemoth. Pharmacol. (submitted for publication)
11. Gulliya, K.S., Fay, J.W., Dowben, R.M., Matthews, J.L.
Life Science (submitted for publication)
12. Gulliya, K.S., Pervaiz, S., Nealon, D.G., VanderMeulen, D.L.
New Directorns in Photodynamic Therapy, Douglas Neckers, editor, Proc. SPIE 907, 1988 (In press)
13. Gulliya, K.S. and Matthews, J.L.
Cell Biol. Int. Rep. 1988 (submitted for publication)
14. Kemshead, J., and Gibson, F.M.
Proc. of First Int. Workshop on bone marrow purging 1987, 2:84-88
15. Kersey, J., LeBien, T., Ramsay, N., Filipovich, A., McGlave, P., Uckun, F., Blazar, B., and Vallera, D.
Proc. of First Int. Workshop on bone marrow purging, 1987, 2:47-49
16. McVie, J.G.
Cancer Treat. Res. 1985, 24:211-21
17. Miale, T.D., Gallagher, M.T., Koester, A., Davis, D.R., Mathew, L. and Thatcher, L.G.
Proc. of First Int. Workshop on bone marrow purging, 1987, 2:136
18. Pendergrass, T.W.
Seminars in Oncol. 1985, 12:80-91
19. Phillip, G.L., Herzig, R.H., Lazarus, H.M., Fay, J.W., Griffith, R., Herzig, G.P.
Clin. Oncol. 1986, 4:480-8
20. Seiber, F., Rao, S., Rowley, S.D., Seiber-Blum, M.S.
Blood 1986, 68:32-36

OPTICAL PROPERTIES OF BIOLOGICAL MATERIALS

Interaction of electromagnetic radiation with biological materials ranging from macromolecules to organized tissue and organs is most conveniently characterized by measurement of the various fractions of incident radiation intensity that are transmitted, T, absorbed, A, and remitted (reflected and back scattered) R. Since these quantities account for all direct physical effects of the interaction, (T+A+R) = 1. Typically, T, A, and R of a specific biological material depend upon both the chemical and structural properties of the material and upon the wavelength of the incident radiation. With knowledge of these electromegnetic properties, the fraction incident light energy transferred to a particular tissue and the variation of its intensity with depth of penetration into that tissue may be computed. This capability will allow a choice of laser radiation wavelengths to effect either optimum light penetration or absorption to achieve a desired clinical effect at a desired depth in tissue, and correlation of biological or therapeutic effects and radiation energy density within the volume of tissue at specified incident wavelength over the output spectrum of the FEL at pulse energies where optical effects are linear.

Radiometer

We have constructed and are calibrating an integrating sphere based radiometer. The design of this system allows the medium under measurement to be placed relative to the detector of light intensity so that all diffusely reflected or transmitted radiation intensity is measured (Wan, et al, 1981; Bastin, et al, 1959). To our knowledge, these systems are not routinely available commercially, although the required components are. The system is built around an 8 inch diameter light integrating sphere (as shown in Figure 1). Its design allows all relative positions of input beam, sample, and detector for measuring both the transmittance and diffuse reflectance of the sample. Its white internal coating is 98% relfective over the wavelength range 300-1000 nm. This range is probably the most interesting for the relavent to clinical applications of photosensitizers. This wavelength range includes those necessary for our development of longer wavelength dyes for photodynamically inactivating blood born infectious agents including viruses. We use standard phase-sensitive lock-in amplifier based detection to increase signal to noise ratio at low light intensity resulting from anticipated small remittance and transmittance values at either large absorbance or with large physical thickness values of the tissue sample. For measurements between 300 and 1000 nm wavelength, we employ an extended range S-1 response end-window (1.375 inch dia.) photomultiplier tube (Hamamatsu, Inc.). The tube is electrostatically and magnetically shielded for noise reduction. In our current measurements on blood and blood-agar composites an Argon ion pumped dye laser is used as the light source for wavelengths between 514 and 1000 nm. Chopping frequency is phaselocked with the lock-in amplifier used to read the photomultiplier tube output (EGG 5209 lock-in amplifier with preamplifier). A commercial beam collimator serves to enlarge the laser beam to cover the entire sample face.

The sample cell which we have designed, constructed and are callibrating enables measurements on samples of any uniform fixed thickness up to 10 mm. As shown in Figure 2, the glass coverslips used as end windows serve to hold the sample perpendicular to the incident light beam and to prevent evaporative loss of water from the sample.

Measurements on Blood Suspension

Because of the importance of relating the light intensity at depth within photo-irradiated flowing blood to the photodynamic viral kill in proposed blood banking applications, we are focusing our current tissue optical measurements on blood suspensions. Initially we are using blood suspended in agar at hematocrit (percent cellular volume) values ranging from 0 to 10. This system was chosen initially because the cells are fixed in position. Thus, potential changes in optical scattering with flow rate due to orientation of the discoidal red blood cells by flow forces and to gradients in cell concentration due to gravity induced sedimentation are avoided.

Results of preliminary measurements of the remittance and transmittance of layers of blood-free agar of thickness ranging between 1 and 7 nm are shown in Figures 3 and 4. The observed decrease in both optical quantities agrees qualitively with prediction of Kubelka Theory (1948). Small fluctuations of measured values about curves of best fit are possibly due to minor fluctuations in sample alignment relative to the beam and possible inclusion of small air bubbles between the agar surface film and the coverslip. We are working to identify and eliminate the sources of these fluctuations before proceeding to work with blood-agar suspensions and whole blood.

References

Bastin, J., E., Mitchell, and J. Whitehouse (1959) Use of an integrating sphere to distinguish between absorption and scattering in solids. Brit. J. App. Phys. 10:412-416.

Kubelka, P. (1948) New contributions to the optics of intensely light scattering materials. Part I. J. Opt. Soc. Am. 38:448-457.

Wan, S., R. Anderson, and J. Parrish (1981) Anayltical modeling for the optical properties of skin within in vitro and in vivo applications. Photochem. and Photobiol. 34:493-499.

R.A.T.S. System

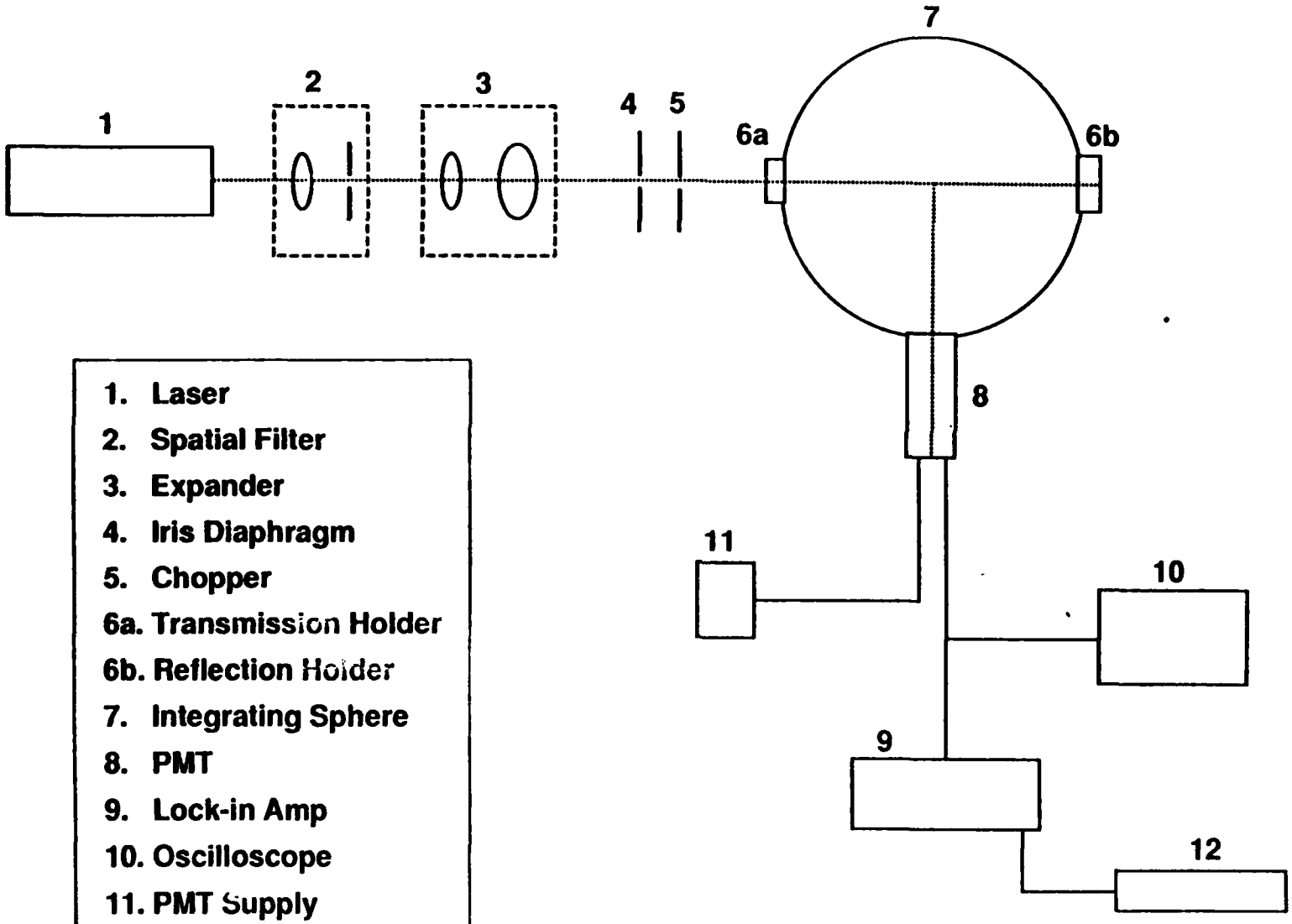

1. Laser
2. Spatial Filter
3. Expander
4. Iris Diaphragm
5. Chopper
6a. Transmission Holder
6b. Reflection Holder
7. Integrating Sphere
8. PMT
9. Lock-in Amp
10. Oscilloscope
11. PMT Supply
12. Recorder

Fig. 1

Sample Holder

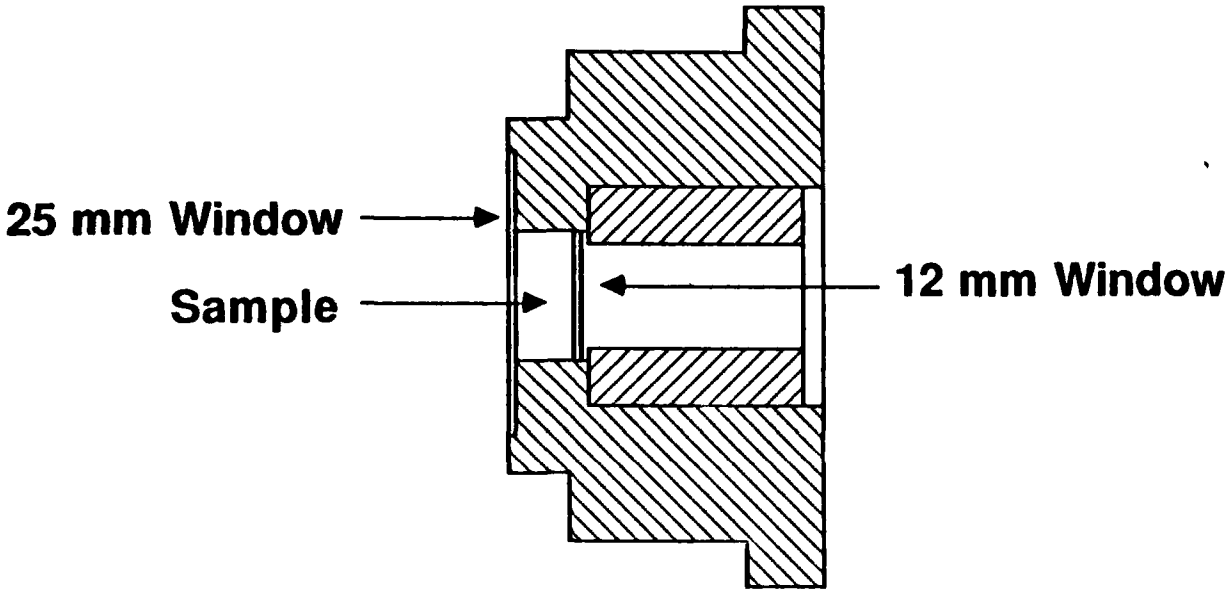

Fig. 2

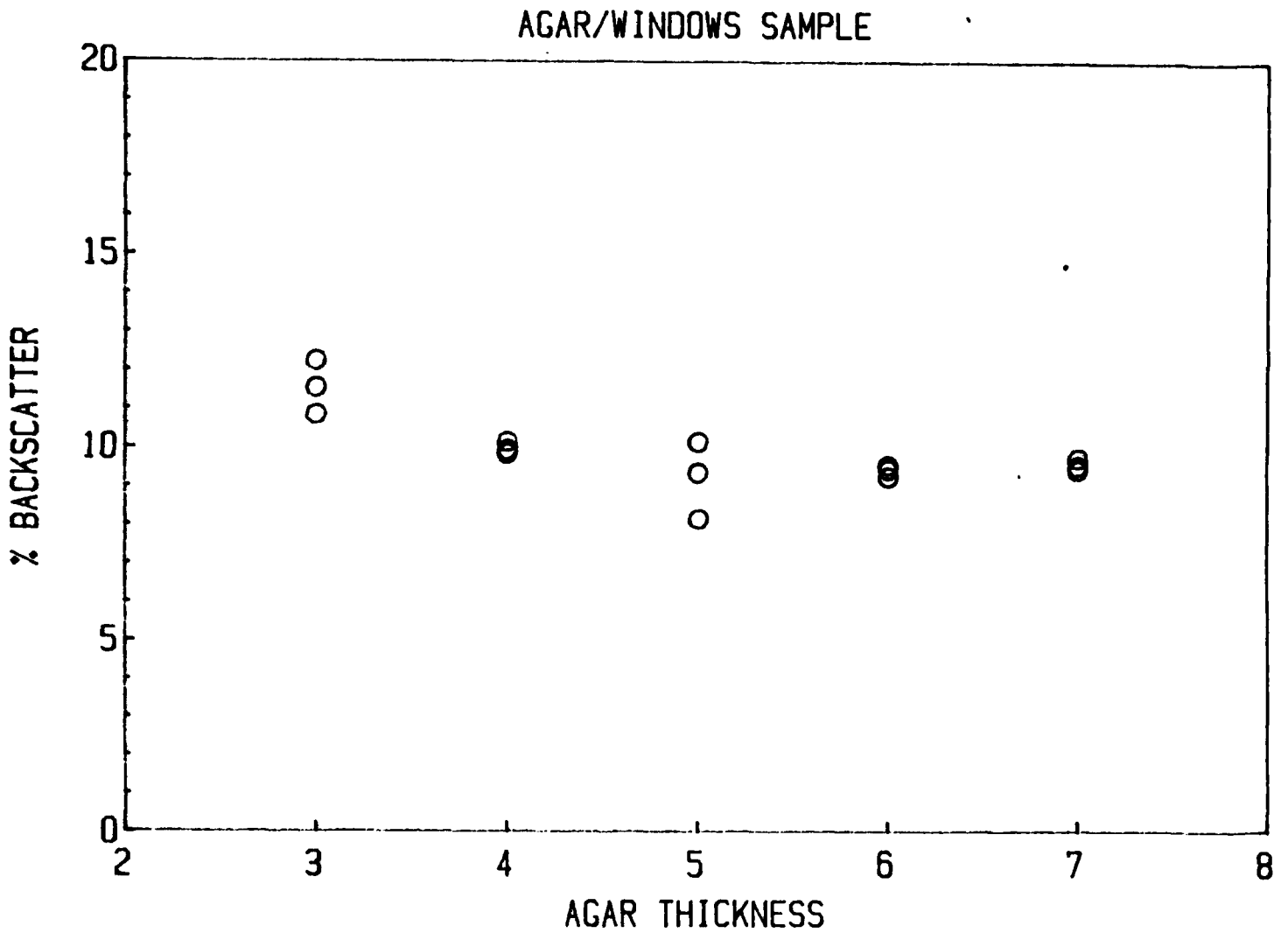
AGAR/WINDOWS SAMPLE
% BACKSCATTER
20
15
10
5
0
2
3
4
5
6
7
8
AGAR THICKNESS

fig. 3

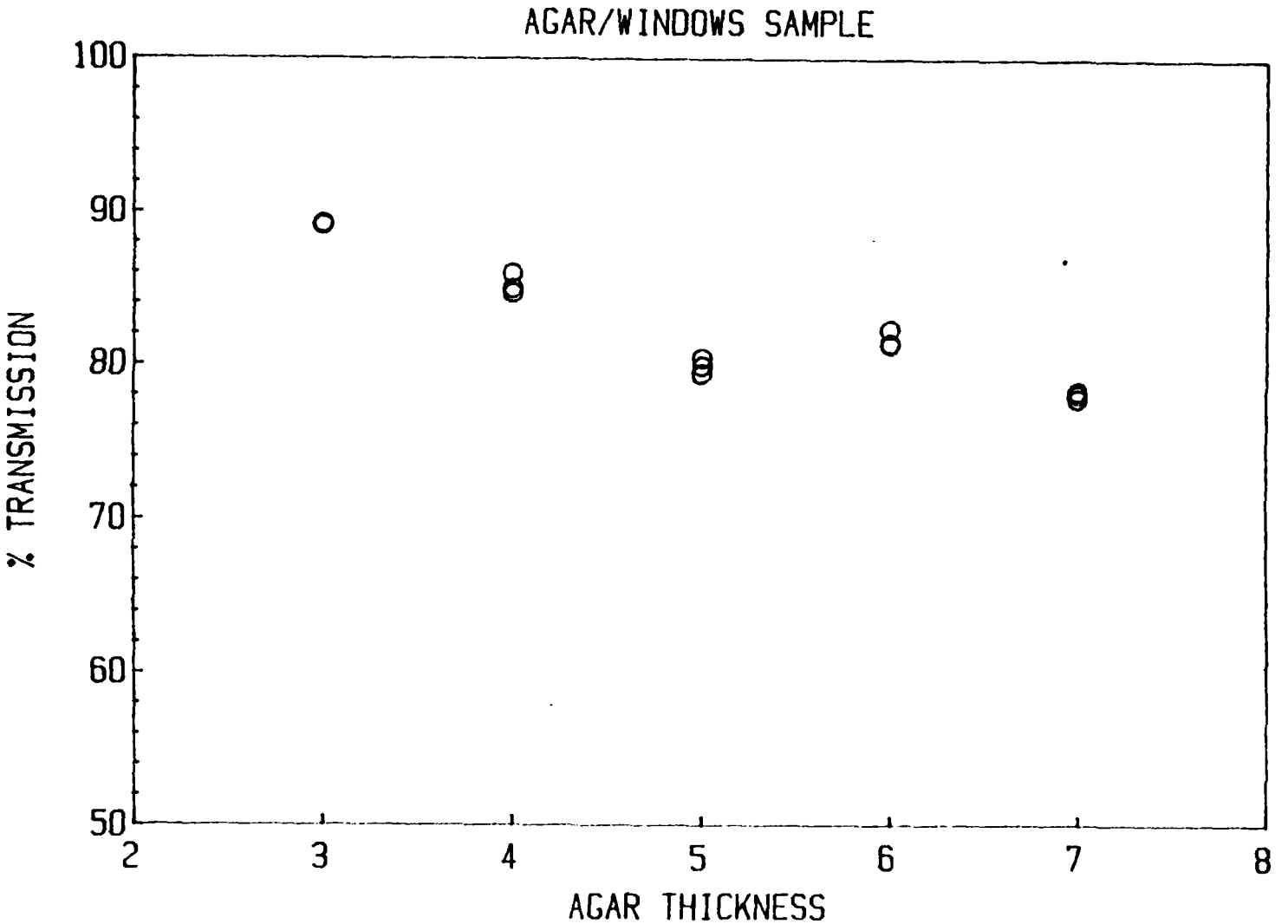
AGAR/WINDOWS SAMPLE
100
90
80
70
60
50
% TRANSMISSION
2
3
4
5
6
7
8
AGAR THICKNESS

Fig. 4

ONR Contract N00014-86-K-0186

	BUDGET'86	BUDGETED 1987-1988	TOTAL BUDGET	EXPENSE 86	EXPENSE 87	EXPENSE 88	TOTAL EXPENSE	BALANCE	PERCENTAGE OF BUDGET
WAGES	276,787.50	384442.50	661,230.00	178129.38	314027.66	79759.82	571916.86	89313.14	86.49%
SUPPLIES	53,800.00	58402.00	112,202.00	49855.21	56347.67	9107.30	115310.18	-3108.18	102.77%
TRAVEL	10,000.00	31505.00	41,505.00	5259.61	13348.61	4664.89	23273.11	18231.89	56.07%
EQUIPMENT	175,775.00	11100.00	186,875.00	141645.34	34505.18	0.00	176150.52	10724.48	94.26%
INDIRECT	82,217.82	114508.18	196,726.00	56305.15	92630.96	22578.63	171514.74	25211.26	87.18%
TOTAL	598,580.32	599957.68	1,198,538.00	431194.69	510860.08	116110.64	1058165.41	140372.59	88.29%

1986 EXPENSES

	JANUARY	FEBRUARY	MARCH	APRIL	MAY	JUNE	JULY	AUGUST	SEPTEMBER	OCTOBER	NOVEMBER	DECEMBER	YEARLY TOTAL EXPENSE
WAGES				25009.56	9010.72	11094.27	13012.83	18659.44	19595.16	22160.38	25639.69	35953.79	178129.38
SUPPLIES				2267.95	1245.64	402.54	1041.19	2591.85	8762.38	6490.05	6344.85	20993.92	49855.21
TRAVEL					1978.93	577.29	320.92	148.36	21.41	0.00	0.00	2212.70	5259.61
EQUIPMENT					0	0	0	0	0.00	6866.10	31908.24	102871.00	141645.34
INDIRECT				6584.79	2954	2914.69	3470.11	5165.88	6850.68	6916.21	7721.07	14281.32	56305.15
TOTAL				33862.3	15189.29	14988.79	17845.05	26565.53	35229.63	42432.74	71613.85	176312.73	431194.69

1987 EXPENSES

	JANUARY	FEBRUARY	MARCH	APRIL	MAY	JUNE	JULY	AUGUST	SEPTEMBER	OCTOBER	NOVEMBER	DECEMBER	YEARLY TOTAL EXPENSE
WAGES	24593.39	25119.75	24181.58	15565.43	33737.60	37990.94	19546.80	25006.14	23326.30	23966.64	33785.76	27207.33	314027.66
SUPPLIES	2701.04	4948.20	9291.46	14065.29	6215.76	5404.65	3043.01	3913.92	1080.01	2839.65	1115.68	1729.00	56347.67
TRAVEL	369.00	1120.88	192.98	1968.88	1508.55	2632.12	0.00	0.00	85.49	1067.23	3328.17	1075.31	13348.61
EQUIPMENT	12404.48	0.00	0.00	6884.01	6976.11	0.00	0.00	0.00	3512.60	0.00	4728.00	0.00	34505.18
INDIRECT	6677.95	7528.98	8126.98	7628.14	10008.91	11111.09	5453.18	6981.30	5912.32	6726.67	9228.63	7244.81	92630.96
TOTAL	46745.84	38717.82	41793.00	46111.75	58446.93	57138.80	28042.99	35901.36	33916.72	34602.19	52186.24	37256.45	510860.08

1988 EXPENSES

	JANUARY	FEBRUARY	MARCH	YEARLY TOTAL EXPENSE
WAGES	27093.76	25534.80	27131.26	79759.82
SUPPLIES	2153.66	4147.66	2805.98	9107.30
TRAVEL	1141.61	1336.73	2184.35	4664.89
EQUIPMENT		0.00	0.00	0.00
INDIRECT	7335.96	7488.52	7754.15	22578.63
TOTAL	37725.19	38509.71	39875.74	116110.64

-Indirect rate is 24.14% as determined by the Office of Naval Research